ARCADA

# Operational State Recognition of a Rotating Machine Based on Measured Mechanical Vibration Data

Jukka Junttila

Master's Thesis

Master of Engineering - Big Data Analytics

2021

| MASTER'S THESIS | |
|---|---|
| Arcada University of Applied Sciences | |
| | |
| Degree Programme: | Master of Engineering - Big Data Analytics |
| | |
| Identification number: | 8273 |
| Author: | Jukka Junttila |
| Title: | Operational State Recognition of a Rotating Machine Based on Measured Mechanical Vibration Data |
| Supervisor (Arcada): | Leonardo Espinosa-Leal |
| | |
| Commissioned by: | VTT Technical Research Centre of Finland Ltd. |


Abstract:
Digital twin is a relatively new concept. Also, it lacks a formal definition and can be applied in virtually any field of technology. Considering digital twins of rotating machines, and especially the in-service phase of their lifecycle, a digital twin should produce valuable information for the owner and operator of the application. The information produced by a digital twin should be accurate, up-to-date, and available anywhere. These requirements act as limiting factors for the complexity of the digital twin and promote the need for efficient data transfer, data acquisition and especially data processing methods at the source of information.
This study investigates how these requirements can be fulfilled in continuous, near real-time operational state recognition of a gas engine genset. Therefore, the objective of this study is to provide a data-based model for operational state recognition and detection of abnormal operation of a gas engine generating set in near real-time.
Two different types of machine learning models for the state recognition of the generating set are presented. The first, a classification model, can identify the current power output level of the generating set using the measured mechanical vibration data. The second, a novelty detection model, can detect abnormal operation of the generating set, in fault situations, at a specific power output level. A two-step state recognition model can be built by combining the classification and novelty detection models.



| Keywords: | Machine learning, classification, novelty detection, feature extraction, signal processing, condition monitoring, state recognition, generating set, internal combustion engine, digital twin, mechanical vibration, structural dynamics, DigiBuzz, VTT, Wärtsilä |
|---|---|
| Number of pages: | 99 |
| Language: | English |
| Date of acceptance: | 1 June 2021 |

# CONTENTS


**1 Introduction ..... 8**

1.1 Background ..... 8

1.2 Research problem ..... 10

1.3 Objectives ..... 11

1.4 Data and methods ..... 11

1.5 Limitations ..... 12

1.6 Structure of the thesis ..... 12

**2 Theory ..... 13**

2.1 Energy generating sets and internal combustion engines ..... 13

2.2 Vibration analysis ..... 24

2.3 Supervised Classification in Machine Learning ..... 29

2.4 Related Work ..... 34

**3 Materials and methods ..... 37**

3.1 Studied genset ..... 38

3.2 Provided dataset and sampling of the data ..... 39

*3.2.1 Test runs ..... 40*

*3.2.2 Data sampling ..... 42*

3.3 Feature extraction ..... 45

3.4 Classification and feature selection ..... 49

3.5 Novelty detection ..... 53

**4 Results ..... 56**

4.1 Data sampling ..... 56

4.2 Feature extraction ..... 60

4.3 Classification and feature selection ..... 61

4.4 Novelty detection ..... 69

**5 Discussion and conclusions ..... 82**

5.1 Discussion ..... 82

5.2 Conclusions ..... 95

5.3 Future work ..... 96

**References ..... 97**

**Appendix A ..... A-1**

## Figures

Figure 1. Engine hall inside Kiisa ERPP 1&2 Power Plant in Estonia (Image courtesy of Wärtsilä.) ©2021 Wärtsilä Corporation. ..... 13
Figure 2. Early reciprocating ICE design (Van Basshuysen, 2016, p. 1) ..... 15
Figure 3. The Otto four-stroke engine cycle (Breeze, 2017, p. 36) ..... 16
Figure 4. Cylinder pressure curves of a four-stroke diesel engine (Van Basshuysen, 2016, p. 54) ..... 17
Figure 5. Cyclic fluctuation in cylinder pressure of an SI engine (Van Basshuysen, 2016, p. 625) ..... 17
Figure 6. Movement types of the piston, the connecting rod, and the crankshaft (Van Basshuysen, 2016, p. 54) ..... 18
Figure 7. Inertial torsional force of a four-stroke diesel engine (Van Basshuysen, 2016, p. 75) ..... 19
Figure 8. Gas torsional force of a four-stroke diesel engine (Van Basshuysen, 2016, p. 75) ..... 20
Figure 9. Resultant harmonic coefficients by Porter (1943) ..... 21
Figure 10. Torsional force curve of a four-stroke diesel engine and its harmonic decomposition (Van Basshuysen, 2016, p. 75) ..... 22
Figure 11. Phase direction diagrams of the first 6 orders for an inline six-cylinder four-stroke engine. (Van Basshuysen, 2016, p. 76) ..... 23
Figure 12. Bending moments caused by internal torque (Van Basshuysen, 2016, p. 70) ..... 24
Figure 13. Digital twin methodology (Johansen, 2019) ..... 34
Figure 14. W20V31SG genset. Image courtesy of Wärtsilä. ©2021 Wärtsilä Corporation. ..... 38
Figure 15. Measurement schedule according to the first and the last time stamp of each file. ..... 40
Figure 16. Screenshot of plant automation system software containing information on a five-hour-long test run. ..... 41
Figure 17. Engine rotation speed curve during assumed abnormal operation. ..... 42
Figure 18. Recommended points for vibration measurement in genset (ISO, 1995, p. 3) ..... 44
Figure 19. Normalised measured velocity amplitudes at 100 % power output ..... 47

Figure 20. Parameter values used in the four rounds of classifier training and testing ..... 52
Figure 21. Normalised total signal variances. ..... 57
Figure 22. Results of the final round: Confusion matrix using sequence length of one engine cycles ..... 68
Figure 23. Results of the final round: Confusion matrix using sequence length of six engine cycles ..... 68
Figure 24. Parameter sweep results for One-class SVM novelty detector fitted to 100 % group data, ν=0.01 ..... 72
Figure 25. Parameter sweep results for LOF novelty detector fitted to 100 % group data, k=16 ..... 72
Figure 26. Results for novelty detections run against data from subset 3 of group 100 %: Low proportion of test data classified as abnormal ..... 78
Figure 27. Results for novelty detections run against data from subset 5 of group 95 %: High proportion of test data classified as abnormal ..... 78
Figure 28. Results for novelty detections run against data from subset 5 of group 95 %: balanced proportions of data classified as normal or abnormal ..... 79
Figure 29. Unbalanced ratios of data classified as abnormal to total amount of data in subset between the novelty detectors trained with features combined and separately ... 80
Figure 30. Effect of training novelty detectors with features extracted using different lengths of signal sequences ..... 81
Figure 31. Results of the classification model trained using the tuned parameter values ……...90
Figure 32. Parameter sweep results for One-class SVM novelty detector fitted to 100 % group data, ν=0.01 ..... 92
Figure 33. Parameter sweep results for LOF novelty detector fitted to 100 % group data, k=16 ..... 92
Figure 34. Results for novelty detections run against data from subset 5 of group 95 %: High proportion of test data classified as abnormal ..... 94

## Tables

Table 1. Parameter names and number of different values per parameter ..... 50
Table 2. size of sampled normal operation data by subsets and by genset power output groups [min] ..... 56
Table 3. The number of subsets of abnormal operation data by genset power output group ..... 56
Table 4. Normalised signal variances of subsets of normal operation ..... 58
Table 5. Normalised signal variances of subsets of abnormal operation ..... 59
Table 6. Results of the first round ..... 62
Table 7. Results of the second round ..... 63
Table 8. Main results of the third round: classification accuracies using the SVM RBF algorithm ..... 64
Table 9. Main results of the fourth round: classification accuracies using the SVM RBF algorithm ..... 65
Table 10. The results of the fourth round: Classification accuracies by the five different algorithms using the features FFT 1.5 and ACC PWR extracted using all sequence lengths from the signals measured at point P1 combined ..... 66
Table 11. The results of the fourth round: Training times by the five different algorithms using the features FFT 1.5 and ACC PWR extracted using all sequence lengths from the signals measured at point P1 combined ..... 66
Table 12. The results of the fourth round: Prediction rates in thousands of samples per second by the five different algorithms using the features FFT 1.5 and ACC PWR extracted using all sequence lengths from the signals measured at point P1 combined 66
Table 13. Grid search results ..... 67
Table 14. Results of the final round ..... 68
Table 15. Parameter sweep results for One-class SVM: Novelty detection against data from the same class as trained ..... 70
Table 16. Parameter sweep results for LOF: Novelty detection against data from the same class as trained ..... 70
Table 17. Parameter sweep result for One-class SVM: Novelty detection against data from the other classes ..... 70
Table 18. Parameter sweep result for LOF: Novelty detection against data from the other classes ..... 71

Table 19. Parameter sweep result for One-class SVM: Novelty detection against data from the other classes presented groupwise ..... 71
Table 20. The number of subsets of abnormal operation data by genset power output group. ..... 73
Table 21. Results for novelty detection runs using the features FFT 1.5 and ACC PWR combined, percentage of abnormal data found in the subsets of abnormal data by the trained novelty detectors..... 74
Table 22. Results for novelty detection runs using only the feature ACC PWR, percentage of abnormal data found in the subsets of abnormal data by the trained novelty detectors ..... 75
Table 23. Results for novelty detection runs using only the feature FFT 1.5, percentage of abnormal data found in the subsets of abnormal data by the trained novelty detectors ..... 76
Table 24. Results of the first round: LR, SVM RBF, and SVM LIN algorithms..... 84
Table 25. Results of the second round: SVM RBF and KNN algorithms..... 85
Table 26. Results of the second round: SVM RBF algorithm..... 87
Table 27. The results of the fourth round: Classification accuracies by the five different algorithms using the features FFT 1.5 and ACC PWR extracted using all sequence lengths from the signals measured at point P1 combined..... 88
Table 28. The results of the fourth round: Prediction rates (thousands of samples per second) by the five different algorithms using the features FFT 1.5 and ACC PWR extracted using all sequence lengths from the signals measured at point P1 combined 89
Table 29. Results of the third round for point P1 ..... A-1
Table 30. Results of the third round for point P2 ..... A-1
Table 31. Results of the third round for point P3 ..... A-2
Table 32. Results of the third round for point P4 ..... A-2
Table 33. Results of the fourth round for combination FFT 1.5 and ACC ABS.... A-3
Table 34. Results of the fourth round for combination FFT 1.5 and ACC ABS.... A-3

# 1 INTRODUCTION

This thesis presents a model for near real-time operational state recognition of a rotating machine based on measured mechanical vibration data. The model was built by applying common machine learning (ML), data analysis and signal processing methods on measured mechanical vibration data. Such a model is a valuable tool for monitoring purposes of machinery or load-bearing structures. A model that predicts the operational state of a mechanical system in near real-time based on sensor data can also act as a building block of a digital twin (DT).

## 1.1 Background

Wärtsilä Finland has a long history of building and designing diesel engines dating back to the 1930's. Later, Wärtsilä started offering energy generating sets (gensets) for ships and power plants. Despite the on-going global energy transition, gensets form an important part of Wärtsilä's offering even in the future. As a response to the growing demand for cleaner energy, Wärtsilä offers gensets that run on greener fuels, as opposed to the traditional diesel or crude oil, such as natural gas, and constantly develops the fuel efficiency and maintainability of their engines. In addition, piston-based power plants are enablers of carbon-free energy production; gensets are commonly used for backing up and balancing the fluctuations in the production of wind and solar energy.

VTT Technical Research Centre of Finland (VTT) and Wärtsilä have collaborated on different fields of engineering during the past decades. The collaboration between the teams, currently known as the Structural Dynamics team at Wärtsilä Energy and the Dynamic Components and Systems team at VTT, started in the 1990s. During this time, the structural dynamics of Wärtsilä internal combustion engines (ICEs) and gensets has been studied extensively by means of simulations and experimental methods. Ultimately the common research interests of VTT and Wärtsilä have moved towards Industry 4.0-related topics. Research themes, such as DTs and hybrid modelling as well as data analysis and ML, have become more relevant.

The concept of DT is relatively new and to this day has not been explicitly defined. Therefore, definitions for a DT are many and as mentioned before. Its origins are in product lifecycle management (PLM): for example, Rasheed (2020) and Tao (2019)

mention the concept of a virtual product connected to a physical product as the first predecessor of a DT. The concept was presented by Grieves in 2003 as part of his University of Michigan Course on PLM (Grieves, 2014). It was the National Aeronautics Association who finally introduced the term digital twin in their roadmap and defined it as follows:

> A digital twin is an integrated multi-physics, multi-scale, probabilistic simulation of a vehicle or system that uses the best available physical models, sensor updates, fleet history, etc., to mirror the life of its flying twin. The digital twin is ultra-realistic and may consider one or more important and interdependent vehicle systems, including propulsion/energy storage, avionics, life support, vehicle structure, thermal management/TPS, etc. In addition to the backbone of high-fidelity physical models, the digital twin integrates sensor data from the vehicle's on-board integrated vehicle health management (IVHM) system, maintenance history, and all available historical/fleet data obtained using data mining and text mining. The systems on board the digital twin are also capable of mitigating damage or degradation by recommending changes in mission profile to increase both the life span and the probability of mission success. (Shafto, 2010)

Another general definition of a DT can be given as a multiphysical and multiscale virtual model of a component, product, system and/or process, which is connected to the real world by ways of data through its entire lifecycle. The definition is very broad and covers a variety of different fields of study. Hence, the variety of different kinds of DTs, and therefore the need for the tools to build them, is immense. (Lämsä, 2019)

Regarding components and products, DTs can exist before their real-world counterparts, the Physical Twins (PTs). The phase before the existence of a PT is called the virtual prototyping phase. It allows free exploration of the design space for different solutions, and various scenarios can be studied for optimising the functionality of the future PT. Digital twin prototypes (DTPs) enable virtual testing, evaluation and analysis, which, compared to physical prototyping, is significantly faster and cheaper. In addition, DTPs facilitate the simulation of product operation, and the perfection of the product for manufacturing. (Lämsä, 2019)

The virtual prototyping phase and the manufacturing of the product is followed by the operating phase, during which the physical product is connected to its DT until it is taken out of use. The connection can be realised by measuring predefined properties of the product. The DT analyses the measured data and produces useful information for the operator and/or owner of the product. In this regard, businesses can use DTs to broaden their offering from products to services. In addition, the operational data can be utilised in the development of new product versions instead of using nominal estimates of operation conditions. (Lämsä, 2019)

Product designers, manufacturers and operators store and have access to substantial amounts of design, production and operational data related to their products. Though in many cases, the full potential of all this data is not used. Tools and technologies like artificial intelligence (AI), especially ML, internet of things (IoT), big data and data analytics enable the transferring and processing of data into useful information for actors in a countless number of fields. (Lämsä, 2019)

## 1.2 Research problem

This study is done as part of a research project called DigiBuzz, in which both VTT and Wärtsilä participate. The DigiBuzz project focuses on simulation-based digital twins of machines and machine systems and their applications, and on the life-cycle management of digital twins. More specifically, DTs of applications involved with structural dynamics is of special interest.

Considering the DTs of rotating machines, such as a genset, and especially the in-service phase of their lifecycle, a functional DT should produce valuable information for the owner and operator of the application. In an ideal case, a DT of a rotating machine would, for example, estimate the current and even the future state of its PT and schedule its maintenance or its shut down before a failure takes place and pass on the information. Therefore, the information produced by a DT should be accurate, up-to-date and available anywhere. These requirements act as limiting factors for the complexity of the DT and promotes the need for efficient data transfer, data acquisition and especially data processing methods at the source of information. This study investigates how these requirements can be fulfilled in continuous, near real-time operational state recognition of a gas engine genset.

## 1.3 Objectives

The objective of this study is to provide a data-based model for operational state recognition and detection of abnormal operation of a gas engine genset in near real-time. To achieve the objective, the following tasks must be completed successfully:

1. Identification and sampling of data that represents different operational states of the genset into labelled datasets from the provided data.
2. Extraction of computationally light features that are sensitive to the changes in the operational state of the genset from the sampled data.
3. Find the best combinations of features and algorithms to build accurate and fast-performing classifier and novelty detection models for the recognition of the operational state of the genset.

## 1.4 Data and methods

The models built in this study are based on mechanical vibration data measured from a gas engine genset. The data was measured at four different locations on the genset during a set of performance test runs. During the test runs, the genset was tested against different fault situations; therefore, the mechanical vibration data was measured during normal and abnormal operations. Periods of both normal and abnormal operation data are identified in the data by visual inspection. The normal and abnormal operation data is sampled into separate subsets according to the power output level of the genset at the time of measurement.

Common statistical and signal processing methods are applied in the feature extraction process. Computationally light feature extraction methods are preferred. The sensitivity of the extracted features to changes in the operational state of the genset is analysed using different classifier algorithms. The effects of the dataset size, measurement point location, feature extraction method and classification algorithm on the classification accuracy are studied. Finally, the periods of abnormal operation in the corresponding sampled subsets are identified using semi-supervised novelty detection methods.

## 1.5 Limitations

The ML models built in this study are based only on measured mechanical vibration acceleration data. For example, the measured stresses or the genset rotation speed were ruled out from the data used in the ML tasks; neither were any simulation models used to generate data for the ML tasks.

The data provided for this study was not labelled; therefore, the labelling is done by visual inspection based on screenshots of the plant automation system software and the measured rpm time histories of the genset during the measurements. The objectives of this study had no influence in the planning of the measurements, such as the election of the measurement point locations, since the measurements were performed before the study began.

Only already-existing ML methods included in the open-source ML library scikit-learn library are used in this study. The default parameter values for the algorithms defined in scikit-learn are preferred.

## 1.6 Structure of the thesis

The rest of the thesis is divided into 4 chapters. Chapter 2 is an introduction to the theory of ICEs, vibration analysis as part of condition monitoring and signal processing applicable to this thesis and finally a short review of past work is included. The materials and methods used in this study are explained in Chapter 3. The results of the study are presented in Chapter 4. First, the results are thoroughly discussed in Chapter 5. The discussion is followed by the conclusions and the proposition of future work made based on the results.

# 2 THEORY

This study focuses on the operational state recognition of a genset through measured mechanical vibration from the genset structure. The mechanical vibrations in the structure of the studied genset are principally excited by its prime mover, a reciprocating ICE. Therefore, basic concepts and theory related to reciprocating ICEs and their dynamics, vibration analysis and diagnostics of rotating machinery and signal analysis are discussed in this chapter.

The operational state recognition model presented in this study is based on common ML classification and novelty detection algorithms. The algorithms and other ML methods used in this study are also presented in this chapter.

## 2.1 Energy generating sets and internal combustion engines

A generating set, or genset, is defined as an electric generator together with and driven by a prime mover (Lackie, 2007, p. 519). A genset with a reciprocating ICE as the prime mover, such as the studied genset, meets the definition of a piston-engine-based power unit (Breeze, 2017, p. 1). Figure 1 presents gensets inside a piston-based power plant.

*Figure 1. Engine hall inside Kiisa ERPP 1&2 Power Plant in Estonia (Image courtesy of Wärtsilä.) ©2021 Wärtsilä Corporation.*

Due to their relatively straightforward installation and operation, and wide ranges of sizes and potential fuels, gensets have a multitude of different types of applications. For example, large or medium-sized gensets, as the studied genset, are commonly used in remote or developing areas where, depending on the need, they can act as the primary or supplementary source of energy. Another typical application for piston-based power plants is to serve as an emergency power supply in the event of failure in the main power source. (Breeze, 2017, pp. 1-2, p. 8)

The gensets used in power plants usually run at a specific constant rotation speed depending on the mains frequency of the grid it is connected to (Breeze, 2017, p. 32). The specific rotation speed is usually considered when designing or choosing the electric generator for the genset. The coincidence of the natural frequencies of the generator structure with the frequencies of the periodic forces that arise from the generator operation at the operating speed can be easily avoided. Therefore, the generators are generally not an important source of vibrational excitations in gensets applications running at constant speed. (Den Hartog, 1985, p. 265) The same does not apply to ICEs (Den Hartog, 1985, pp. 170-224).

The first reciprocating ICEs were made in the 19$^{th}$ century (Breeze, 2017, p. 6). Since then, they have become a frequently used power source for a variety of different kinds of vehicles, as well as stationary power plants (Breeze, 2017, p. 1). Due to their popularity, they have been studied widely, and numerous inventions and improvements have been made since they were introduced, mainly to increase their efficiency, reliability and comfort and to decrease their environmental impact. (Van Basshuysen, 2016, pp. 1-7, pp. 745-809) However, the most important early technological inventions, such as the two- and four-stroke spark-ignited (SI) gasoline engines, as well as the compression ignition engine, i.e. diesel engine, form the backbone of modern ICEs and serve as a common basis for classification of ICEs (Van Basshuysen, 2016, p. 10). Reciprocating ICE designs from the late 19$^{th}$ century and the early 20$^{th}$ century are presented in Figure 2.

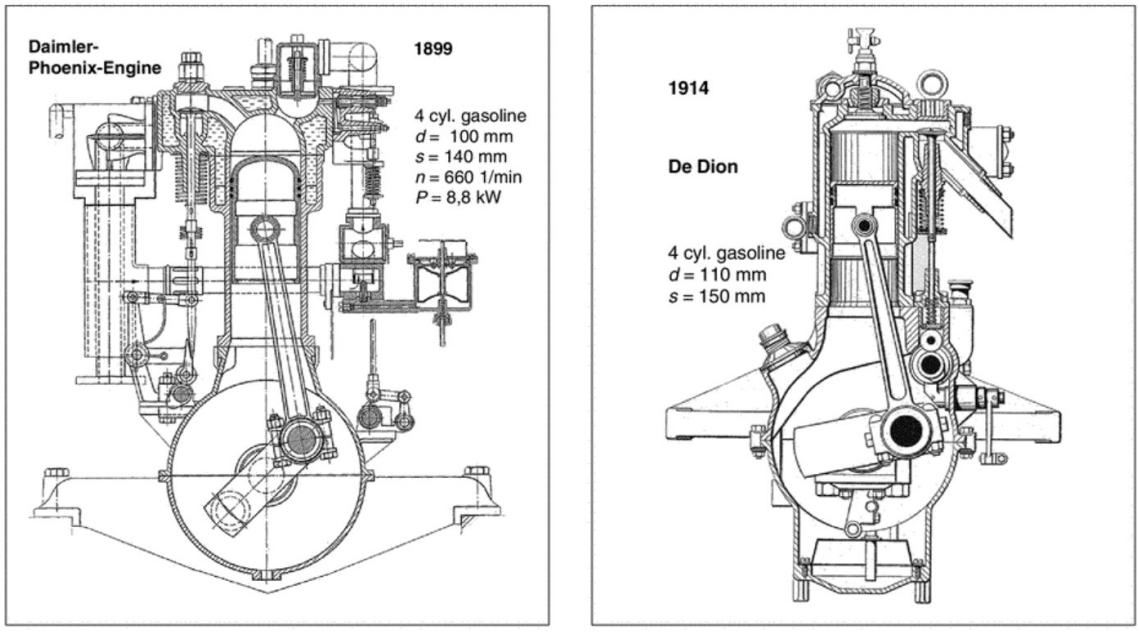


*Figure 2.Early reciprocating ICE design (Van Basshuysen, 2016, p. 1)*

Reciprocating ICEs are a type of driving piston engines. That is, they transform the chemical energy of the fuel to kinetic energy by means of a piston. The piston receives the energy released from the fuel through combustion and turns it to motion. (Van Basshuysen, 2016, pp. 9-10)

The piston of a reciprocating engine moves back and forth in a cylinder between two points called top dead centre (TDC) and bottom dead centre (BDC) (Breeze, 2017, p. 37). The movement from one extreme to the other is called a stroke (Breeze, 2017, p. 36). In most reciprocating ICEs, the oscillating motion of the piston is converted to a rotating motion of a crankshaft (Breeze, 2017, p. 24). The power of the engine is transmitted to the driven application by the crankshaft (Breeze, 2017, p. 23). The two most common engine cycles for crankshaft engines are the two-stroke and four-stroke cycles (Breeze, 2017, p. 21).

The genset studied in this thesis is driven by a four-stroke SI engine. The four strokes of a four-stroke cycle are as follows: intake, compression, expansion and exhaust. An intake stroke starts with the piston moving from TDC towards BDC. The inlet valve(s) are opened, and the cylinder is filled with fresh air or air-fuel mixture depending on the engine type. The intake stroke ends when the piston reaches BDC and a compression stroke starts. During the compression stroke, the valves are closed and the gas inside the cylinder is compressed while the piston moves back to TDC. The combustion starts before the piston reaches TDC. The compression stroke is followed by a power stroke. The

combustion of the fuel-air mixture occurs principally during the power stroke. The burning gases inside the cylinder expand, elevating the pressure in the cylinder which forces the piston towards BDC. By the end of the stroke, the exhaust valve(s) open and the burned gases start flowing away from the cylinder. Within the exhaust stroke, the rest of the burned gases are forced to exit the cylinder by the piston moving from BDC to TDC. A new cycle begins after the piston reaches TDC. The strokes of the four-stroke engine cycle of an SI engine, also known as the Otto engine, are illustrated in Figure 3. (Breeze, 2017, pp. 36-38)

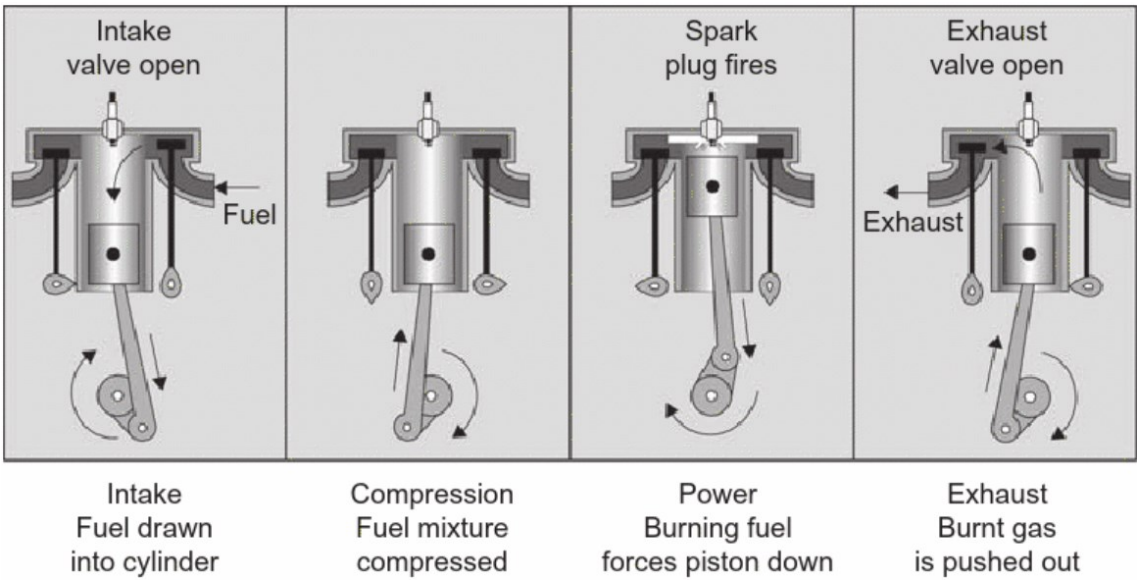


*Figure 3.The Otto four-stroke engine cycle (Breeze, 2017, p. 36)*

The four-stroke engine cycle takes two revolutions of crankshaft to complete. During only one of the four strokes, the power stroke, energy is released from the fuel, and power is generated to the system. This causes highly fluctuating forces acting on the piston during the engine cycle. This can be seen, for example, from a cylinder pressure curve which depicts the gas pressure in the cylinder against the angular position of the crankshaft. Cylinder pressure curves of a four-stroke diesel engine at different levels of power output are presented in Figure 4. A crankshaft angle value of 360° equals the beginning of the power stroke and value 540° the end of the power stroke in Figure 4. (Van Basshuysen, 2016, p. 49, p. 52) Substantial fluctuation in the cylinder pressure of consecutive power strokes is typical for SI engines, as can be seen from Figure 5 (Van Basshuysen, 2016, p. 624).

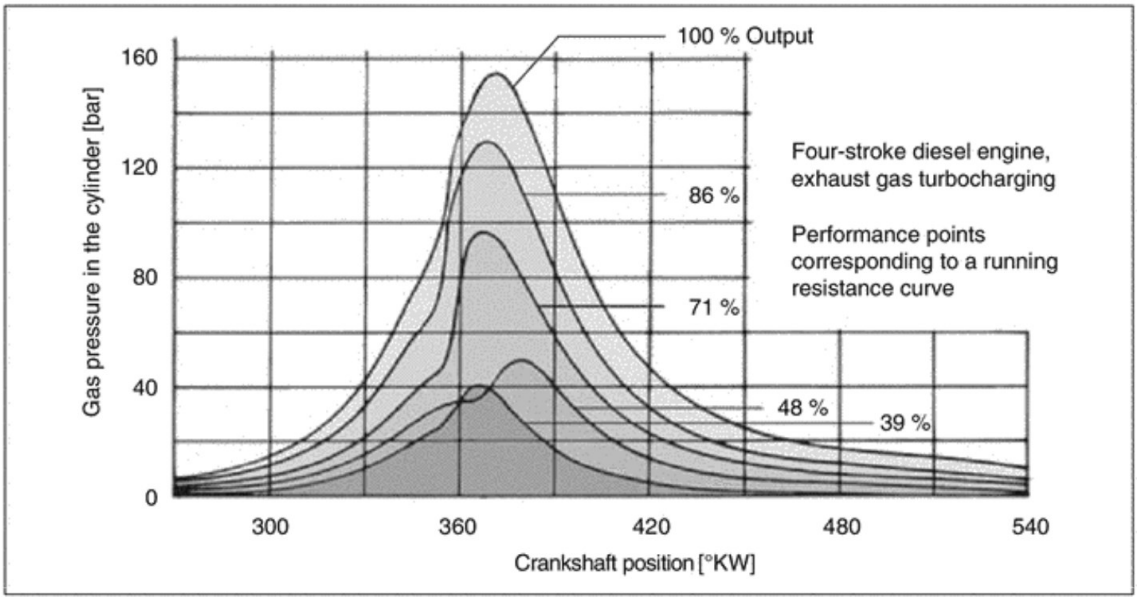


*Figure 4.Cylinder pressure curves of a four-stroke diesel engine (Van Basshuysen, 2016, p. 54)*

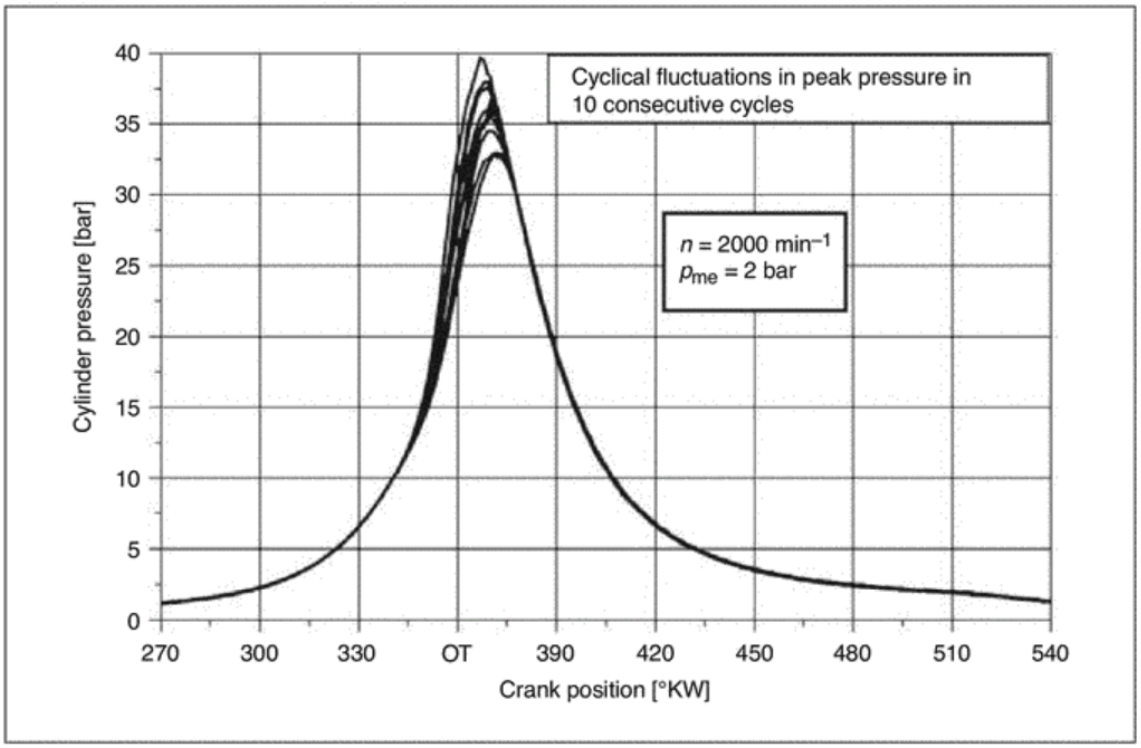


*Figure 5.Cyclic fluctuation in cylinder pressure of an SI engine (Van Basshuysen, 2016, p. 625)*

The piston is connected to the crankshaft through a connecting rod. All three parts belong to a functional group called the crank gear or crankshaft drive. While the engine is operating, the crank gear is in motion. The piston, the connecting rod and the crank shaft are the most active parts of the crank gear, and they all have different types of movements presented in Figure 6. (Van Basshuysen, 2016, pp. 53-54)

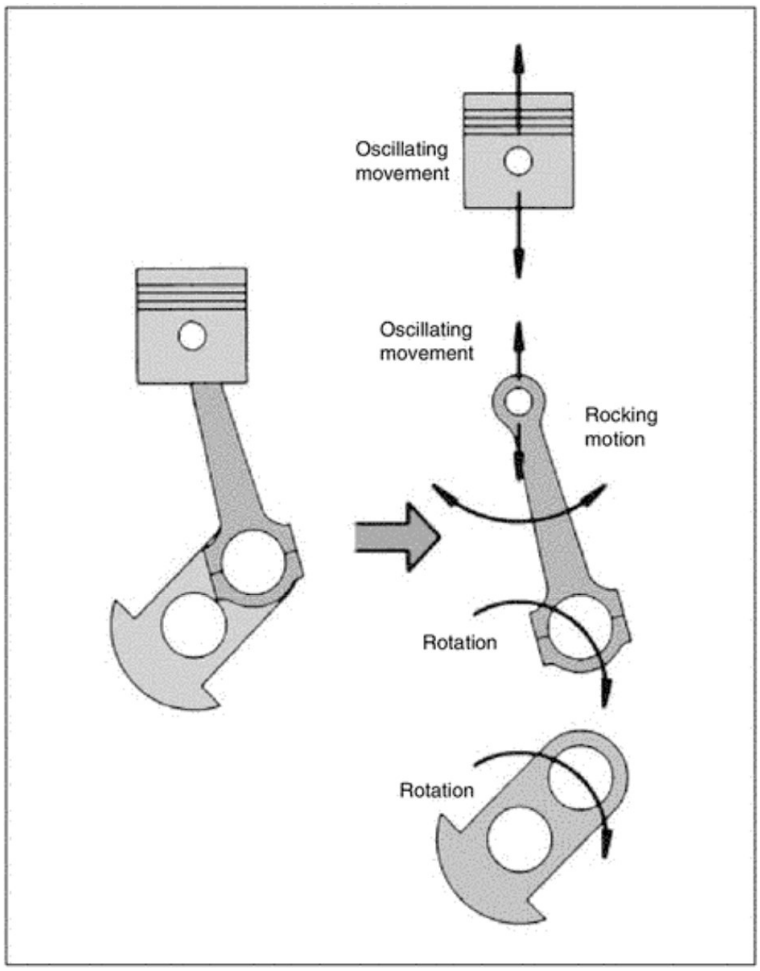


*Figure 6.Movement types of the piston, the connecting rod, and the crankshaft (Van Basshuysen, 2016, p. 54)*

Although the piston, the connecting rod and the crankshaft have different types of movements, common to all of them is that they are under non-uniform acceleration. The direction of the acceleration of the parts depends on the angular position of the crankshaft and the magnitude of the acceleration depends on the angular position and the angular velocity of the crankshaft. That is, the higher the rotation speed, the higher the amplitude of acceleration at a given angular position of the crankshaft and at a constant crankshaft rotation speed, the variation in the acceleration is identical between complete rotations of the crankshaft. (Den Hartog, 1985, pp. 174-177)

Alternating accelerations of the moving parts of the engine cause alternating inertia forces, and the alternating cylinder pressure causes alternating gas forces. According to Newton´s third law, there must be equal and opposing alternating forces acting on the fixed side of the engine. The effect of the alternating inertia and gas forces are observed as vibrations in the engine and its mounting structures, as well as torsional vibrations in the crankshaft. (Den Hartog, 1985, pp. 170-177)

At a constant engine rotation speed, the inertia forces, and therefore the resulting vibrations, are periodic, repeating themselves every engine cycle. The inertial torque acting at the crankshaft, induced by the inertia forces, is caused by the reciprocating mass, that is the whole mass of the piston and partially the mass of the connecting rod. The inertial torque is dependent of the crank angle and the crank gear dimensions. It is accurately approximated using Equation 1. (Den Hartog, 1985, p. 178)

$$M = \frac{1}{2} m_{rec} \omega^2 r^2 \left( \frac{r}{2l} \sin \omega t + \sin 2\omega t + \frac{3r}{2l} \sin 3\omega t \right) \quad (1)$$

Where $m_{rec}$ is the reciprocating mass

$\omega$ is the angular rotation speed

r is the crank radius

l is the length of the connecting rod

The inertial torsional force of a four-stroke diesel engine is presented in Figure 7.

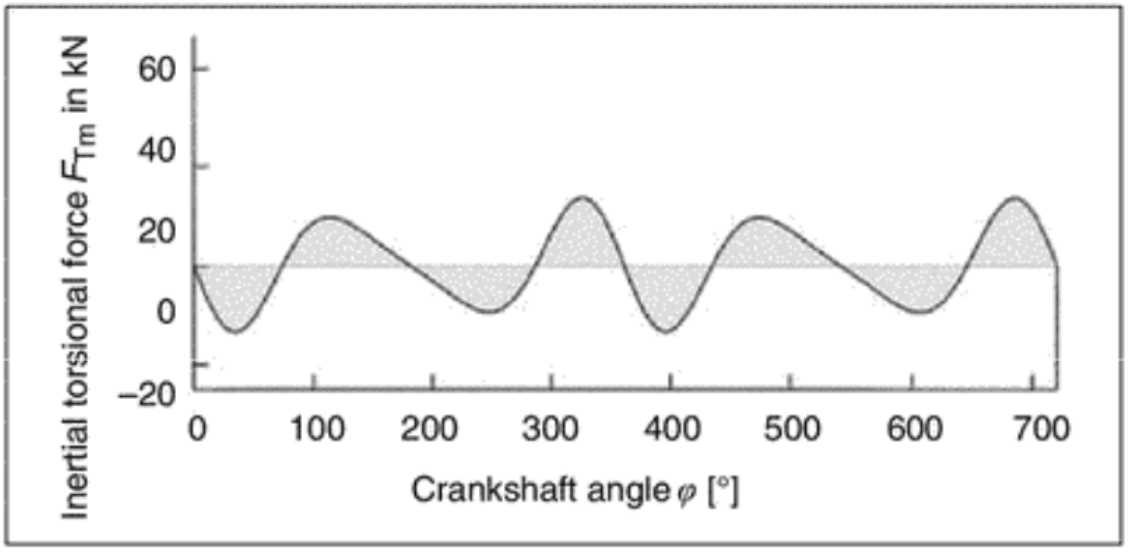


*Figure 7.Inertial torsional force of a four-stroke diesel engine (Van Basshuysen, 2016, p. 75)*

Although the cylinder pressure varies not just during but between engine cycles, even at a constant rotation speed and load, as was shown in Figure 5, the cylinder pressure is often treated as periodic over an engine cycle when it is simulated. Due to the substantial differences between the strokes of an operating cycle in a thermodynamical sense, the gas forces can only be described analytically by a piecewise function of the crank angle (Eriksson, 2002). The gas torsional force of a four-stroke diesel engine is presented in Figure 8.

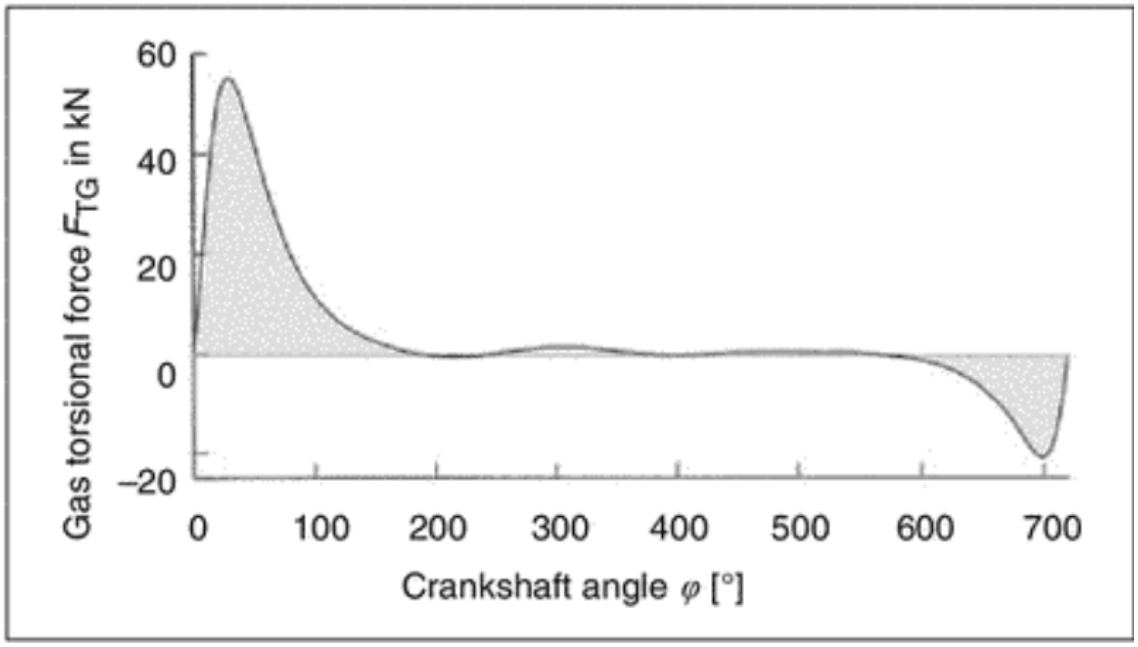


*Figure 8.Gas torsional force of a four-stroke diesel engine (Van Basshuysen, 2016, p. 75)*

Assuming the gas forces as periodic over the engine cycle, the gas torque can be described as a Fourier series. The Fourier series is an infinitely large sum of sinusoidal functions, that is sines and cosines with individual weights called the Fourier coefficients. The sinusoidal functions of the Fourier series are based on the fundamental frequency of the periodic function and its integer multiples. The integer multiples of the fundamental frequency are called the harmonics and the corresponding Fourier coefficients are called the harmonic coefficients. The integer multiples, also known as the harmonic numbers, equal the number of repetitions a harmonic has in one engine cycle. The term order number equals the number of repetitions of a harmonic during one revolution of the crankshaft. The Fourier coefficients represent the amplitudes of engine torque due to the combined forces at corresponding harmonic. The Fourier analysis, of which the Fourier series is an important factor, as part of vibration analysis of rotating machines, is dealt with in more detail in the following chapter. (Porter, 1943, p. A-33)

As mentioned before, one engine cycle of a four-stroke process takes two revolutions of crankshaft, i.e., the fundamental frequency for four-stroke engines is half of the rotational frequency of the engine. Therefore, the order numbers for four-stroke engines are integer multiples of 0.5: order number 0.5 corresponds to the engine cycle frequency, order number 1 corresponds to the rotating frequency and so on. Porter (1943) calculated the harmonic coefficients of the engine torque due to gas pressure affecting on a single crank until the 18$^{th}$ order for different types of engines at different levels of engine load.

Common to all four-stroke engine types, the values of the harmonic coefficients tend to decrease as the order number grows after, at the latest, the fourth harmonic. The resultant harmonic coefficients, i.e., the square root of squared sum of the harmonic coefficients at orders 0 - 18 for a four-stroke gasoline engine at idle and at full load, calculated by Porter (1943), are presented in Figure 9. The value of the harmonic coefficients at order number 0 correspond to the mean value of engine torque over an engine cycle (Den Hartog, 1985, p. 199). The engine torque curve of a four-stroke diesel engine and the first 6 harmonics of its harmonic decomposition are presented in Figure 10. (Porter, 1943)

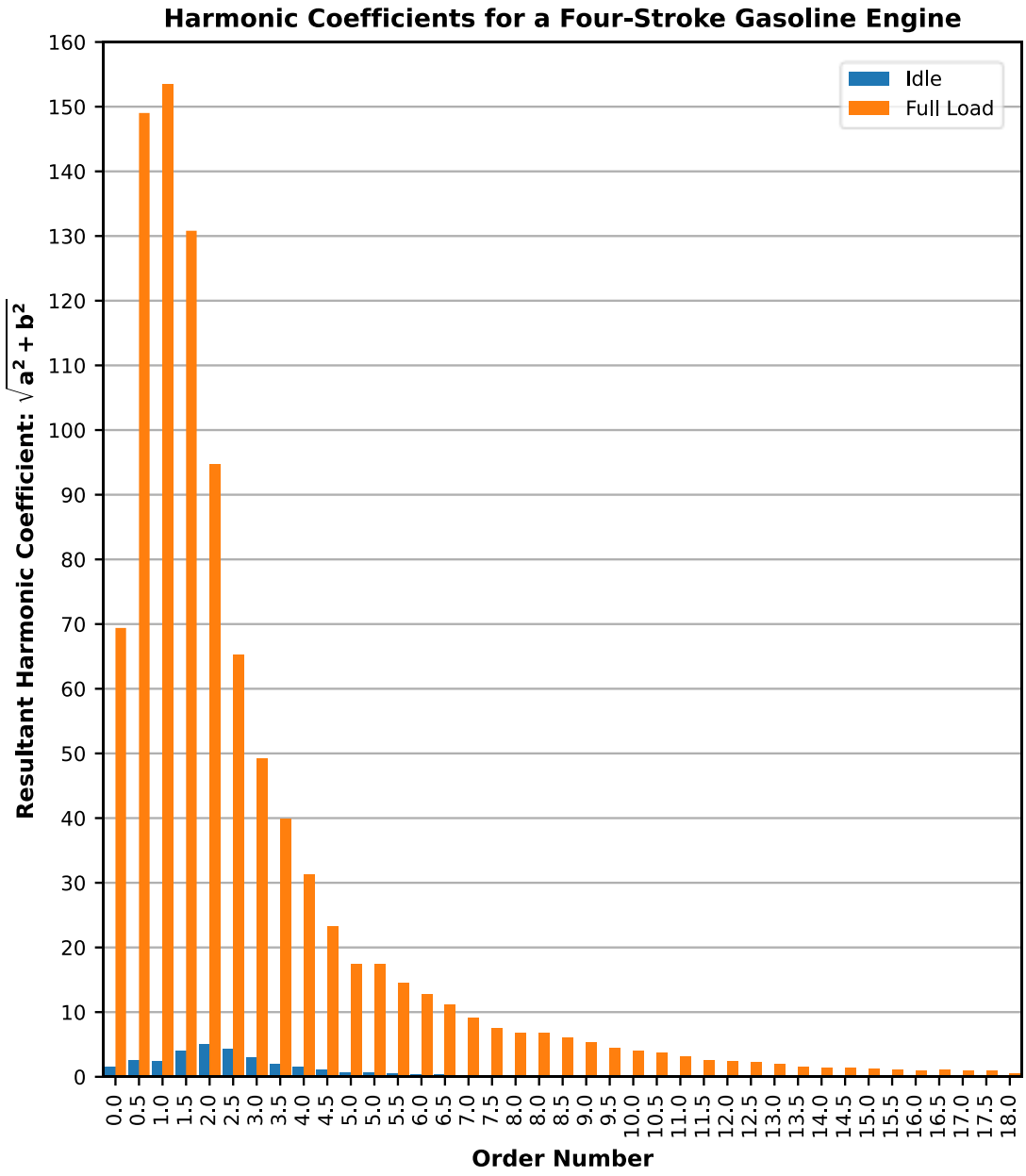


*Figure 9. Resultant harmonic coefficients by Porter (1943)*

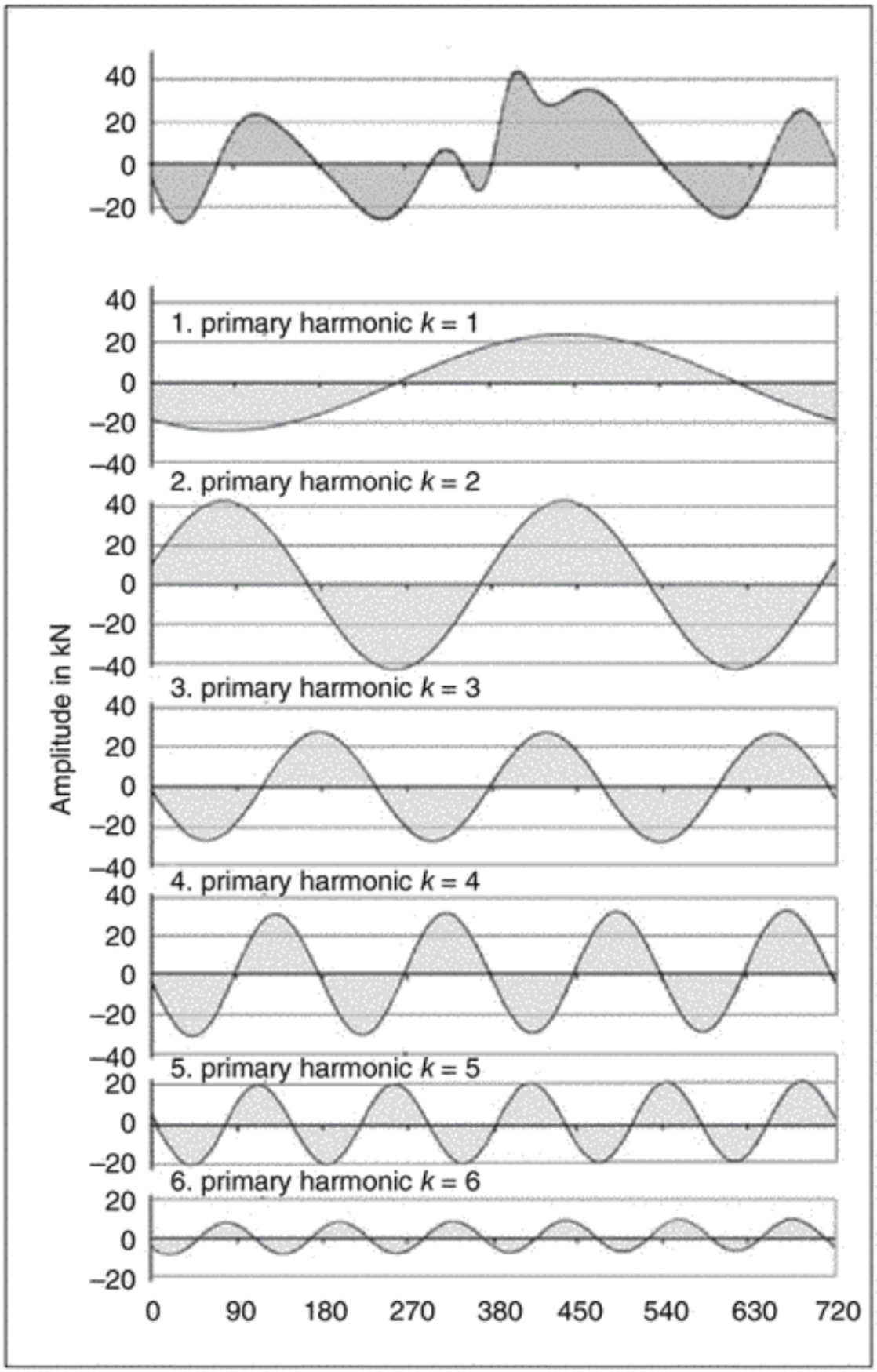


*Figure 10. Torsional force curve of a four-stroke diesel engine and its harmonic decomposition (Van Basshuysen, 2016, p. 75)*

In multi-cylinder engines, smoother operation is accomplished by firing the cylinders at even intervals of a crankshaft angle instead of firing them all at the same time or at uneven intervals (Van Basshuysen, 2016, p. 59, p. 71). When the individual effects of the torsional forces of all pistons of an evenly firing multi-cylinder engine are added up, it results in that, depending on the number of cylinders, they cancel each other out totally or partially at certain harmonics, and reinforce the total torsional forces at others. As an example, in the case of an evenly firing inline six-cylinder engine, the individual effects of the torsional forces of all pistons at the first five harmonics cancel each other out, and the torsional forces of the sixth harmonic are all in the same phase. The worst order numbers for a four-stroke engine are the integer multiples of the number of cylinders halved, because for these orders, all the excitation forces resulting from the individual pistons are aligned. The phase direction diagrams (individual cranks projected on the plane of gravity of the engine) of the first six orders for an inline six-cylinder four-stroke engine are presented in Figure 11. (Van Basshuysen, 2016, pp. 75-76)

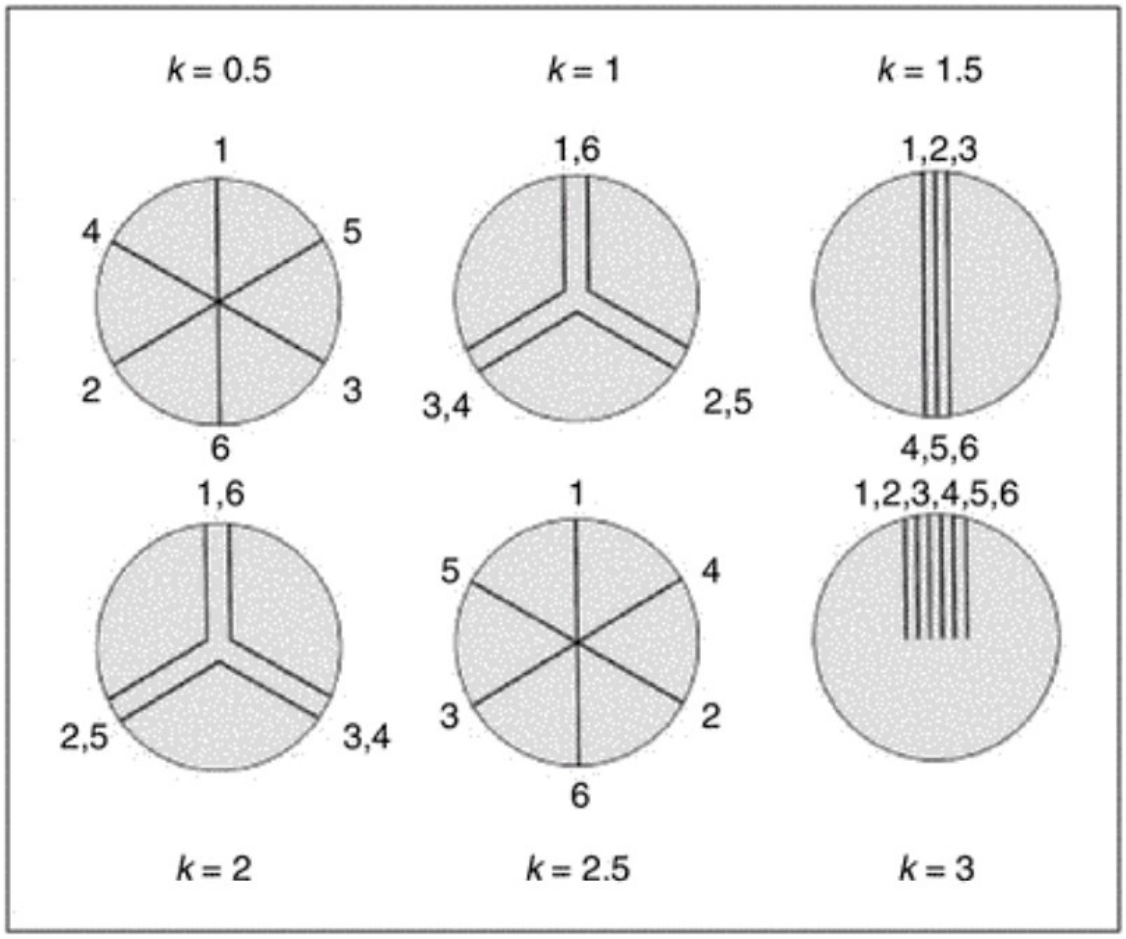


*Figure 11. Phase direction diagrams of the first 6 orders for an inline six-cylinder four-stroke engine. (Van Basshuysen, 2016, p. 76)*

The gas and inertial forces of a multi-cylinder engine do not act on the centre of gravity of the engine. Therefore, the forces may cause imbalanced or internal torques, which in turn excite vibrations in the engine structure. For example, the internal torques cause bending moments in the crankshaft, which affect the main bearings and the crankcase (Figure 12). (Van Basshuysen, 2016, pp. 63-64, p. 70)

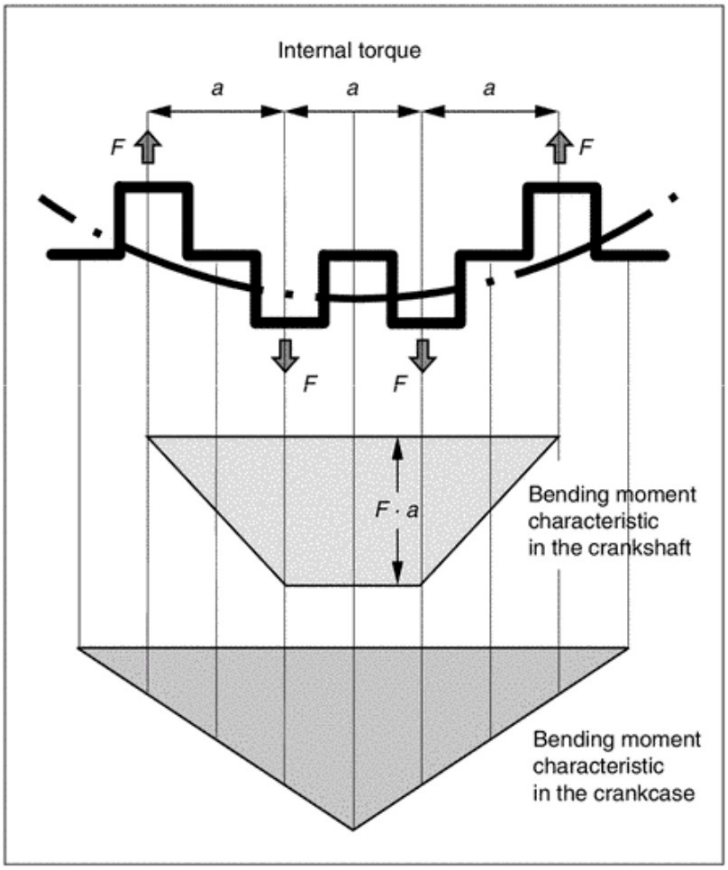


*Figure 12. Bending moments caused by internal torque (Van Basshuysen, 2016, p. 70)*

## 2.2 Vibration analysis

Condition-based maintenance (CBM), or predictive maintenance (PM), is a maintenance strategy for a wide range of industrial machinery that has gained increasing popularity during the last decades. Compared to traditional maintenance strategies, such as performing maintenance after failure or following a scheduled maintenance plan, CBM has proven to be more cost efficient and to improve safe operation. On the other hand, it requires reliable condition monitoring (CM) methods for staying up to date with the current state and more importantly to give accurate estimates of the remaining useful life of the machinery. (Randall, 2011, pp. 1-3)

While operating, most machines vibrate, and certain types of machines usually have characteristic vibrational behaviour of its own kind. A change in the vibrational behaviour may indicate a fault in the machine. Vibration analysis is a CM method based on detecting changes in a certain feature or features of the vibrational behaviour that are known to point out developing faults or other irregularities in a machine. Vibration analysis techniques enable real-time monitoring of machines and the identification of faults in individual parts of a machine. Due to its wide applicability, fast response and accuracy, it is the most-used CM method. (Randall, 2011, pp. 3-6)

Possible sources of vibration in a machine are numerous and are dependent on the type of machine. Monitored vibrations may originate from periodically repeating events in the machine's operation, such as rotations of shafts or meshing of gear teeth, as well as from irregular events caused, for example, by flowing fluids. ICEs have a particular vibrational behaviour that is not perfectly periodic due to the crank gear mechanism and the fluctuating gas forces, both during and between engine cycles, as explained in the previous chapter. (Randall, 2011, pp. 3-4, p. 56)

The monitored vibrations can be classified as translational or torsional, and the translational vibrations can be further classified as absolute or relational. Relational vibrations are commonly measured between a shaft and bearing housing. Monitoring of the torsional vibration of crankshafts is common in ICE applications. It can be used, for example, for monitoring misfiring in cylinders. However, the vibration data used in this study was measured from different parts on the outer surfaces of the genset; that is the data can be classified as absolute translational vibration data. (Randall, 2011, p. 4, p. 60)

Translational vibrations in CM applications are usually measured using piezoelectric accelerometers, mainly due to their ability to measure vibration in wide ranges of frequency and amplitude. They take advantage of the property of piezoelectric materials to generate a strain-related electric charge. The piezoelectric elements of an accelerometer act as a spring between the base of the accelerometer and a mass inside the accelerometer. When attached to the measured object, the base of the accelerometer follows the motion of the object. If the motion is accelerated, the inertial forces of the mass inside the accelerometer cause strain in the piezoelectric elements, which in turn generate electric charge proportional to the acceleration. The vibrations are finally measured as a varying voltage in which the electric charge is converted to avoid the undesired effect of the

impedance in the electric circuit of the measurement set-up on the signal by means of a charge amplifier. (Randall, 2011, p. 4, pp. 13-17)

An important downside of utilizing accelerometers in CM applications is their high cost. Therefore, only the most critical machinery, or parts of a machine, are monitored continuously. Since, in most cases, the ability to predict the need of maintenance well in advance creates the greatest economic advantage of CM, it is often enough to monitor a machine only at certain intervals. Hence, the same measurement equipment, including accelerometers, can be used in the CM of various machines. (Randall, 2011, p. 4, pp. 6-8)

The mere acquisition of the vibration signal is usually not enough for CM purposes. In most cases, the signal needs processing before obtaining the information it carries in a useful form. The usage of digital signal processing methods requires the conversion of the continuous time signal into discrete form. This is done by taking samples of the continuous time signal at a constant time interval, called the *sampling period*, or in other words at a constant *sampling frequency*. (Oppenheim, 1997, p. 516, p. 534)

Choosing the appropriate sampling frequency for sampling a periodic signal depends on the highest frequency of interest. The Sampling Theorem states that any periodic signal of which the Fourier series has only zero-valued coefficients after a certain limit frequency, that is a frequency band-limited signal, can be uniquely defined by samples taken at a sampling frequency higher than the so-called Nyquist frequency. The Nyquist frequency is related to the limit frequency of the periodic signal being one half of the limit frequency. (Oppenheim, 1997, pp. 516-520) In (Randall, 2011, p. 72), the Nyquist frequency is defined as one-half of the sampling frequency.

Applicable signal processing methods for a given vibration signal depend on the type of the signal. However, some methods in time-domain, such as the signal energy and signal power, are applicable to all types of signals, independent of what physical phenomena the signal represents. Signal energy for a discrete time signal $s(n)$ over an interval $[n_0, n_N]$ is expressed in Equation 2. (Oppenheim, 1997, pp. 5-7)

$$E = \sum_{n=n_0}^{n_N} |s(n)|^2 \quad (2)$$

The average signal power for a discrete time signal is calculated by dividing the signal energy by the number of points in the interval $[t_0, t_n]$ (Oppenheim, 1997, p. 6). It can be

remarked that if the signal has zero mean, the signal power equals variance, and that acceleration vibration signals of stationary machinery should have a zero or close to zero mean. Nonzero-mean acceleration implies that the machinery has changed its location permanently during the measurement. However, a small direct current component is typically introduced to the signal during the signal acquisition process, which causes the signal to be a nonzero mean. Therefore, the mean value of a sequence of measured vibration signal can be subtracted from the values of the signal sequence before further processing it. (Lyons, 2011, pp. 761-762)

As already mentioned in Chapter 2.1, a periodic series can be expressed as a sum of harmonic sinusoidal components by the Fourier series. The Fourier series is closely related to the Fourier transform, by which the frequency domain representation of a time domain series, or signal is obtained. The Fourier transform can be applied to both periodic and aperiodic signals, as well as continuous time and discrete time signals. As the signals processed as part of this study are discrete time signals of finite duration, the Fourier analysis is explained briefly only on that behalf. Fourier analysis methods are thoroughly explained theoretically in, for example, (Oppenheim, 1997).

The frequency domain representation, or frequency spectrum, of a discrete time signal of finite duration can be obtained by the discrete Fourier transform (DFT) presented in equation (3). The DFT is also discrete and of finite length. The time domain representation of the signal can be retrieved by the inverse DFT (IDFT) presented in equation (4). (Randall, 2011, pp. 71-73)

$$S(k) = \frac{1}{N}\sum_{n=0}^{N-1} s(n)e^{\frac{-i2\pi kn}{N}} \tag{3}$$

$$s(n) = \sum_{k=0}^{N-1} S(k)e^{\frac{i2\pi kn}{N}} \tag{4}$$

where N is the number of samples in the signal.

The DFT and the IDFT are usually solved using computationally efficient algorithms called the fast Fourier transform (FFT) and the inverse FTT (IFFT), respectively. The computational complexity of the FFT and IFFT algorithms is $2Nlog_2N$, where N is the number of samples in the signal. (Randall, 2011, pp. 71-73)

In equation (4), the DFT is presented in the "forward normalised" form in which it is scaled by the length of the signal. As can be seen from equations (3) and (4), the

representations of the signal have equal length in time and frequency domains. The frequency range of the DFT is double-sided: that is, it has an equal amount of both positive and negative frequency terms, ranging incrementally between negative one-half of the sampling frequency to positive one-half of the sampling frequency. Hence, the size of the frequency increment, that is the sampling resolution, is the sampling frequency divided by the number of samples in the signal. (National Instruments Inc., 2020)

The DFT is complex valued: that is, it carries the information about the amplitude and phase of the signal. Therefore, taking the magnitude of the DFT at each frequency gives the amplitude spectrum of the signal. For a real valued signal, the amplitude spectrum is always symmetric with respect to zero frequency. Hence, the double-sided format of the amplitude spectrum can be converted to a one-sided format by doubling all the amplitude values on the positive side of the spectrum, except for the last and discarding the negative side. A one-sided amplitude spectrum of a vibration acceleration signal gives the amplitudes of the vibration acceleration at different frequencies. (National Instruments Inc., 2020)

The International Organization for Standardization (ISO) has provided a procedure for measuring and evaluation of external mechanical vibration behaviour of generating sets (ISO, 1995). The standard presents primarily root mean square (RMS) velocity as the unit for the evaluation, although the RMS acceleration and RMS displacement are also accepted. The definition of RMS velocity in time domain over an interval $[t_1, t_2]$ is presented in equation (5) and in frequency domain in equation (6). (ISO, 1995, pp. 1-2)

$$v_{rms} = \sqrt{\frac{\int_{t_1}^{t_2} v^2 dt}{t_2 - t_1}} \tag{5}$$

$$v_{rms} = \sqrt{\frac{\sum_{i=1}^{n} \hat{v}_i}{2}} \tag{6}$$

where $\hat{v}_i$ are the vibration velocities at angular frequencies $\omega_i$.

Velocity is the integral over time of acceleration. The acceleration signal can be converted to velocity signal by integration in time domain or by the accumulation property of Fourier transform, presented in equation (7), in frequency domain (Oppenheim, 1997, p. 375 - 376). The latter method is referred to as Omega Arithmetics (Jablonski, 2021, p.142, pp.201 - 202).

$$\mathcal{F}\left(\sum_{k=-\infty}^{n} s[k]\right) = \frac{1}{1-e^{-i\omega}} S\left(e^{j\omega}\right) + \pi S\left(e^{i0}\right) \sum_{k=-\infty}^{+\infty} \delta(\omega - 2\pi k) \quad (7)$$

The right summation term in equation (7) equals zero for zero-mean signals (Oppenheim, 1997, p. 376). Therefore, the velocity amplitude spectrum is obtained from the acceleration amplitude spectrum by multiplying the acceleration at each frequency component by 1/ω, that is 1/(2πf). Hence, the low frequency components of acceleration have a notably higher impact on the total vibration velocity than the high frequency components for an evenly distributed acceleration spectrum. After the multiplication, the RMS velocity can then be calculated, either in frequency domain by equation (6) or in time domain by first applying IDFT on the velocity spectrum and taking the RMS of the inverse transform. (Jablonski, 2021, p.142, pp.201-202)

## 2.3 Supervised Classification in Machine Learning

Classification and regression are the two most common problem types considering supervised learning. The objective of supervised classification is to classify: that is, predict the correct class of a new sample of data into a class of a predefined set of classes. If the classification is done between two different classes it is called binary classification, and in the case of three or more classes, the term multiclass classification is used. In supervised regression, the aim is to predict a continuous number instead of a class as in classification. (Müller, 2016, pp. 25-26)

A supervised classification model is built, or fitted, based on a set of data called the training set or training data. The data in the training set contains an array of samples. Each sample has a set of values of the properties, that is the features, used in the training of the classification model. In supervised classification, a sample also carries information about the class it belongs to, that is the class label. Therefore, the relation between the features and the different classes are known. The term generalisation is used to describe the ability of a classification model to predict the correct class of data carrying new, unseen values of the same features as the training data had. Simply put, an accurate classification model generalises well to new, unseen data. (Müller, 2016, p. 4, p. 26)

In order to evaluate a classification model, the set of data available before training can be divided into two subsets, of which one is used for training the model and the other for testing the model after it has been fitted. The part of the data left out from training the

model is called the test set or the test data. A simple metrics for evaluating a classification model is its accuracy. The accuracy is the ratio of the test samples classified into the correct class to the total number of samples in the test set. (Müller, 2016, p. 17, p. 22)

A more reliable estimate of how well a model generalises is achieved by cross-validation than by splitting the available data into training and test sets only once. Cross-validation is done by splitting the available data into a chosen number of equally sized sets called folds. For example, if the available data is split into five folds, the following procedure is called five-fold cross-validation. The training and testing of a model are repeated until all folds have been used exactly once as the test set, while the others form the training set. Hence, the number of folds equals the number of repetitions of training and testing a model, and therefore also the number of values for model accuracy. It is common to use the mean of the cross-validation accuracies for estimating the accuracy of a model built based on the available data. The reliability of the estimate of how well a model generalises can be enhanced by using stratified cross-validation. Cross-validation is stratified if the relation of samples per class in the available data is maintained in the folds. (Müller, 2016, pp. 252-256)

The amount and variety of the data available for training and testing a classification model determines how complex and well generalising a model can be built. The complexity of a model describes the amount of different relations between the features it describes. Using a small set of data with a high variance for training a complex model easily leads to an overfitting model. Hence, the model accurately predicts using only the data that was available before training but does not generalise well to new data. By including more samples of data with high variation to the dataset, the coverage of the feature space is increased, and therefore a more complex model can be trained without overfitting it. If a model is too simple, where it does not describe the relevant relations between the features well enough, it is called underfitting. (Müller, 2016, pp. 27-29)

Various algorithms for building a supervised classification model have been developed. The five different algorithms used in this study are briefly presented in this chapter. All five are among the most popular, and one of them, called the K-Nearest Neighbours (KNN), is also the simplest. It basically needs no training because the model is fitted by merely storing the training data. Predicting is done by finding a predefined integer number of nearest datapoints in the training data to the sample being classified. The predefined

integer number is given to the algorithm before the model is fitted into the form of an input parameter, referred to as k. The predicted class of the sample being classified is the class with the greatest representation within the set of the k nearest points to the sample. The complexity of the model trained using the KNN algorithm depends on the value of the parameter k. A lower value of k results in a more complex model, because it increases the amount of different definitions for a class. (Müller, 2016, pp. 35-38)

Logistic regression and linear support vector machines are the two most common linear classification algorithms. When used for binary classification, the linear classification algorithms are based on the following decision function, which forms a linear separator, a hyperplane, between the two classes: (Müller, 2016, p. 45, p. 56)

$$\hat{y} = b + \sum_{i=0}^{p} w_i x_i > 0 \quad (8)$$

where $\hat{y}$ is the prediction

b is the intercept

$w_i$ are the individual weights for the features

$x_i$ are the values of different features of a sample.

The greater-than sign in equation (8) should be interpreted as a comparison operator. That is, the predicted class of a sample depends on the sign of the value of $\hat{y}$. How the individual weights for the features are calculated is what makes the linear classification algorithms different from each other. Model complexity is controlled using regularisation of the weight factors. High regularisation forces the weights closer to zero and therefore decreases the complexity of the model. Training and predicting with linear models are generally fast, and they can be used for very large datasets. (Müller, 2016, p. 5, p. 56, p. 67)

The family of naïve Bayes classifier algorithms offers an even faster option for classifier training than the linear classifier algorithms. The faster training is due to the Naïve Bayes algorithms ignoring the possible relations between different features. However, for the same reason, the naïve Bayes classification models tend to be less accurate than the linear classification models. The Gaussian naïve Bayes (GNB) algorithm accepts continuous data for training a classification model. Training a GNB model is done by calculating the average and standard deviation of the feature values of each feature for each class. GNB

is usually used for data with a very high number of different features. (Müller, 2016, pp. 68-70)

The kernelized support vector machines (SVMs) are an extension to the linear classification algorithms. They offer an option to build more complex models than the linear classification algorithms by allowing nonlinearity into the definition of the separators formed between classes. For example, if the radial base function (RBF) is used as the kernel function, the distance between two data points $x_1$ and $x_2$ is calculated using function (9). (Müller, 2016, pp. 92-98)

$$k_{rbf}(x_1,x_2) = e^{-\gamma\|x_1-x_2\|^2} \quad (9)$$

where $\gamma > 0$ (gamma), is used to control the size of the kernel

$\|x_1 - x_2\|$ is the Euclidean distance between the points $x_1$ and $x_2$

The distance is calculated between the data point being classified and all the support vectors defined during the training. The closest support vectors to the data point being classified define the predicted class. The definition of the support vectors assumes that only the datapoints that are close to the hyperplane which separates the different classes are meaningful for the classification purposes. Therefore, the points close to the hyperplane are chosen as the support vectors. (Müller, 2016, pp. 97-98)

If the RBF kernel is used, the complexity of the SVM model can be adjusted by regulating the effect of the support vectors to the classification and by varying the value of γ in equation (9), which controls the effect of the distance between the points on the classification results. The regulation of the effect of the support vectors resembles the regulation of the weights of a linear classification model. Therefore, higher regulation leads to simpler models. Decreasing the value of γ, that is increasing the radius of the kernel, results in a simpler model, because support vectors from a larger space influence the classification of a datapoint. (Müller, 2016, pp. 99-100)

SVM models tend to work well on datasets of which features are similar and the feature values are scaled equally. Using large datasets and complex SVM models can lead to long training or predicting times and require a lot of memory. (Müller, 2016, p. 104)

Decision trees represent a different approach for solving the classification problem compared to the algorithms described previously. A model trained by a decision tree

algorithm has a hierarchical tree-like structure. The structure is formed of a series of Boolean questions, which finally lead to the predicted class. (Müller, 2016, pp. 70-71)

Ideally, the sets of data at the lowest level of hierarchy, referred to as the leaves, contain only data that belongs to one class. In that case, the leaves are called pure. However, in practise, if the algorithm trains the tree until all leaves are pure, the model is highly overfitted. The complexity of a decision tree depends on the number of levels of hierarchy in the model or simply put, the depth of the model. Therefore, overfitting can be avoided by restricting the depth of the tree. Also, the size of the leaves affects the complexity of the model trained, using a decision tree algorithm in a similar manner as the parameter k affects the complexity of a classification model trained using the KNN algorithm. In other words, a small leaf size and a large number of leaves lead to more complex models. (Müller, 2016, p. 74)

Novelty detection is a classification method which is used for identifying data from a previously (to training) unknown class. A novelty detection model is trained using data from a known class or known classes. After training, a novelty detector can be used for detecting novel data samples, that is samples of data that do not belong to the same class as the training data, in a set of new data. Various methods for novelty detection have been developed. The applicability of a novelty detection method depends on the properties of the data being processed. Some of them are based on or related to the classification methods presented earlier in this chapter, such as the KNN (Markou, 2003, p. 2490) and SVM algorithms (Markou, 2003, p. 2483). (Markou, 2003, p. 2480)

Novelty detection algorithms called the one-class SVM, which as the name suggests, is based on SVMs, and the local outlier factor (LOF) are used in this study. The term factor in the name of LOF refers to the ability of the algorithm to give a degree of outlierness of a sample. The term local refers to the property of the algorithm to define the value of the factor in relation to a predefined number of samples closest to the sample being evaluated. The LOF is fully described in the publication by Breunig et al. (2000).

## 2.4 Related Work

Bevilacqua et al. (2020), Rasheed et al. (2020) and Tao et al. (2019) extensively reviewed the current state of DTs in the context of risk control and prevention, modelling and industrial applications respectively. All three mention big data analytics (BDA) as one of the key enablers of DTs. The large amount of data generated by a DT during all the different phases of its lifecycle need BDA and AI tools to be processed effectively (Bevilacqua, 2020), (Rasheed, 2020).

Methodology for building a digital twin for condition monitoring purposes of marine drivetrains was discussed by Johansen et al. (2019). The approach proposed by Johansen et al. (2019) is simplified in Figure 13. Vibration analysis of measured and simulated mechanical vibration data is proposed as the condition monitoring method. The importance of measurement point location and sensitivity analysis was mentioned. A ML-based approach is considered in the study, but the verification of the presented methods for building the virtual model is purely simulation based.

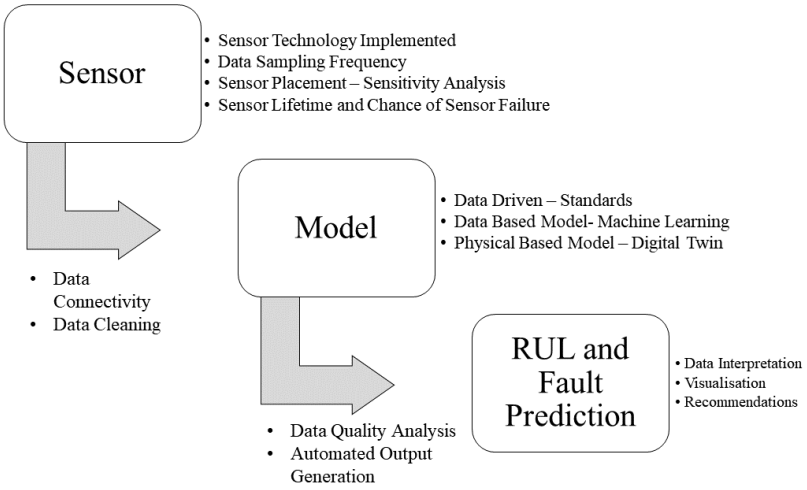


*Figure 13. Digital twin methodology (Johansen, 2019)*

Tiainen et al. (2019) developed a testbench for demonstrating a digital twin concept of a long rotating shaft. In addition to the physical testbench, the proposed concept covered the collection and integration of data from multiple sources, a user interface and a virtual sensor. Deep learning was used to create a virtual sensor for predicting the location of a point on the centreline of the rotor. The virtual sensor used windowed sequences of acceleration or force signals measured from the ends of the shaft as input. A converging

model of the virtual sensor was finally achieved using only the measured force signal. Over 99 % accuracy was reached with the converging model.

Detection of abnormal operation of a genset, using classifier and neural network models, was studied by Palestini et al. (2019). The training of the models was done using features extracted from simulated flywheel rotation speed. Measured cylinder pressure was given as input for the simulation. As well as normal operation conditions, three different fault situations, namely misfire, knocking and overpressure, were simulated. The operation of the genset was simulated at full-power output level only. The best accuracy in the classification between normal and abnormal operation was achieved using the KNN algorithm, that is 97 %. However, the neural network model was more suitable for the identification of the different abnormal operation conditions than the rest.

A few years before the famous Course on PLM, held by Grieves in 2003 (Grieves, 2014), that is the origin of the DT, Nairac et al. (1997) used novelty detection for the recognition of abnormal operation of jet engines. The novelty detection algorithms used in the study were based on SVMs. The features were extracted from measured mechanical vibration signals, that is the vibration amplitudes at different orders. The novelty detection algorithms developed in the study were evaluated using cross-validation with data containing previously known abnormalities.

A few years after, the LOF algorithm was experimented by Breunig et al. (2000) on, for example, finding outstanding football players of the first Bundesliga of Germany based on the statistics of the 1998/99 Bundesliga season. Remarkable players, such as the top goal-scorer of the season, “Der Torschützenkönig” Michael Preetz, and Hans-Jörg Butt, a penalty kick executing goalkeeper, who scored altogether 7 goals during the season, were spotted as outliers with the highest and the third highest LOF of all of the 375 players in the dataset respectively.

The different feature extraction methods developed based on vibration analysis techniques are many. Depending on the problem, the applied feature extraction methods range from simple to very complex, that is from methods in time domain to frequency domain or even time-frequency domain. Examples of common time domain methods are signal power, skewness or kurtosis, while FFT is commonly used for finding out the frequency content of the signal. The frequency content can be further processed into different features using, for example, statistical methods. Short-time Fourier transform,

or wavelets, are some examples of common vibration analysis methods used for the extraction of features from non-stationary or transient signals. (Caesarendra, 2017)

The feature extraction methods used in this study were relatively simple due to the requirement of computational efficiency defined at the beginning of the study. The parts of vibration analysis theory related to the feature extraction methods used in this study were presented previously in Chapter 2.2.

# 3 MATERIALS AND METHODS

This chapter first describes the source of the measured mechanical vibration data used in this study, that is the genset, the data itself, and how the applicable data was identified and sampled into subsets. The data was sampled into subsets regarding the power output level at time of measurement and the type of operation, that is normal or abnormal.

The data sampling was followed by a feature extraction process. The characteristics of ICEs on which the feature extraction was done, and the functions applied to extract the features from the data are explained. Features were extracted by applying five different functions to short sequences of the sampled signals, based on two different characteristics of ICEs introduced later in this chapter.

The sensitivity of the extracted features to changes in power output level of the genset was compared by building various classification models using five different classification algorithms. At the same time, different classification algorithms were compared. Also, the effect of the measurement point location to the classification accuracy was studied. A combination of two features extracted from one measurement point was found for building an accurate and fast-performing classification model using the SVM algorithm.

Finally, the applicability of two different algorithms was studied for detecting abnormal operation from the data sampled into the subsets of abnormal operation. Both were found applicable with small differences in accuracy and larger differences in performance.

The data sampling was done using MathWorks Matlab R2020a software and tools from the Python libraries NumPy, Pandas and MatPlotLib. The functions used in feature extraction were written in Python programming language using tools found in the NumPy library. All pre-processing, classification and novelty detection algorithms used in this study were included in the open-source ML library called scikit-learn, version 0.24.1.

The training and testing of the classification models of this study were principally done on a high-performance laptop with 128 GB of memory and an Intel® Xeon® W-10885M processor with eight cores running Windows 10 operating system and Python version 3.8.5. A server with 1.5 TB of memory and two processors Intel® Xeon® Gold 6246 with 24 cores each, running Windows Server 2016 operating system and Python version 3.7.10 was used in the second, the third and the fourth rounds of training and testing of the classification models with the high-performance laptop. The training and testing of the

novelty detection models were done on the high-performance laptop alone, as well as the definition of all training and predicting times of different algorithms presented in this study.

## 3.1 Studied genset

The studied genset is based on a Wärtsilä 20V31SG four-stroke internal combustion engine (Wärtsilä, 2021); a 20-cylinder V-engine with a cylinder bore size of 31 cm and gas used as fuel. The engine and the generator are mounted on a common base frame. The base frame is a steel structure made of steel plates welded together. The coupling between the engine crankshaft and the generator rotor is flexible. The flexible coupling restricts the transmission of torsional vibrations from the engine crankshaft to the generator rotor. To isolate the genset vibrationally from its surroundings, the base frame is resiliently mounted to the ground by spring mounts.

The rotation speed of the studied genset is 750 rpm, and the rated electrical power is approximately 12 MW. The maximum transportation dimensions (length, width and height) and weight of a Wärtsilä 20V31SG genset are 14 412, 3 893, and 5 090 mm, and 182 000 kg. A Wärtsilä 20V31SG genset is presented in Figure 14.

*Figure 14. W20V31SG genset. Image courtesy of Wärtsilä. ©2021 Wärtsilä Corporation.*

## 3.2 Provided dataset and sampling of the data

The data used in this study was measured between the 19th and 30th of September 2019 during a fault ride through (FRT) and other performance tests of a Wärtsilä 20V31SG genset in Vaasa. No measurements took place on the 18th and 22nd of September. The data consists of a time series of measured mechanical vibration accelerations at 4 different locations on the genset outer surfaces, measured stresses from two locations on the genset outer surfaces and measured rotation speed of the engine. In addition, screenshots of the plant automation system software presenting general performance information, such as engine rotation speed and generator active power output against time, measured during the tests were included in the dataset.

The size of the dataset is 28.8 gigabytes. It includes 47 hours, 26 minutes and 7 seconds of measured data. The vibration accelerations were measured at a sampling rate of 2 048 Hz. The vibration accelerations were measured using triaxial accelerometers at four different locations on the studied genset. That is nearly 350 million individual observations in the time of each of the 12 different measurement variables. The measured rotation speed of the genset included in the dataset was stored both at the original high sampling rate (a function of the rotation speed itself) as well as at a down-sampled rate to 1 Hz. The measured stresses were measured at the same sampling rate as the accelerations. The measured stresses were not considered in this study.

The measured acceleration data is divided into 118 files of different sizes, containing at most one hour of measured data. The measurement schedule according to the first and the last time stamps of each file is presented in Figure 15. Adjacent files are separated from each other by colour in Figure 15.

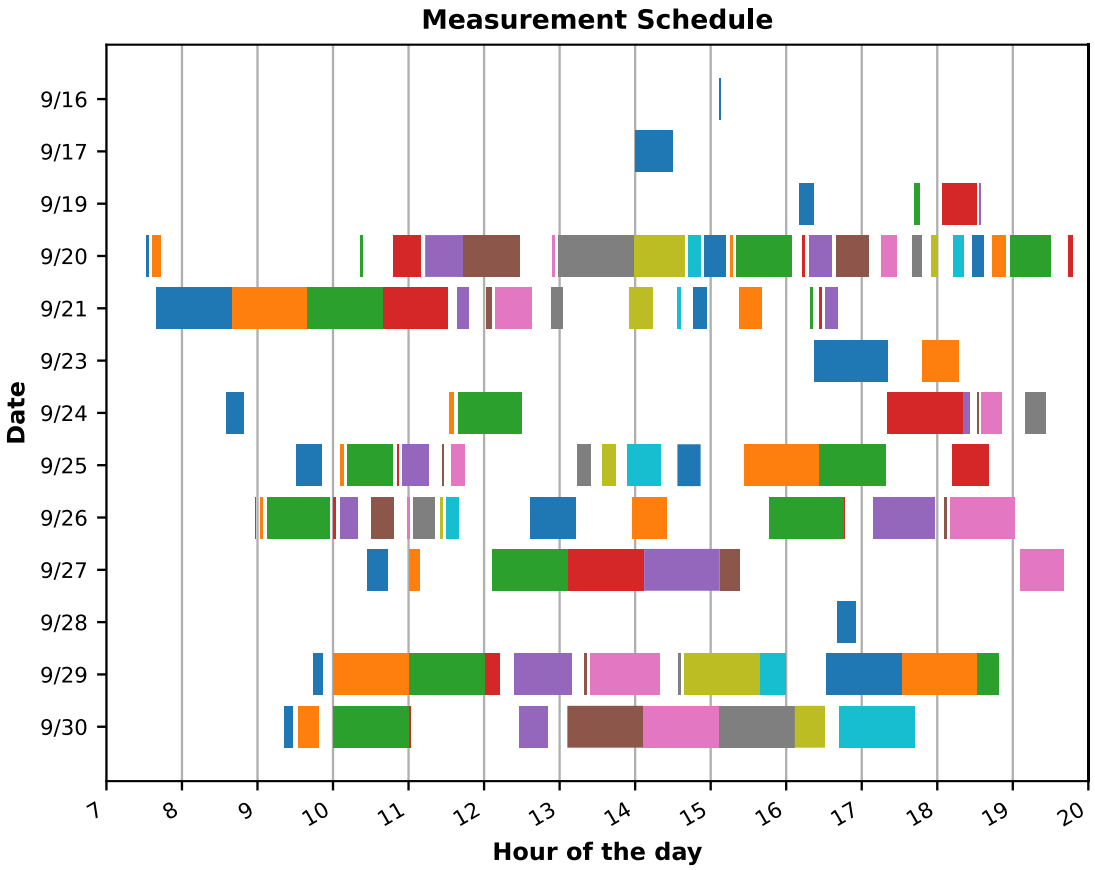


*Figure 15. Measurement schedule according to the first and the last time stamp of each file.*

### 3.2.1 Test runs

The purpose of the FRT and performance tests was to study the operation of the genset during abnormal operation conditions, such as sudden voltage changes in the electrical grid. However, since the studied abnormal phenomena are transient, and their frequency of occurrence during the tests was relatively low, most of the measured data consists of normal operation. As an example of a typical test run, a screenshot of the plant automation system software containing graphs of a five-hour-long test session is presented in Figure 16.


*Figure 16. Screenshot of plant automation system software containing information on a five-hour-long test run.*

From the engine rotation curve (black graph in Figure 16), it can be seen that there have been three start-ups and shutdowns, the test runs, during the test session. The generator active power output curve (green graph in Figure 16) shows that the second half of the first run has been run on full power output and that there are two peaks in the curve during that time. Similar peaks can be seen in the generator active power output curve during the second run; two peaks take place during the first half of the run at half power output and another two during the second half of the run at full power output. The spikes are due to abnormal operation of the genset.

During the tests, the genset was run at different constant power output levels. Figure 16 shows that during the test session in question, the genset was run at 0 %, 50 % and 100 % constant power output levels of full power output. The other constant power output levels, at which the genset was run significant amounts of time during the tests, were as follows: 75 %, 90 % and 95 % of full power output. The genset was run through faults while running at all aforementioned levels of power output except for 0 % power output.

### 3.2.2 Data sampling

The first of the three tasks defined at the beginning of this study was to identify and sample data that represents different operational states of the genset into labelled datasets from the provided dataset. The measured mechanical acceleration data was, therefore, inspected and sampled into subsets of normal operation at different power output levels and subsets of abnormal operation at different power output levels of the genset. The time intervals of constant operation at different power levels were identified from the power output graphs presented in the screenshots of the plant automation system software. The timings of abnormal operation were first estimated roughly from the peaks in the power output curves; thereafter, the timings were estimated more precisely from the engine rotation speed data. An engine rotation speed curve before, during and after the assumed abnormal operation is presented in Figure 17.

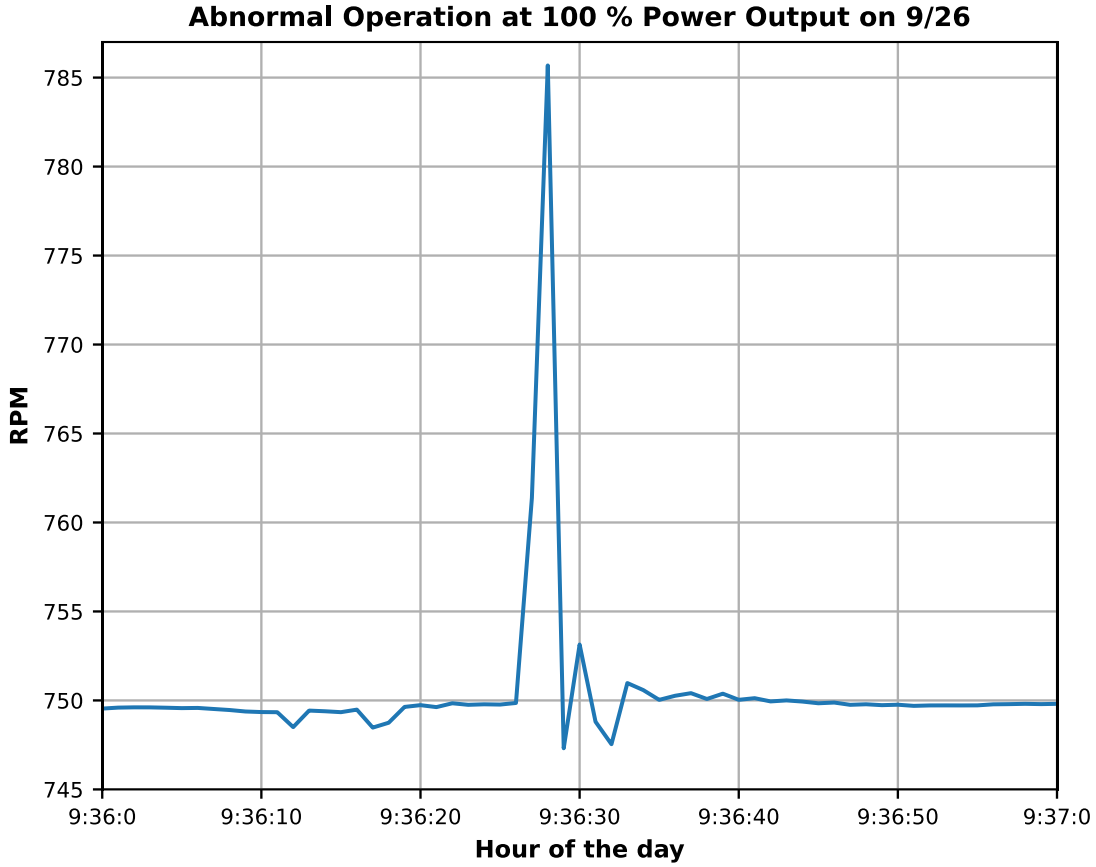


*Figure 17. Engine rotation speed curve during assumed abnormal operation.*

The subsets of abnormal operation are all one minute in length. The intention was to include measured data acquired before, during and after a fault at a specific power output

level. The data for the subsets of abnormal operation was sampled starting approximately half a minute before the largest peak in the rpm curve to ensure data acquired during normal operation is included in the subset as described.

The lengths of the samples of normal operation vary according to the lengths of the test run, and the file containing the data, as well as the occurrence of changes in power output level, or abnormal operation during the test runs. When found, continuous periods of normal operation signal longer than ten minutes were split into subsets shorter than ten minutes due to the feature extraction method explained in Chapter 3.3. A subset of normal operation includes data acquired while the genset has been running at only one constant power output level.

The sampled subsets of signals acquired during normal operation were labelled and divided into six groups by different power output levels: 100 %, 95 %, 90 %, 75 %, 50 % and 0 % of the full power output of the genset. All subsets include twelve zero-mean made and equally spaced (in time) signals of equal length of the twelve different measurement variables; that is, the accelerations are measured from 4 different locations on the genset in 3 orthogonal directions. For convenience, the groups of subsets are hereafter called by their percentage value of the full power output, i.e., 100 % group, 95 % group … 0 % group, and likewise the measurement variables are called hereafter by the measurement point number and direction, i.e., P1X, P1Y … P4Z.

Recommended points of vibration measurement in gensets presented in Figure 18 have been given in the standard (ISO, 1995, p. 3). The measurement points and their numbers used in this study correspond best to the points and point numbers in Figure 18 as follows: P1 = 2, P2 = 8, P3 = 5 and P4 = 7. The coordinate system used in this study corresponds with the one presented in Figure 18.

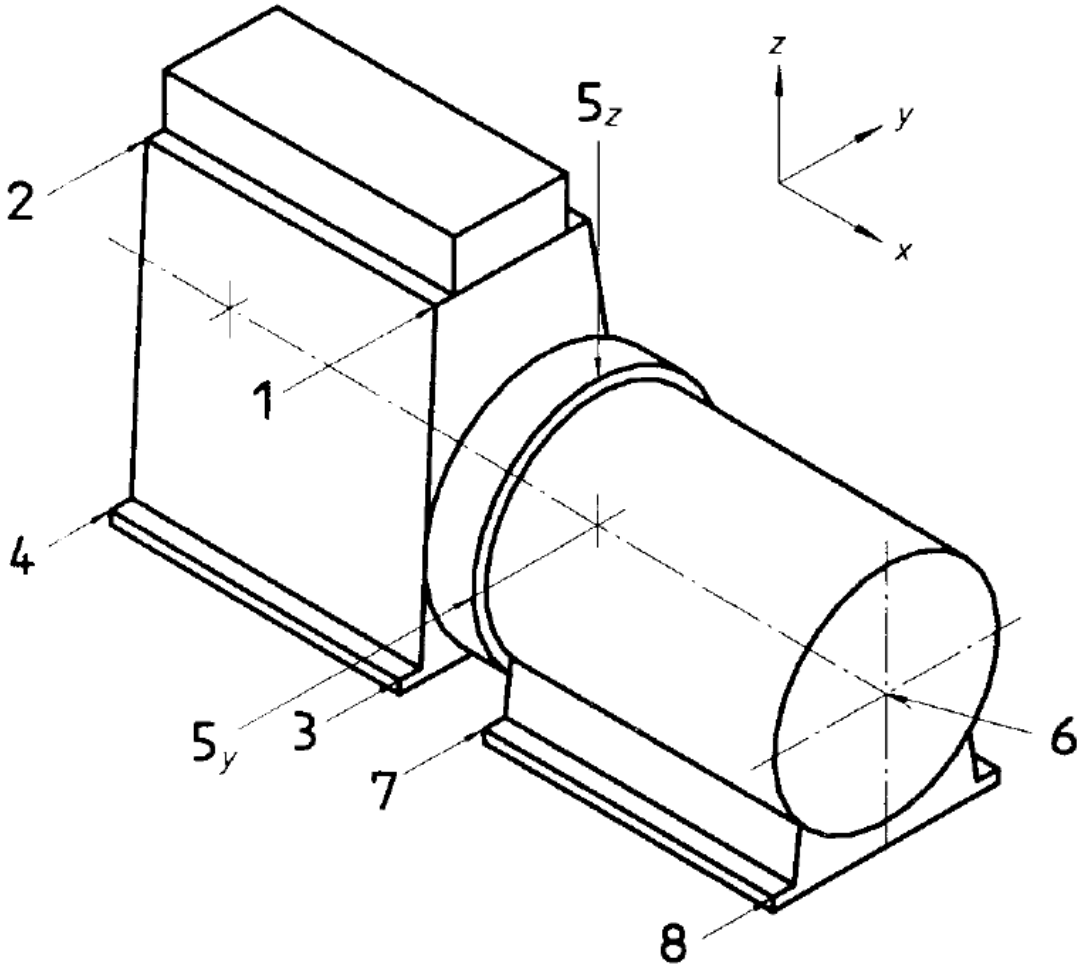


*Figure 18. Recommended points for vibration measurement in genset (ISO, 1995, p. 3)*

The sampled subsets were statistically analysed by comparing the variances of the signals. Since the signals have zero mean, the variance equals average signal power. First, the signals of all the subsets belonging to a group were concatenated into twelve signals, and variances of all the twelve concatenated signals were calculated to form the total signal variances of each group. Then, the total signal variances of each group were normalised by the total signal variances of the 100 % group, and the normalised total signal variances of each group were compared with each other. Finally, the variances of the signals in each subset of normal and abnormal operation were calculated and normalised by the total signal variances of the corresponding group. The signal variances of each subset of normal operation were group-wise compared with each other as well as the signal variances of abnormal operation.

## 3.3 Feature extraction

It was foreseen that reaching the objective of this study, computationally light features that are sensitive to the changes in the operational state of the genset needed to be extracted from the sampled datasets. The feature extraction was based on two characteristics of the operation of an ICE presented in Chapter 2.1:

1. The operation of the genset at constant operation speed can be treated as periodic and analysed using suitable signal processing methods to achieve accurate results, although fluctuations between engine cycles are constant.
2. The mechanical vibrations of a genset, based on an ICE result, are mainly from the gas and inertia forces of the ICE. The amplitude of the gas forces increases as the engine load, that is the power output of the engine, increases. It is also universally known that force is relational to acceleration; therefore, the level of mechanical vibrations of an ICE at constant operating speed is higher at a higher level of power output at constant operation speed.

The first of the above-mentioned characteristics was considered in the feature extraction process by calculating the values of each feature, by applying different functions to sequences of the sampled signals equalling the length of the duration of an engine cycle or its integer multiples. Before applying the different functions to a sequence of a sampled signal, the sequence of the sampled signal was zero-meaned for the reasons mentioned in chapter 2.2.

The inclusion of the second characteristic in the feature extraction process was done by means of the different functions applied to the sequences of the sampled signals. Five different functions were used to extract five different features from each of the 12 different measured variables. The extracted features and their abbreviations are the following:

1. The average signal power (ACC PWR)
2. The average of the absolute values of the signal (ACC ABS)
3. The velocity RMS using Omega Arithmetics (VEL RMS)
4. The amplitude of acceleration at order number 1.0 using FFT (FTT 1.0)
5. The amplitude of acceleration at order number 1.5 using FFT (FTT 1.5)

The methods for calculating the features have been presented in Chapter 2.2, except for the method for calculating the second feature. The method for calculating the second feature is in its description. Clearly, the first three features correspond with the second characteristic. The values of the first three features get higher values as the vibration levels rise. Squaring the values puts more weight on the higher absolute values of an array. Therefore, the average of the absolute values was chosen as a feature to see if squaring the values has a significant effect on the sensitivity of the feature.

The fourth and the fifth features are individual factors of the third feature, as explained in chapter 2.2. In equation (1) of chapter 2.1, it was shown that the analytical expression of the inertial torque has factors only at orders 1.0, 2.0 and 3.0. If the amplitude of the inertial torque is comparable to the amplitude of the gas torque at order 1.0, the fact that the amplitude of the inertial torque is only dependent of the rotation velocity, i.e., independent of the load level, suggests that the fourth feature might not be sensitive to changes in the power output level. On the other hand, the amplitude of acceleration at order 1.5 is independent of the inertial torque and could, therefore, be more sensitive to changes in the power output level than the velocity RMS.

The normalised velocity amplitudes at orders 0.5 to 6.0, calculated using FFT and Omega Arithmetics from the measured accelerations of the studied genset at 100 % power output for all measurement points in all three orthogonal directions, are presented in Figure 19. It can be seen that the velocity amplitudes at orders 1.0 and 1.5 are the most dominant overall from Figure 19.

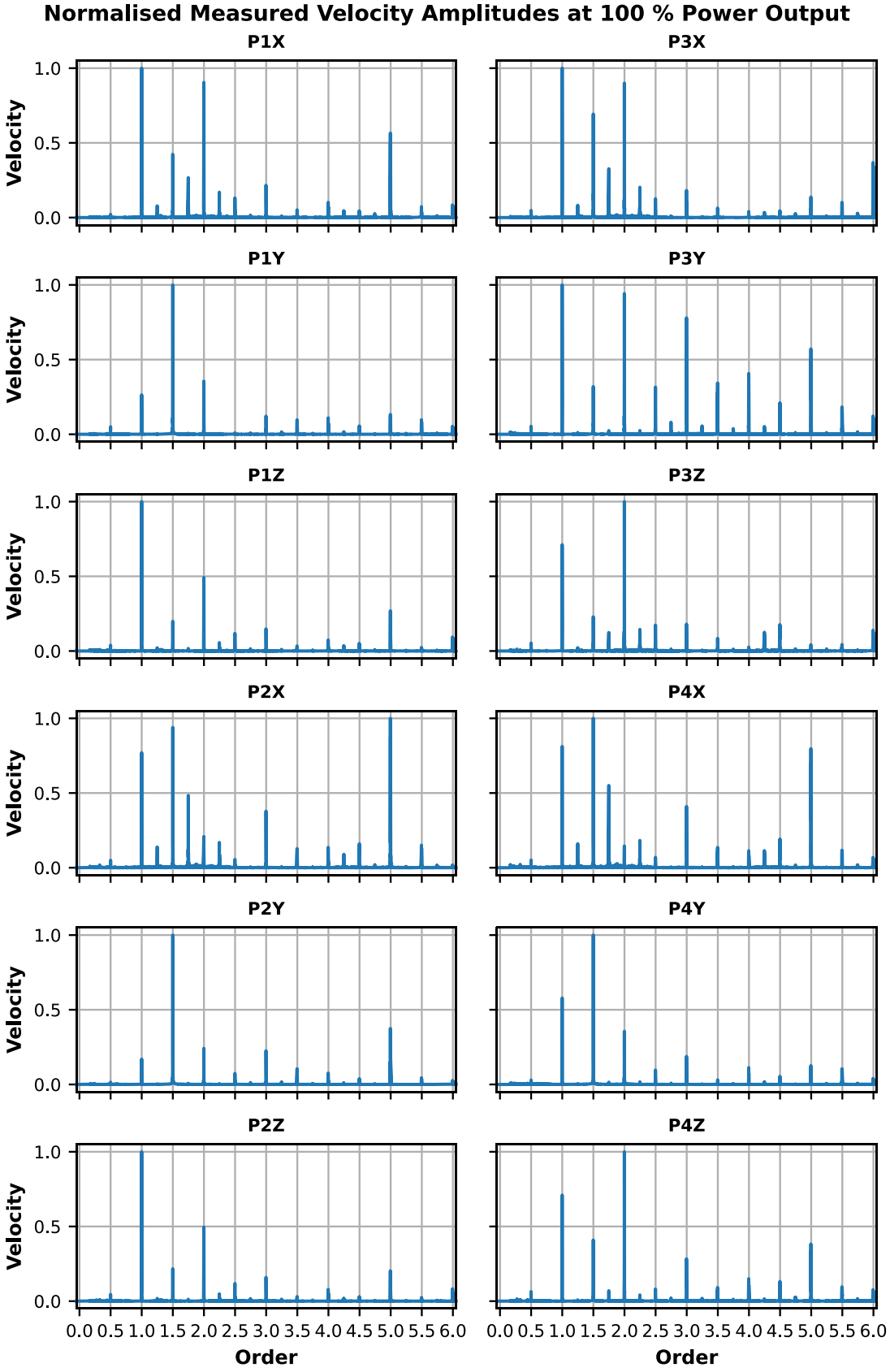


*Figure 19. Normalised measured velocity amplitudes at 100 % power output*

Another goal of this study was to identify the operational state of the genset near real time. Achieving this goal requires the usage of computationally light feature extraction algorithms. Evidently, the shorter the sequence used for calculating the feature values, the faster it is to process, and the closer it is to real time. However, features calculated over longer sequences are probably less sensitive to the irregularities in the mechanical vibrations caused by the fluctuations in the gas forces between engine cycles. Therefore, the feature values were calculated using sequences of different lengths for finding the optimal sequence length in terms of computational cost and classification accuracy. Considering the functions used for calculating the feature values, the computational cost is the lowest for the first two feature values, and for the third it is the highest. The computational cost of the fourth and the fifth feature values is equal at least if FFT is used.

It should be mentioned that by using sequence lengths equalling integer multiples of an engine cycle, the frequencies at different orders are integer multiples of the sampling resolution of the FFT of the sequence. For example, for the sequence of which length is one engine cycle, the frequency resolution equals the frequencies at different orders.

The chronological order of the feature values calculated from the signals sampled to the subsets of abnormal operation was required for the identification of the moment in time of the possibly detected occurrence of abnormal operation. The chronological order was maintained by calculating the feature values using a sliding window technique. The length of the sequence was used as the window size, and to cover all possible sequences of given length in the signal, one was used as the step size.

The chronological order of the feature values of normal operation was redundant for the purposes of this study, and calculating the feature values using the rolling window technique with step size of 1 would have led to an unnecessarily large amount of data for the purposes of this study. Therefore, instead of applying the rolling window technique with a fixed step size for calculating the feature values for normal operation, the feature values were calculated from sequences of the sampled signals with starting points chosen by random selection without duplicates. The same randomly chosen starting points were used for the sequences of different sizes. The number of feature values calculated from a subset of normal operation was proportional to the size of the subset compared to the size of all the subsets combined of the corresponding group of power output level.

## 3.4 Classification and feature selection

To find the best combinations of features and algorithms to build accurate and fast performing classifier and novelty detection models, the feature selection method used in this study was model based. By the chosen approach, both the sensitivity of the extracted features to changes in power output level and the different classifier algorithms were studied simultaneously. Since the training data was divided into six different groups and labelled accordingly, the classification problem type of this study was supervised multiclass classification. The objective of the classification tasks of this study were to predict the correct state of normal operation, that is the power output level of the genset based on the measured mechanical vibration data.

These were the classification algorithms and their abbreviations used in this study: logistic regression (LR), support vector machine using the linear and radial base function kernels (SVM LIN & SVM RBF), decision trees (DT), k-nearest neighbours (KNN) and Gaussian Naïve Bayes (GNB). The applicability of each algorithm for the studied problem was studied by comparing the accuracies of the classifier models. A short introduction to all the classifier algorithms used in this study was given in chapter 2.3.

The selected algorithms efficiently cover the different levels of complexity and different types of algorithms commonly used for supervised classification problems. As mentioned in chapter 2.3, the KNN and GNB algorithms are the simplest of the commonly used algorithms, whereas the linear algorithms LR and SVM LIN are more complex, and the SVM with RBF kernel is the most complex. The decision tree has a different approach to solving the classification problem as explained in chapter 2.3. The accuracy of the classifier is important as always, but also the time it takes to make a prediction has to be considered. The sampling frequency used to measure mechanical vibrations is very high, which makes reaching real-time predictions challenging.

Four rounds of training and testing different classifiers were performed to find out the effects of the size of the dataset, the length of the sequence used in feature extraction, the different features and the measurement point location on the accuracy of the trained classifiers. The results of a preceding round were used in the definition of the following round of training and testing of the classifiers, when applicable.

The classification and pre-processing of the extracted features was done using algorithms included in the scikit-learn ML library. The workflow of the four rounds of classification included pre-processing of the data using the "StandardScaler" algorithm, training and testing the classification models using the different classification algorithms with five-fold stratified cross-validation. The "StandardScaler"-algorithm was used to convert the feature values used for training to zero-mean and unit variance, and to scale the feature values used for testing using the values fitted with the training data.

The default values for the parameters of the classification algorithms defined by scikit-learn were used except for the parameters n_neighbours (the number of neighbours, referred to hereafter as parameter k) of the KNN algorithm and the min_samples_leaf (the minimum number of samples required to be at a leaf node) of the DT algorithm. The values used for the parameters k and min_samples_leaf was defined as the square root of the number of samples per class in the training data.

Values of five different parameters were varied during the rounds of training and testing the classifiers. The different parameter names and the number of different values for each parameter type are presented in Table 1.

*Table 1. Parameter names and number of different values per parameter*

| Parameter Name | Values |
|---|---|
| **Dataset Size** | 7 |
| **Classifier Algorithm** | 6 |
| **Sequence Length Used in Feature Extraction** | 7 |
| **Extracted Feature** | 5 |
| **Measurement Point Location(s)** | 5 |

The seven different dataset sizes used in this study were 100, 500, 1 000, 5 000, 10 000, 50 000 and 100 000 samples per class. The samples were chosen using random selection method without duplicates from the datasets of normal operation data created during the feature extraction process. The contents of the different datasets of normal operation data are described in Chapter 0. The same randomly selected samples were used throughout the four rounds of training and testing the classifiers.

Performing classifier training and testing with all possible combinations of parameter values was not necessary. The main goal of the first round of training and testing the classifiers was to find the impact of the dataset size on the classifier accuracy and decide the dataset size for the following rounds accordingly. Also, the choice between the two

SVM kernels for the remaining rounds was made based on the results of the first round. The first round consisted of 294 different classification tasks formed of the combinations of the six different classifier algorithms, seven sequence lengths and obviously the seven different sizes of datasets. Only the extracted feature was not varied. Hence, all classification tasks of the first round were performed using only the ACC PWR feature extracted from the twelve signals using the seven different sequence lengths.

The sensitivity of the different extracted features to changes in power output level was validated in the second and third rounds of classifier training and testing. The classification tasks of the second and the third round were performed combining the five remaining classifier algorithms, the seven sequence lengths and the five different extracted features. In the classification tasks of the second round, the features extracted from the twelve different measurement variables were included in the same task. Whereas, in the classification tasks of the third round, they were divided according to the measurement points into four different tasks; that is the effect of measurement point location was studied. Hence, the five different values of parameter measurement point locations referred to in Table 1 are the measurement points combined (All) and separately (P1, P2, P3 and P4).

The best combination of two different extracted features from a single measurement point was sought after in the fourth round of classifier training and testing. Not all possible combinations of two features were studied, but only two different combinations were selected based on the results of the third round. The classification tasks of the fourth round were performed combining the five remaining classifier algorithms, the seven sequence lengths and the two chosen combinations separately for each measurement point. After the fourth round, the parameters of the best performing classifier algorithm were tuned, and a final round of classifier training and testing was performed using the most suitable parameter values. In the last round, the classifier training and testing times were also studied.

The flow diagram presented in Figure 20 represents the parameter values used in each of the four rounds of classifier training and testing. In the flow diagram, the parameter values studied separately are divided by a vertical bar, and the combined parameter values studied are inside brackets and divided by a comma.

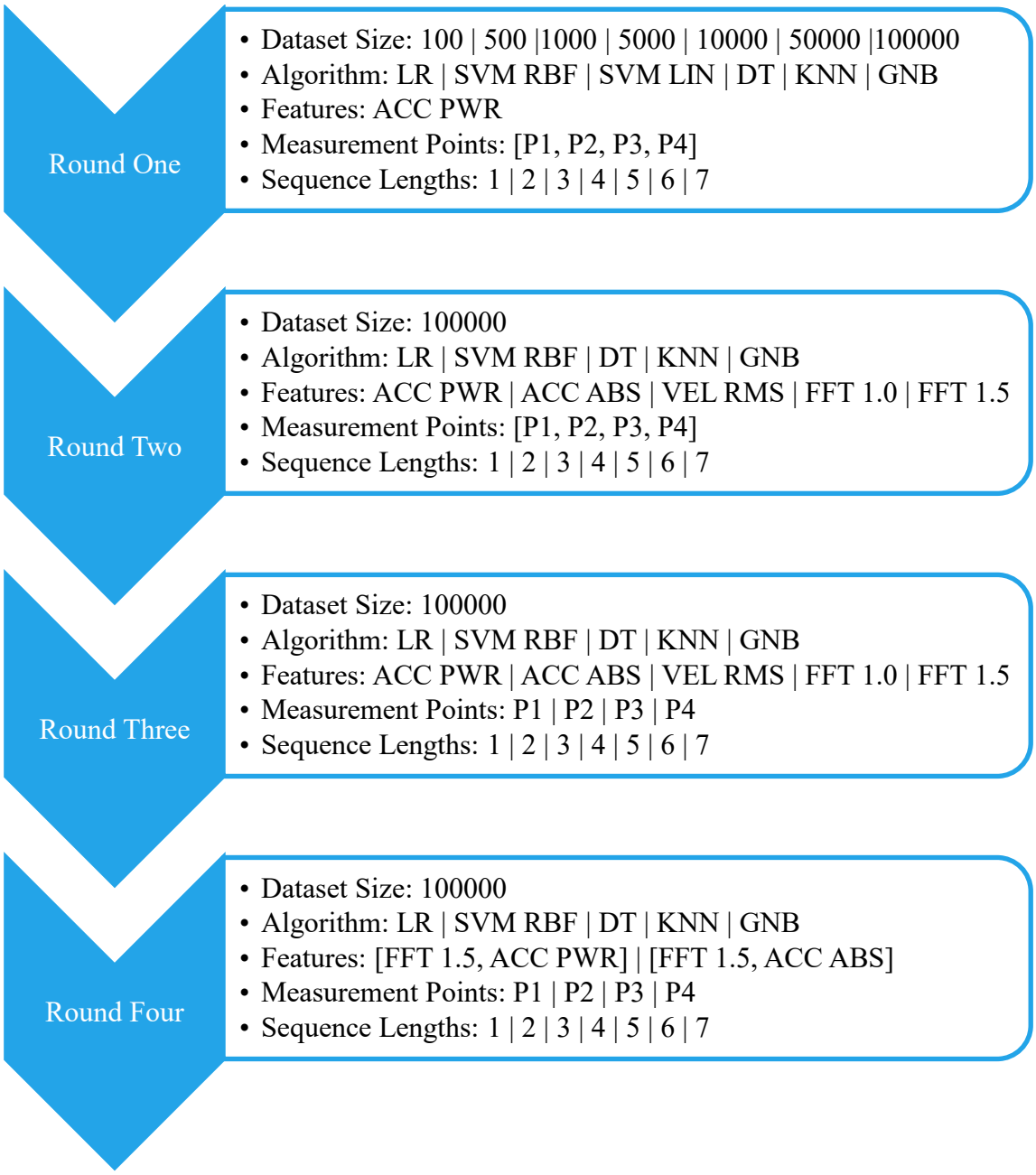


*Figure 20. Parameter values used in the four rounds of classifier training and testing*

## 3.5 Novelty detection

The detection of abnormal operation of the genset was done using the novelty detection method. As mentioned in Chapter 2.3, data from only one class is used for training novelty detection models. In this study the normal operation data was used as the training data and afterwards for the validation of the trained novelty detection models. After validation the novelty detector models were run against the data sampled in the subsets of abnormal operation data.

When the abnormal operation data was sampled, the intention was to include some amount of both normal and abnormal operation data into the sampled subsets of abnormal operation data. Hence, the data in the subsets of abnormal operation was not labelled. It must be considered that the genset was tested against different fault situations at different levels of power output. The duration and severity of the fault situations was not exactly known. Hence, even if abnormal operation data was included in the training datasets the relation of normal and abnormal operation data in the sampled datasets is unknown and probably varies significantly between the subsets of abnormal operation data.

Two different novelty detector algorithms in Scikit-learn called the One-class SVM and the LOF were used for building the novelty detectors for this study. The normal operation data used previously for training the classifiers of normal operation was used for training the novelty detectors. However, normal operation data was divided into six different classes. Therefore, six different novelty detectors had to be trained using both algorithms, that is one for each group of power output level. The features used for training the novelty detectors were chosen based on the results of the preceding classification and model-based feature selection step.

The maximum proportion of abnormal data in the training data should be known when using the One-class SVM algorithm. The LOF algorithm assumes that there is some amount of abnormal data in the training data. One could say, that since the training data originates from normal operation, it therefore contains no abnormal operation data. Hence, the One-class SVM and LOF algorithms would not be applicable for the purposes of this study. However, a relatively small proportion of the normal data can be defined as abnormal and used later as a threshold value for detecting abnormal operation from a series of continuous predictions; that is, a proportion of the continuous predictions greater

than the threshold value has to be classified as novel for the operation to be classified abnormal.

The threshold values for both algorithms are related to the input parameters of the algorithms, and they were therefore defined by a parameter sweep. The upper limit for the proportion of abnormal data in the training data is given to the One-class SVM algorithm as a parameter called ν. At the same time, the parameter ν acts as a lower limit for the fraction of support vectors. Hence, the lower the value of parameter ν, the faster the training of the novelty detector, and more importantly, considering the objective of this study, the prediction with the trained novelty detector. Therefore, a parameter sweep was performed to find a suitable value for the parameter ν with preference for lower values. Novelty detectors were trained separately for each of the six groups of power output level, varying the value of the parameter ν. The tested values for the parameter ν were 0.00001, 0.0001, 0.001, 0.005, 0.01, 0.02.

The LOF algorithm is based on the KNN classifier and, therefore, takes the number of nearest neighbours as the principal input parameter. The fraction of abnormal data in the training data can be given as input parameter but is not obligatory, since the algorithm has a built-in method to define the limit automatically, which is used as default. Since the exact amount of abnormal data in the training data is not known, the fraction of abnormal data in the training data is not given as an input in this study. A parameter sweep was performed to find a suitable value for the parameter k. The values used for k were 8, 16, 32, 64, 128, 256 and 512.

The trained novelty detectors were then validated by running them against new normal operation data that was not used in the training, both from their own respective class and from the other classes. When run against new normal operation data from the same class as the training data, it was assumed that an ideal novelty detector trained using the One-class SVM algorithm would find a proportion of novel data from the new data equal to or lower than the value of the parameter ν used during the training. Whereas, since the proportion of abnormal data in the training data was not given as input for the LOF algorithm, the above rule could not be applied for the novelty detectors trained using the LOF algorithm. Therefore, the lowest number of abnormal data points found in the data was considered as the best result, since test data represents the same class as the training data. The threshold value for detecting abnormal operation in a series of continuous

predictions for the SVM algorithm is the value of the parameter ν itself, and for the LOF algorithm, the proportion of abnormal data found from the test data of the same class.

When run against new normal operation data from the other classes, it was assumed that an ideal novelty detector would predict all new data as novel, independent of the algorithm used for the training.

The most suitable values for the parameters ν and k novelty detectors, according to the parameter sweeps, were chosen. Novelty detectors were trained by the two algorithms with the features chosen based on the results of the preceding classification and model-based feature selection step. The trained novelty detectors were run against the data sampled into the subsets of abnormal operation data. The proportions of abnormal operation data detected in the test data by the different novelty detectors was studied and compared. Also, the training and predicting times of the different novelty detectors were studied and compared. The LOF algorithm supports parallel computing. Therefore, the training and predicting times were defined using both one CPU and four CPUs to discover the performance gained when using parallelisation.

# 4 RESULTS

## 4.1 Data sampling

As a result of the data sampling, 67 subsets of normal operation data and 40 subsets of abnormal operation data were formed. The total amount of sampled normal operation data is not divided equally between the groups, nor is it divided equally between the subsets inside the groups. The subset and group sizes, as well as the total size of sampled normal operation data are presented in Table 2.

*Table 2. size of sampled normal operation data by subsets and by genset power output groups [min]*

| | Group | | | | | |
|---|---|---|---|---|---|---|
| **Subset #** | **100 %** | **95 %** | **90 %** | **75 %** | **50 %** | **0 %** |
| **1** | 5 | 8 | 8 | 9 | 5 | 9 |
| **2** | 5 | 8 | 7 | 6 | 5 | 9 |
| **3** | 5 | 8 | 3 | 3 | 6 | 9 |
| **4** | 3 | 6 | 5 | 2 | 8 | 9 |
| **5** | 8 | 5 | 5 | 5 | 9 | 9 |
| **6** | 8 | 5 | 7 | 5 | 7 | 9 |
| **7** | 8 | 5 | 6 | 8 | 9 | 9 |
| **8** | 8 | 7 | 5 | 5 | 5 | 9 |
| **9** | 8 | 6 | | 3 | 5 | 9 |
| **10** | 8 | 6 | | 2 | | 9 |
| **11** | 8 | 7 | | 3 | | |
| **12** | 8 | 6 | | 8 | | |
| **13** | 7 | 8 | | 7 | | |
| **14** | 7 | | | | | |
| **Group Sums** | **96** | **85** | **46** | **66** | **59** | **90** |
| **Total Sum** | | | | | | **442** |

The sampled signals in the subsets of abnormal operation data are all one minute long. No abnormal operation data acquired during 0 % genset power output was found from the provided dataset. The number of the subsets of abnormal operation data in the rest of the groups are presented in Table 3.

*Table 3. The number of subsets of abnormal operation data by genset power output group*

| Group | | | | |
|---|---|---|---|---|
| **100 %** | **95 %** | **90 %** | **75 %** | **50 %** |
| 8 | 6 | 6 | 12 | 8 |

The calculated normalised total signal variances, i.e., the normalised signal powers of all groups of normal operation are presented in Figure 21. The signal variances in the subsets of normal and abnormal operation normalised by the total signal variances of the corresponding group are presented in Table 4 and in Table 5 respectively.

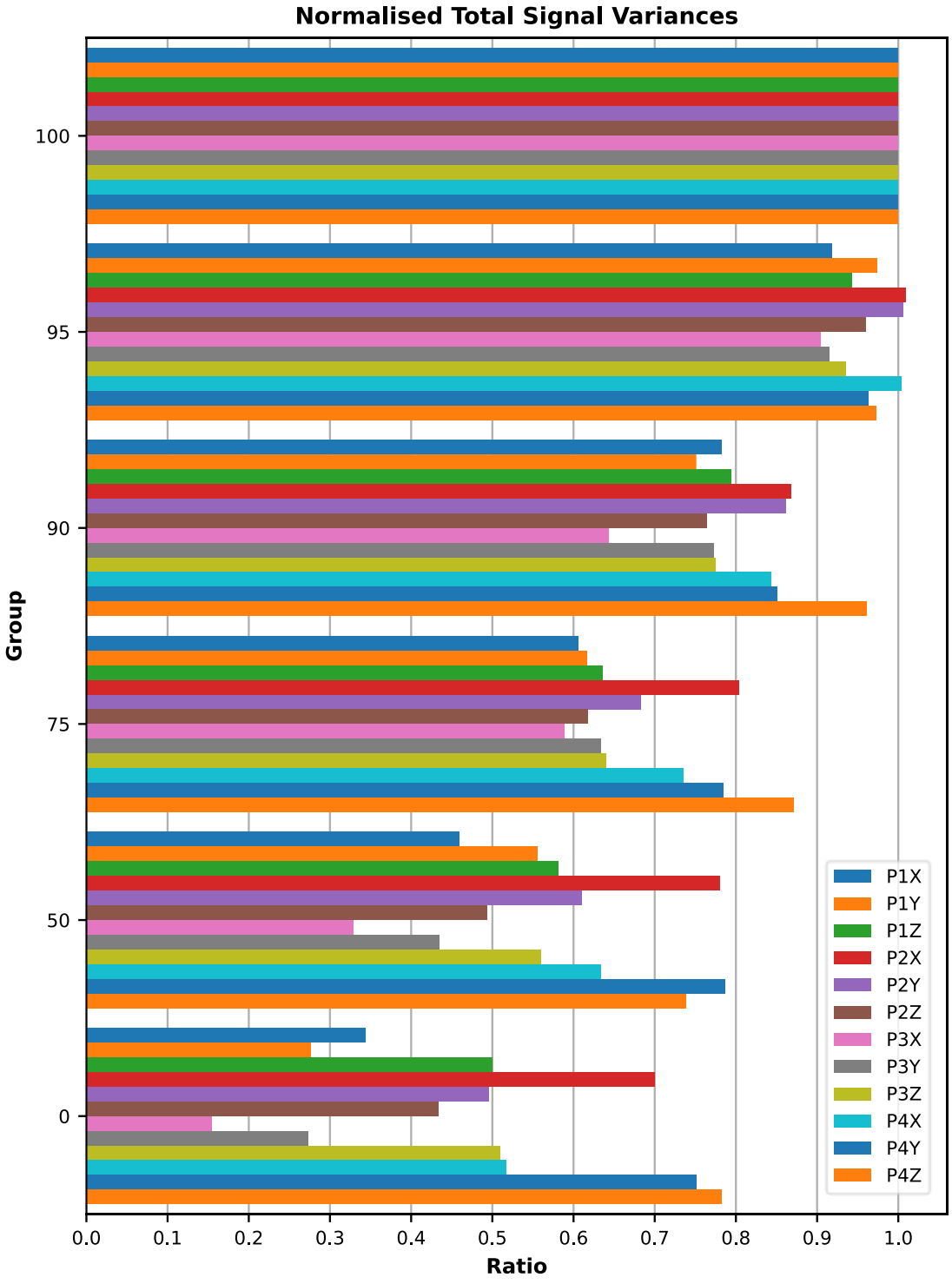


*Figure 21. Normalised total signal variances.*

*Table 4. Normalised signal variances of subsets of normal operation*

| Group | Subset | Measurement Point and Direction | | | | | | | | | | | |
|---|---|---|---|---|---|---|---|---|---|---|---|---|---|
| | | P1X | P1Y | P1Z | P2X | P2Y | P2Z | P3X | P3Y | P3Z | P4X | P4Y | P4Z |
| | 1 | 104.07 % | 101.90 % | 100.88 % | 98.77 % | 101.20 % | 98.91 % | 101.16 % | 101.37 % | 99.46 % | 98.95 % | 97.30 % | 97.49 % |
| | 2 | 99.47 % | 100.11 % | 98.74 % | 97.84 % | 97.30 % | 98.19 % | 100.93 % | 98.01 % | 98.29 % | 99.57 % | 96.67 % | 96.94 % |
| | 3 | 97.81 % | 99.60 % | 99.02 % | 97.01 % | 96.40 % | 98.08 % | 101.29 % | 98.09 % | 98.36 % | 99.05 % | 96.86 % | 96.94 % |
| | 4 | 108.31 % | 110.66 % | 106.61 % | 107.35 % | 107.59 % | 107.38 % | 108.29 % | 105.80 % | 102.74 % | 106.11 % | 99.71 % | 100.52 % |
| | 5 | 97.52 % | 104.26 % | 98.88 % | 100.19 % | 97.56 % | 101.81 % | 103.57 % | 99.41 % | 98.17 % | 102.41 % | 96.20 % | 98.30 % |
| 1 | 6 | 97.11 % | 104.31 % | 100.59 % | 100.09 % | 97.96 % | 103.06 % | 105.15 % | 98.90 % | 99.88 % | 105.21 % | 96.69 % | 97.18 % |
| 0 | 7 | 102.30 % | 95.91 % | 101.63 % | 102.36 % | 108.77 % | 103.17 % | 99.91 % | 100.29 % | 105.82 % | 97.95 % | 110.01 % | 106.41 % |
| 0 | 8 | 104.75 % | 97.68 % | 102.47 % | 104.11 % | 108.94 % | 105.68 % | 103.70 % | 101.14 % | 107.07 % | 99.87 % | 107.81 % | 105.03 % |
| | 9 | 100.47 % | 96.91 % | 98.64 % | 96.21 % | 97.15 % | 95.15 % | 92.55 % | 100.12 % | 96.34 % | 95.58 % | 96.83 % | 99.60 % |
| % | 10 | 100.37 % | 99.73 % | 99.34 % | 98.59 % | 98.02 % | 98.70 % | 97.67 % | 101.19 % | 98.71 % | 98.06 % | 99.75 % | 100.61 % |
| | 11 | 99.64 % | 98.93 % | 99.69 % | 98.87 % | 97.72 % | 98.91 % | 98.19 % | 100.51 % | 99.23 % | 100.16 % | 100.33 % | 99.96 % |
| | 12 | 98.69 % | 99.33 % | 100.07 % | 99.83 % | 96.98 % | 98.75 % | 99.21 % | 100.07 % | 99.35 % | 101.09 % | 100.75 % | 99.45 % |
| | 13 | 97.38 % | 99.19 % | 99.06 % | 99.39 % | 96.06 % | 98.00 % | 99.56 % | 99.71 % | 99.37 % | 101.68 % | 99.76 % | 96.89 % |
| | 14 | 97.22 % | 98.41 % | 97.21 % | 101.24 % | 100.59 % | 95.77 % | 94.39 % | 97.66 % | 96.77 % | 96.52 % | 96.82 % | 101.06 % |
| | 1 | 100.46 % | 98.68 % | 99.61 % | 99.09 % | 99.72 % | 100.80 % | 98.18 % | 101.66 % | 99.47 % | 99.47 % | 101.05 % | 98.24 % |
| | 2 | 99.88 % | 97.92 % | 99.15 % | 97.64 % | 99.50 % | 99.75 % | 97.86 % | 101.58 % | 98.89 % | 98.64 % | 99.70 % | 95.69 % |
| | 3 | 98.92 % | 97.58 % | 98.34 % | 96.46 % | 98.38 % | 96.76 % | 98.30 % | 100.45 % | 98.05 % | 97.15 % | 97.08 % | 92.57 % |
| | 4 | 97.00 % | 101.41 % | 97.45 % | 100.31 % | 94.69 % | 96.45 % | 99.46 % | 98.64 % | 96.22 % | 100.63 % | 97.57 % | 96.15 % |
| 9 | 5 | 96.37 % | 102.27 % | 97.35 % | 99.93 % | 96.68 % | 97.48 % | 103.60 % | 97.60 % | 98.91 % | 104.05 % | 97.86 % | 101.09 % |
| 5 | 6 | 97.02 % | 101.41 % | 97.72 % | 100.21 % | 98.37 % | 97.17 % | 103.06 % | 97.03 % | 100.04 % | 105.58 % | 98.01 % | 103.38 % |
| | 7 | 95.78 % | 101.97 % | 98.13 % | 99.48 % | 96.80 % | 97.24 % | 104.14 % | 96.35 % | 99.33 % | 104.66 % | 97.59 % | 102.17 % |
| | 8 | 100.55 % | 104.05 % | 102.92 % | 104.83 % | 103.67 % | 99.70 % | 110.62 % | 99.73 % | 102.93 % | 97.77 % | 97.93 % | 105.14 % |
| % | 9 | 106.09 % | 100.84 % | 103.59 % | 102.09 % | 107.98 % | 104.94 % | 97.80 % | 101.38 % | 104.12 % | 98.44 % | 103.08 % | 102.26 % |
| | 10 | 103.53 % | 98.69 % | 102.66 % | 99.95 % | 105.75 % | 106.08 % | 96.74 % | 101.20 % | 103.56 % | 98.19 % | 102.40 % | 101.03 % |
| | 11 | 101.75 % | 99.14 % | 100.98 % | 100.40 % | 100.27 % | 101.46 % | 97.59 % | 99.79 % | 100.59 % | 99.58 % | 102.05 % | 101.69 % |
| | 12 | 99.98 % | 99.41 % | 101.03 % | 100.92 % | 98.31 % | 100.10 % | 98.36 % | 100.16 % | 99.80 % | 100.33 % | 102.42 % | 103.67 % |
| | 13 | 100.53 % | 99.23 % | 100.21 % | 100.04 % | 99.00 % | 101.08 % | 97.47 % | 101.34 % | 98.83 % | 99.94 % | 102.17 % | 101.05 % |
| | 1 | 102.61 % | 101.60 % | 100.30 % | 101.86 % | 103.07 % | 103.66 % | 105.41 % | 99.24 % | 107.13 % | 100.90 % | 100.17 % | 97.43 % |
| | 2 | 99.79 % | 100.93 % | 99.58 % | 99.68 % | 100.40 % | 100.57 % | 102.98 % | 96.11 % | 106.12 % | 100.46 % | 99.76 % | 98.91 % |
| 9 | 3 | 102.34 % | 102.63 % | 103.88 % | 101.34 % | 106.16 % | 103.44 % | 106.28 % | 103.50 % | 101.43 % | 98.49 % | 96.92 % | 93.43 % |
| 0 | 4 | 95.89 % | 95.16 % | 99.86 % | 90.49 % | 98.72 % | 100.45 % | 90.77 % | 108.53 % | 91.54 % | 95.16 % | 95.59 % | 97.40 % |
| | 5 | 98.61 % | 96.07 % | 102.95 % | 95.47 % | 101.53 % | 102.35 % | 94.33 % | 105.87 % | 97.37 % | 98.59 % | 99.34 % | 100.95 % |
| % | 6 | 101.07 % | 99.95 % | 99.90 % | 102.53 % | 98.64 % | 97.74 % | 99.40 % | 98.56 % | 98.12 % | 101.02 % | 101.61 % | 102.63 % |
| | 7 | 100.34 % | 101.46 % | 99.14 % | 103.69 % | 97.47 % | 97.50 % | 99.27 % | 97.52 % | 97.70 % | 101.30 % | 102.72 % | 103.87 % |
| | 8 | 98.31 % | 101.64 % | 96.16 % | 102.73 % | 95.53 % | 94.65 % | 100.03 % | 95.14 % | 95.64 % | 102.08 % | 101.46 % | 102.90 % |
| | 1 | 99.85 % | 104.13 % | 104.46 % | 103.05 % | 97.73 % | 101.81 % | 107.27 % | 99.42 % | 105.34 % | 105.86 % | 101.90 % | 98.46 % |
| | 2 | 96.10 % | 101.32 % | 102.17 % | 102.77 % | 97.31 % | 97.98 % | 103.22 % | 94.84 % | 102.76 % | 103.38 % | 98.96 % | 98.45 % |
| | 3 | 95.46 % | 101.40 % | 103.17 % | 102.99 % | 98.43 % | 97.92 % | 103.29 % | 95.76 % | 103.11 % | 103.59 % | 98.14 % | 99.00 % |
| | 4 | 96.39 % | 102.98 % | 101.21 % | 103.51 % | 100.41 % | 98.69 % | 104.74 % | 96.26 % | 103.31 % | 105.05 % | 97.93 % | 100.47 % |
| 7 | 5 | 98.58 % | 93.16 % | 95.74 % | 93.68 % | 93.01 % | 101.52 % | 85.56 % | 107.87 % | 98.18 % | 92.92 % | 103.78 % | 99.54 % |
| 5 | 6 | 99.60 % | 91.94 % | 95.62 % | 94.62 % | 95.98 % | 102.29 % | 88.88 % | 107.05 % | 99.98 % | 94.42 % | 102.12 % | 101.06 % |
| | 7 | 101.90 % | 96.47 % | 96.72 % | 98.12 % | 101.11 % | 103.05 % | 93.59 % | 102.58 % | 100.01 % | 97.63 % | 103.11 % | 101.04 % |
| | 8 | 100.54 % | 96.09 % | 98.27 % | 97.01 % | 103.06 % | 99.18 % | 91.73 % | 98.66 % | 99.36 % | 95.25 % | 97.19 % | 100.32 % |
| % | 9 | 100.73 % | 97.33 % | 97.22 % | 96.95 % | 103.75 % | 98.66 % | 94.54 % | 97.88 % | 98.08 % | 94.30 % | 93.20 % | 97.80 % |
| | 10 | 100.00 % | 97.59 % | 98.55 % | 97.36 % | 104.63 % | 98.94 % | 96.45 % | 97.39 % | 99.40 % | 97.59 % | 94.70 % | 98.15 % |
| | 11 | 99.33 % | 99.92 % | 96.82 % | 96.12 % | 98.48 % | 98.75 % | 101.12 % | 96.96 % | 97.77 % | 99.19 % | 96.67 % | 96.15 % |
| | 12 | 102.26 % | 104.80 % | 102.12 % | 103.46 % | 103.44 % | 98.31 % | 108.08 % | 98.99 % | 96.13 % | 102.38 % | 100.10 % | 102.11 % |
| | 13 | 102.65 % | 105.95 % | 102.40 % | 103.83 % | 103.97 % | 98.38 % | 110.25 % | 99.51 % | 96.61 % | 102.50 % | 99.80 % | 102.46 % |
| | 1 | 101.32 % | 90.00 % | 103.37 % | 98.42 % | 104.30 % | 98.19 % | 96.27 % | 95.64 % | 100.42 % | 106.22 % | 101.49 % | 96.77 % |
| | 2 | 101.88 % | 90.86 % | 101.89 % | 98.24 % | 105.69 % | 98.82 % | 96.29 % | 97.01 % | 101.43 % | 108.29 % | 101.97 % | 97.20 % |
| | 3 | 98.35 % | 98.77 % | 96.80 % | 102.70 % | 98.13 % | 99.33 % | 95.19 % | 97.32 % | 100.33 % | 91.83 % | 98.76 % | 107.51 % |
| 5 | 4 | 98.13 % | 106.14 % | 96.94 % | 102.67 % | 99.01 % | 102.13 % | 103.71 % | 103.37 % | 98.31 % | 91.95 % | 96.59 % | 103.01 % |
| 0 | 5 | 98.46 % | 105.99 % | 97.75 % | 105.10 % | 99.90 % | 102.53 % | 101.98 % | 103.80 % | 98.35 % | 94.86 % | 97.07 % | 102.89 % |
| | 6 | 100.89 % | 97.42 % | 105.38 % | 105.19 % | 106.18 % | 100.36 % | 94.75 % | 95.68 % | 102.96 % | 111.25 % | 103.01 % | 94.48 % |
| % | 7 | 100.07 % | 102.31 % | 103.99 % | 97.79 % | 96.20 % | 98.93 % | 103.05 % | 99.09 % | 101.38 % | 99.26 % | 102.96 % | 98.08 % |
| | 8 | 100.77 % | 102.58 % | 99.65 % | 95.97 % | 97.45 % | 99.39 % | 100.17 % | 101.07 % | 99.32 % | 104.50 % | 100.44 % | 96.55 % |
| | 9 | 101.77 % | 102.41 % | 98.81 % | 96.42 % | 97.73 % | 99.56 % | 101.76 % | 101.89 % | 100.20 % | 105.96 % | 101.02 % | 96.73 % |
| | 1 | 99.61 % | 98.48 % | 92.54 % | 109.06 % | 116.05 % | 113.29 % | 105.09 % | 102.92 % | 97.21 % | 113.56 % | 111.73 % | 108.53 % |
| | 2 | 99.18 % | 100.20 % | 99.35 % | 109.24 % | 111.64 % | 103.93 % | 105.14 % | 116.72 % | 100.66 % | 109.15 % | 112.36 % | 111.81 % |
| | 3 | 100.28 % | 103.17 % | 107.91 % | 106.12 % | 105.89 % | 100.24 % | 102.05 % | 113.23 % | 104.02 % | 103.08 % | 108.87 % | 110.34 % |
| 0 | 4 | 100.63 % | 102.28 % | 108.19 % | 100.85 % | 100.31 % | 97.95 % | 101.48 % | 103.10 % | 104.03 % | 99.26 % | 103.70 % | 104.49 % |
| | 5 | 99.87 % | 100.77 % | 105.00 % | 98.46 % | 97.09 % | 96.52 % | 100.15 % | 95.89 % | 101.32 % | 97.61 % | 99.22 % | 98.90 % |
| % | 6 | 99.86 % | 98.91 % | 99.91 % | 95.74 % | 94.38 % | 96.95 % | 97.99 % | 92.85 % | 98.60 % | 95.39 % | 94.23 % | 94.14 % |
| | 7 | 99.75 % | 98.85 % | 96.98 % | 95.25 % | 93.68 % | 97.09 % | 96.89 % | 93.12 % | 98.34 % | 95.07 % | 93.65 % | 93.45 % |
| | 8 | 99.84 % | 99.05 % | 97.12 % | 95.71 % | 93.89 % | 97.56 % | 96.66 % | 93.67 % | 97.90 % | 94.83 % | 92.35 % | 92.34 % |
| | 9 | 100.28 % | 98.94 % | 96.14 % | 94.84 % | 93.61 % | 98.23 % | 97.03 % | 93.83 % | 98.61 % | 95.75 % | 92.18 % | 92.98 % |
| | 10 | 100.70 % | 99.34 % | 96.86 % | 94.72 % | 93.45 % | 98.23 % | 97.53 % | 94.68 % | 99.31 % | 96.28 % | 91.70 % | 93.03 % |
| Colourbar | | 85.00 % | 88.00 % | 91.00 % | 94.00 % | 97.00 % | 100.00 % | 103.00 % | 106.00 % | 109.00 % | 112.00 % | 115.00 % | 118.00 % |

*Table 5. Normalised signal variances of subsets of abnormal operation*

| Group | Subset | Measurement Point and Direction | | | | | | | | | | | |
|---|---|---|---|---|---|---|---|---|---|---|---|---|---|
| | | P1X | P1Y | P1Z | P2X | P2Y | P2Z | P3X | P3Y | P3Z | P4X | P4Y | P4Z |
| 100% | 1 | 98.84 % | 95.19 % | 102.96 % | 109.30 % | 109.44 % | 105.71 % | 92.83 % | 101.33 % | 104.62 % | 104.58 % | 110.28 % | 108.40 % |
| | 2 | 103.89 % | 103.09 % | 103.02 % | 103.61 % | 102.72 % | 104.58 % | 103.10 % | 101.49 % | 101.85 % | 102.85 % | 101.09 % | 100.24 % |
| | 3 | 98.75 % | 100.49 % | 99.70 % | 99.55 % | 97.96 % | 99.76 % | 101.62 % | 99.34 % | 99.30 % | 100.37 % | 98.55 % | 98.13 % |
| | 4 | 104.22 % | 103.87 % | 102.70 % | 105.85 % | 104.06 % | 106.28 % | 104.53 % | 102.59 % | 103.01 % | 105.09 % | 101.87 % | 102.36 % |
| | 5 | 98.60 % | 101.75 % | 101.62 % | 102.08 % | 100.94 % | 101.76 % | 102.43 % | 99.88 % | 100.62 % | 102.89 % | 99.38 % | 100.69 % |
| | 6 | 102.44 % | 100.26 % | 107.11 % | 104.99 % | 103.75 % | 103.47 % | 92.82 % | 102.66 % | 100.95 % | 102.62 % | 102.09 % | 104.58 % |
| | 7 | 97.34 % | 95.76 % | 101.83 % | 107.94 % | 103.53 % | 100.67 % | 88.37 % | 98.23 % | 100.63 % | 103.40 % | 103.68 % | 106.32 % |
| | 8 | 99.50 % | 100.44 % | 103.71 % | 104.66 % | 100.94 % | 103.07 % | 93.03 % | 101.10 % | 99.99 % | 101.71 % | 102.53 % | 103.73 % |
| 95% | 1 | 92.73 % | 92.66 % | 96.47 % | 101.26 % | 96.80 % | 95.88 % | 85.40 % | 97.12 % | 96.71 % | 100.77 % | 99.38 % | 97.22 % |
| | 2 | 92.08 % | 94.04 % | 96.87 % | 102.09 % | 97.35 % | 95.71 % | 87.96 % | 96.63 % | 97.39 % | 102.89 % | 99.74 % | 100.07 % |
| | 3 | 98.19 % | 98.02 % | 103.40 % | 106.55 % | 100.75 % | 98.48 % | 93.81 % | 100.38 % | 102.50 % | 103.20 % | 101.92 % | 106.90 % |
| | 4 | 96.00 % | 95.52 % | 99.49 % | 104.62 % | 98.29 % | 97.37 % | 92.11 % | 96.47 % | 100.82 % | 101.73 % | 100.85 % | 104.25 % |
| | 5 | 95.15 % | 93.19 % | 97.50 % | 102.63 % | 98.88 % | 96.29 % | 85.23 % | 96.28 % | 99.36 % | 101.39 % | 100.39 % | 103.31 % |
| | 6 | 95.64 % | 94.14 % | 98.82 % | 104.46 % | 99.72 % | 98.86 % | 87.59 % | 98.19 % | 104.25 % | 102.62 % | 102.70 % | 102.71 % |
| 90% | 1 | 108.22 % | 107.16 % | 111.25 % | 119.49 % | 112.66 % | 116.55 % | 104.91 % | 105.73 % | 113.71 % | 112.66 % | 116.25 % | 106.84 % |
| | 2 | 97.77 % | 99.84 % | 103.49 % | 108.99 % | 102.07 % | 104.87 % | 93.18 % | 97.18 % | 103.23 % | 106.34 % | 107.99 % | 102.19 % |
| | 3 | 102.07 % | 101.56 % | 103.47 % | 102.68 % | 104.14 % | 104.98 % | 104.34 % | 104.36 % | 104.63 % | 98.72 % | 100.03 % | 98.16 % |
| | 4 | 101.88 % | 100.49 % | 104.22 % | 101.06 % | 103.48 % | 102.05 % | 101.31 % | 102.52 % | 102.75 % | 100.26 % | 99.10 % | 97.88 % |
| | 5 | 107.09 % | 104.43 % | 109.04 % | 109.61 % | 108.69 % | 110.93 % | 104.86 % | 108.56 % | 107.80 % | 108.52 % | 109.01 % | 106.40 % |
| | 6 | 101.65 % | 102.17 % | 101.84 % | 103.89 % | 100.28 % | 100.79 % | 99.77 % | 101.94 % | 101.07 % | 102.68 % | 102.48 % | 101.61 % |
| 75% | 1 | 102.21 % | 104.16 % | 107.69 % | 104.29 % | 103.03 % | 106.00 % | 99.51 % | 103.12 % | 104.93 % | 105.77 % | 103.62 % | 99.91 % |
| | 2 | 101.68 % | 103.87 % | 107.01 % | 105.38 % | 103.93 % | 105.17 % | 99.61 % | 102.33 % | 104.27 % | 105.94 % | 103.26 % | 100.65 % |
| | 3 | 99.07 % | 102.17 % | 104.80 % | 102.87 % | 101.44 % | 101.35 % | 98.11 % | 100.73 % | 102.48 % | 103.27 % | 100.69 % | 99.96 % |
| | 4 | 104.10 % | 108.39 % | 108.46 % | 106.93 % | 106.99 % | 107.00 % | 96.85 % | 103.66 % | 106.56 % | 107.09 % | 103.18 % | 100.73 % |
| | 5 | 105.07 % | 101.46 % | 106.21 % | 103.80 % | 105.85 % | 109.55 % | 95.75 % | 108.45 % | 105.80 % | 103.82 % | 107.04 % | 103.14 % |
| | 6 | 106.19 % | 103.84 % | 107.76 % | 105.03 % | 108.69 % | 109.63 % | 97.97 % | 106.83 % | 106.31 % | 104.67 % | 106.61 % | 102.45 % |
| | 7 | 105.22 % | 103.14 % | 107.02 % | 103.09 % | 107.51 % | 107.36 % | 96.66 % | 104.99 % | 105.13 % | 102.92 % | 103.11 % | 101.08 % |
| | 8 | 103.74 % | 101.92 % | 105.41 % | 102.84 % | 107.67 % | 105.98 % | 94.78 % | 103.74 % | 104.68 % | 101.86 % | 100.15 % | 99.99 % |
| | 9 | 104.05 % | 102.81 % | 106.36 % | 103.23 % | 106.84 % | 106.97 % | 97.51 % | 103.78 % | 104.53 % | 103.28 % | 102.12 % | 99.46 % |
| | 10 | 104.22 % | 103.71 % | 105.80 % | 102.16 % | 105.99 % | 106.14 % | 98.86 % | 103.38 % | 103.87 % | 103.95 % | 101.75 % | 99.50 % |
| | 11 | 106.28 % | 107.14 % | 108.58 % | 105.35 % | 107.39 % | 109.71 % | 101.37 % | 105.04 % | 106.52 % | 106.59 % | 104.37 % | 100.40 % |
| | 12 | 104.86 % | 106.57 % | 108.76 % | 107.33 % | 108.68 % | 108.11 % | 101.63 % | 105.09 % | 105.02 % | 106.65 % | 105.52 % | 101.21 % |
| 50% | 1 | 99.35 % | 96.69 % | 98.48 % | 101.69 % | 99.91 % | 102.25 % | 96.00 % | 99.83 % | 101.10 % | 96.50 % | 102.05 % | 106.36 % |
| | 2 | 98.17 % | 102.79 % | 98.98 % | 100.52 % | 98.17 % | 99.51 % | 106.35 % | 104.95 % | 100.57 % | 95.65 % | 97.99 % | 102.02 % |
| | 3 | 96.30 % | 100.78 % | 98.86 % | 101.54 % | 99.08 % | 98.67 % | 101.03 % | 104.95 % | 99.65 % | 95.75 % | 98.07 % | 103.44 % |
| | 4 | 100.67 % | 102.75 % | 100.20 % | 102.48 % | 101.32 % | 102.02 % | 101.26 % | 101.00 % | 97.58 % | 98.91 % | 98.45 % | 101.90 % |
| | 5 | 99.64 % | 97.92 % | 103.52 % | 100.75 % | 101.21 % | 100.21 % | 95.88 % | 100.20 % | 101.89 % | 104.54 % | 101.31 % | 99.92 % |
| | 6 | 100.29 % | 99.59 % | 103.76 % | 102.73 % | 102.50 % | 101.11 % | 95.06 % | 100.11 % | 101.59 % | 106.36 % | 101.86 % | 98.91 % |
| | 7 | 97.49 % | 99.27 % | 101.39 % | 98.58 % | 96.35 % | 99.39 % | 99.02 % | 97.33 % | 101.10 % | 97.20 % | 102.86 % | 102.00 % |
| | 8 | 101.07 % | 104.71 % | 102.13 % | 98.85 % | 98.77 % | 100.50 % | 101.99 % | 101.36 % | 100.50 % | 101.76 % | 101.19 % | 98.61 % |
| Colourbar | | 80.00 % | 83.64 % | 87.27 % | 90.91 % | 94.55 % | 98.18 % | 101.82 % | 105.46 % | 109.09 % | 112.73 % | 116.36 % | 120.00 % |

## 4.2 Feature extraction

The feature extraction was based on the engine operating cycle of the studied genset. The studied genset has a four-stroke engine operating at 750 rpm. That is, the duration of one operating cycle is 0.16 s at nominal speed, and therefore the frequency of the operating cycles is 6.25 Hz. The sampling frequency used in the measurement was 2048 Hz, hence one operating cycle consists of 327.68 samples. The chosen sequence lengths were multiples from one to seven of the duration of one engine cycle rounded to the nearest integer. One second was chosen as the maximum length of a sequence to be used in this study. Therefore, seven engine cycles was the longest length used in this study, as it is the first multiple of engine cycles to exceed one second in length.

The sampling frequency used in the measurements excessively covers the necessary frequency range for this study. According to the Sampling Theorem presented in Chapter 2.2, vibrations at frequencies up to 1024 Hz, that is 81 first harmonic orders, were measured correctly. The harmonic coefficients of the first 18 harmonic orders presented in Figure 9 of Chapter 2.1 show that the higher half of the harmonic orders have negligible effect on the total gas torque.

As mentioned in Chapter 3.3, the feature values for the data in the subsets of abnormal operation were defined using a sliding window with the length of the sequence as the window size and one as step size. Forty subsets of abnormal operation were sampled, each of them containing 60 seconds of measured data from each of the 12 different measurement variables. Hence, 1400 datasets (40 subsets x 5 features x 7 sequence lengths) of abnormal operation data were created containing 12 arrays of almost 123 000 values (60 seconds at 2048 Hz).

The feature values for the data in the subsets of normal operation were calculated from randomly chosen sequences of the signals sampled to subsets of normal operation. In total, 35 (5 features x 7 sequence lengths) datasets of normal operation data were created containing 12 arrays of 1800 000 feature values (300 000 feature values for each class) and one array of equal length containing the labels.

The number of feature values calculated from a subset of normal operation was proportional to the size of the subset compared to the size of all the subsets in the corresponding group of power output level. This means, 300 000 feature values equal a

signal length of approximately 147 seconds, if calculated using a sliding window with step size one, as was done for the abnormal operation data. The largest amount of data sampled in the subsets of a single group was 96 minutes of signals. Using the shortest window length, that is 328 samples, each value in a 96-minutes-long signal measured at a sampling rate of 2048 Hz is included in one of the 300 000 sequences 8.37 times on average.

## 4.3 Classification and feature selection

Four rounds of training and testing the classifiers were performed to find out the effects of the size of the dataset, the length of the sequence used in feature extraction, the different features and the measurement point location on the accuracy of the classification models. Also, the different classifier algorithms were evaluated in the process. The results, that is the average accuracies of the cross-validation of each trained classifier, of the four rounds are presented in the following tables.

The complete results of the first and the second rounds are presented in Table 6 and in Table 7 respectively. The results presented in the first column of Table 7 were presented already in the last column of Table 6. The results are repeated to allow easier comparison between the results calculated using all five different features. The results for the most accurate classifier algorithm of the third and the fourth rounds, that is the SVM, are presented in Table 8 and in Table 9. The complete results of the third and the fourth rounds are presented in Appendix A.

*Table 6. Results of the first round*

| Classifier | Cycles | Samples per Class 100 | 500 | 1000 | 5000 | 10000 | 50000 | 100000 | Colour bar |
|---|---|---|---|---|---|---|---|---|---|
| LR | 1 | 94.67 % | 96.10 % | 96.27 % | 96.80 % | 96.88 % | 96.89 % | 96.95 % | 100.0 % |
| | 2 | 97.50 % | 98.40 % | 98.28 % | 98.61 % | 98.63 % | 98.65 % | 98.69 % | 99.76 % |
| | 3 | 97.83 % | 98.63 % | 98.87 % | 99.02 % | 99.12 % | 99.19 % | 99.18 % | 99.51 % |
| | 4 | 98.50 % | 98.90 % | 99.13 % | 99.38 % | 99.41 % | 99.44 % | 99.45 % | 99.27 % |
| | 5 | 99.17 % | 99.03 % | 99.22 % | 99.43 % | 99.56 % | 99.58 % | 99.58 % | 99.02 % |
| | 6 | 99.17 % | 99.20 % | 99.28 % | 99.60 % | 99.63 % | 99.68 % | 99.69 % | 98.78 % |
| | 7 | 99.17 % | 99.20 % | 99.42 % | 99.67 % | 99.71 % | 99.74 % | 99.75 % | 98.54 % |
| SVM RBF | 1 | 96.50 % | 96.53 % | 96.93 % | 97.20 % | 97.34 % | 97.37 % | 97.45 % | 98.29 % |
| | 2 | 98.50 % | 98.73 % | 98.83 % | 98.88 % | 98.99 % | 99.03 % | 99.08 % | 98.05 % |
| | 3 | 98.83 % | 99.20 % | 99.28 % | 99.36 % | 99.40 % | 99.51 % | 99.52 % | 97.80 % |
| | 4 | 99.33 % | 99.40 % | 99.53 % | 99.62 % | 99.67 % | 99.72 % | 99.74 % | 97.56 % |
| | 5 | 99.33 % | 99.47 % | 99.65 % | 99.71 % | 99.76 % | 99.81 % | 99.83 % | 97.32 % |
| | 6 | 99.67 % | 99.63 % | 99.65 % | 99.80 % | 99.83 % | 99.87 % | 99.89 % | 97.07 % |
| | 7 | 100.0 % | 99.80 % | 99.70 % | 99.85 % | 99.87 % | 99.91 % | 99.92 % | 96.83 % |
| SVM LIN | 1 | 90.83 % | 92.70 % | 92.53 % | 93.06 % | 92.90 % | 92.99 % | 92.99 % | 96.59 % |
| | 2 | 96.17 % | 96.57 % | 97.00 % | 96.93 % | 97.11 % | 97.12 % | 97.15 % | 96.34 % |
| | 3 | 97.50 % | 96.97 % | 97.60 % | 97.84 % | 97.94 % | 97.99 % | 97.98 % | 96.10 % |
| | 4 | 98.00 % | 97.97 % | 98.37 % | 98.52 % | 98.64 % | 98.73 % | 98.74 % | 95.85 % |
| | 5 | 98.17 % | 98.37 % | 98.33 % | 98.74 % | 98.90 % | 98.93 % | 98.94 % | 95.61 % |
| | 6 | 98.50 % | 98.60 % | 98.60 % | 99.03 % | 99.15 % | 99.20 % | 99.23 % | 95.37 % |
| | 7 | 98.83 % | 98.73 % | 98.85 % | 99.10 % | 99.21 % | 99.29 % | 99.31 % | 95.12 % |
| DT | 1 | 91.67 % | 93.57 % | 93.92 % | 94.84 % | 95.11 % | 95.57 % | 95.79 % | 94.88 % |
| | 2 | 96.83 % | 96.80 % | 96.68 % | 97.42 % | 97.43 % | 97.58 % | 97.78 % | 94.63 % |
| | 3 | 96.33 % | 97.30 % | 97.42 % | 97.85 % | 97.89 % | 98.20 % | 98.33 % | 94.39 % |
| | 4 | 97.17 % | 97.77 % | 97.70 % | 98.18 % | 98.32 % | 98.60 % | 98.72 % | 94.15 % |
| | 5 | 98.33 % | 98.50 % | 98.07 % | 98.34 % | 98.39 % | 98.87 % | 98.93 % | 93.90 % |
| | 6 | 98.33 % | 98.63 % | 98.10 % | 98.62 % | 98.65 % | 98.99 % | 99.13 % | 93.66 % |
| | 7 | 98.17 % | 98.67 % | 98.52 % | 98.64 % | 98.85 % | 99.08 % | 99.18 % | 93.41 % |
| KNN | 1 | 91.83 % | 93.53 % | 94.28 % | 95.33 % | 95.62 % | 95.98 % | 96.14 % | 93.17 % |
| | 2 | 95.17 % | 97.30 % | 97.07 % | 97.73 % | 98.03 % | 98.19 % | 98.27 % | 92.93 % |
| | 3 | 97.00 % | 98.23 % | 97.70 % | 98.52 % | 98.57 % | 98.87 % | 98.90 % | 92.68 % |
| | 4 | 97.67 % | 98.63 % | 98.45 % | 99.01 % | 99.12 % | 99.30 % | 99.36 % | 92.44 % |
| | 5 | 97.33 % | 98.70 % | 98.72 % | 99.26 % | 99.37 % | 99.50 % | 99.54 % | 92.20 % |
| | 6 | 98.67 % | 98.97 % | 99.07 % | 99.46 % | 99.47 % | 99.64 % | 99.69 % | 91.95 % |
| | 7 | 98.67 % | 98.90 % | 99.18 % | 99.56 % | 99.56 % | 99.72 % | 99.75 % | 91.71 % |
| GNB | 1 | 93.33 % | 93.07 % | 93.12 % | 93.42 % | 93.28 % | 93.31 % | 93.34 % | 91.46 % |
| | 2 | 96.00 % | 94.87 % | 94.65 % | 94.72 % | 94.89 % | 94.85 % | 94.89 % | 91.22 % |
| | 3 | 96.33 % | 95.53 % | 95.63 % | 95.57 % | 95.61 % | 95.63 % | 95.66 % | 90.98 % |
| | 4 | 96.17 % | 96.07 % | 95.88 % | 96.03 % | 96.05 % | 96.06 % | 96.06 % | 90.73 % |
| | 5 | 97.17 % | 96.70 % | 96.15 % | 96.40 % | 96.43 % | 96.33 % | 96.35 % | 90.49 % |
| | 6 | 97.17 % | 96.90 % | 96.50 % | 96.58 % | 96.63 % | 96.54 % | 96.53 % | 90.24 % |
| | 7 | 96.83 % | 96.97 % | 96.62 % | 96.70 % | 96.75 % | 96.67 % | 96.70 % | 90.00 % |

According to the results of the first round, the SVM with the RBF kernel and LR classifiers give more accurate results than the SVM with the linear kernel. The results of the first round showed also that using bigger datasets yields more accurate results, but the differences in the accuracies between the largest dataset sizes is moderate. Therefore, in the following rounds, the SVM classifier was used with the RBF kernel only and the dataset size was 100 000 samples per class.

*Table 7. Results of the second round*

| | | Feature | | | | | Best | | Colour |
|---|---|---|---|---|---|---|---|---|---|
| Classifier | Cycles | ACC PWR | ACC ABS | VEL RMS | FFT 1.0 | FFT 1.5 | Feature | | bar |
| LR | 1 | 96.95 % | 97.07 % | 95.82 % | 72.00 % | 93.26 % | ACC ABS | | 100.0 % |
| | 2 | 98.69 % | 98.90 % | 99.39 % | 88.89 % | 99.14 % | VEL RMS | | 99.18 % |
| | 3 | 99.18 % | 99.33 % | 96.71 % | 87.83 % | 98.14 % | ACC ABS | | 98.35 % |
| | 4 | 99.45 % | 99.61 % | 96.69 % | 92.99 % | 99.74 % | FFT 1.5 | | 97.53 % |
| | 5 | 99.58 % | 99.71 % | 98.76 % | 91.43 % | 99.23 % | ACC ABS | | 96.71 % |
| | 6 | 99.69 % | 99.79 % | 98.91 % | 94.98 % | 99.87 % | FFT 1.5 | | 95.88 % |
| | 7 | 99.75 % | 99.85 % | 99.23 % | 93.36 % | 99.61 % | ACC ABS | | 95.06 % |
| SVM RBF | 1 | 97.45 % | 97.46 % | 97.59 % | 89.18 % | 96.53 % | VEL RMS | | 94.24 % |
| | 2 | 99.08 % | 99.15 % | 99.62 % | 93.74 % | 99.72 % | FFT 1.5 | | 93.41 % |
| | 3 | 99.52 % | 99.54 % | 98.38 % | 94.93 % | 99.29 % | ACC ABS | | 92.59 % |
| | 4 | 99.74 % | 99.77 % | 98.61 % | 96.50 % | 99.94 % | FFT 1.5 | | 91.76 % |
| | 5 | 99.83 % | 99.85 % | 99.44 % | 96.46 % | 99.74 % | ACC ABS | | 90.94 % |
| | 6 | 99.89 % | 99.91 % | 99.53 % | 97.62 % | 99.98 % | FFT 1.5 | | 90.12 % |
| | 7 | 99.92 % | 99.94 % | 99.62 % | 97.31 % | 99.90 % | ACC ABS | | 89.29 % |
| DT | 1 | 95.79 % | 95.99 % | 96.36 % | 82.26 % | 94.06 % | VEL RMS | | 88.47 % |
| | 2 | 97.78 % | 98.12 % | 99.12 % | 90.69 % | 99.13 % | FFT 1.5 | | 87.65 % |
| | 3 | 98.33 % | 98.62 % | 97.98 % | 91.21 % | 98.28 % | ACC ABS | | 86.82 % |
| | 4 | 98.72 % | 99.05 % | 98.49 % | 94.22 % | 99.70 % | FFT 1.5 | | 86.00 % |
| | 5 | 98.93 % | 99.18 % | 98.99 % | 93.54 % | 99.13 % | ACC ABS | | 85.18 % |
| | 6 | 99.13 % | 99.34 % | 99.21 % | 95.82 % | 99.70 % | FFT 1.5 | | 84.35 % |
| | 7 | 99.18 % | 99.37 % | 99.24 % | 94.83 % | 99.44 % | FFT 1.5 | | 83.53 % |
| KNN | 1 | 96.14 % | 95.84 % | 96.62 % | 82.22 % | 94.82 % | VEL RMS | | 82.71 % |
| | 2 | 98.27 % | 98.00 % | 99.44 % | 90.04 % | 99.46 % | FFT 1.5 | | 81.88 % |
| | 3 | 98.90 % | 98.70 % | 97.48 % | 90.52 % | 98.76 % | ACC PWR | | 81.06 % |
| | 4 | 99.36 % | 99.19 % | 97.53 % | 94.25 % | 99.87 % | FFT 1.5 | | 80.24 % |
| | 5 | 99.54 % | 99.41 % | 99.14 % | 93.08 % | 99.54 % | ACC PWR | | 79.41 % |
| | 6 | 99.69 % | 99.59 % | 99.31 % | 95.93 % | 99.95 % | FFT 1.5 | | 78.59 % |
| | 7 | 99.75 % | 99.68 % | 99.41 % | 94.99 % | 99.79 % | FFT 1.5 | | 77.76 % |
| GNB | 1 | 93.34 % | 93.80 % | 93.94 % | 80.27 % | 90.82 % | VEL RMS | | 76.94 % |
| | 2 | 94.89 % | 95.51 % | 97.96 % | 88.21 % | 96.27 % | VEL RMS | | 76.12 % |
| | 3 | 95.66 % | 96.25 % | 95.45 % | 88.52 % | 94.05 % | ACC ABS | | 75.29 % |
| | 4 | 96.06 % | 96.71 % | 94.97 % | 91.31 % | 96.65 % | ACC ABS | | 74.47 % |
| | 5 | 96.35 % | 97.01 % | 97.46 % | 90.90 % | 95.50 % | VEL RMS | | 73.65 % |
| | 6 | 96.53 % | 97.23 % | 97.45 % | 92.77 % | 96.89 % | VEL RMS | | 72.82 % |
| | 7 | 96.70 % | 97.40 % | 97.79 % | 91.94 % | 96.26 % | VEL RMS | | 72.00 % |

*Table 8. Main results of the third round: classification accuracies using the SVM RBF algorithm*

| Feature | Cycles | Point P1 | P2 | P3 | P4 | Best Point | Colour bar |
|---|---|---|---|---|---|---|---|
| ACC PWR | 1 | 91.49 % | 79.19 % | 93.64 % | 70.12 % | P3 | 100.0 % |
| | 2 | 93.54 % | 83.97 % | 96.21 % | 78.22 % | P3 | 98.50 % |
| | 3 | 94.12 % | 85.83 % | 96.94 % | 81.51 % | P3 | 97.00 % |
| | 4 | 94.62 % | 87.02 % | 97.59 % | 83.49 % | P3 | 95.50 % |
| | 5 | 94.85 % | 87.74 % | 97.86 % | 84.63 % | P3 | 94.00 % |
| | 6 | 95.08 % | 88.34 % | 98.12 % | 85.45 % | P3 | 92.50 % |
| | 7 | 95.18 % | 88.80 % | 98.25 % | 86.02 % | P3 | 91.00 % |
| ACC ABS | 1 | 91.97 % | 78.82 % | 93.35 % | 67.42 % | P3 | 89.50 % |
| | 2 | 93.96 % | 84.17 % | 96.61 % | 76.25 % | P3 | 88.00 % |
| | 3 | 94.57 % | 86.26 % | 97.33 % | 79.96 % | P3 | 86.50 % |
| | 4 | 95.00 % | 87.56 % | 98.03 % | 82.11 % | P3 | 85.00 % |
| | 5 | 95.24 % | 88.30 % | 98.24 % | 83.43 % | P3 | 83.50 % |
| | 6 | 95.44 % | 89.02 % | 98.57 % | 84.35 % | P3 | 82.00 % |
| | 7 | 95.53 % | 89.51 % | 98.68 % | 85.08 % | P3 | 80.50 % |
| VEL RMS | 1 | 91.17 % | 93.66 % | 93.52 % | 92.40 % | P2 | 79.00 % |
| | 2 | 96.43 % | 97.44 % | 97.15 % | 97.95 % | P4 | 77.50 % |
| | 3 | 93.74 % | 95.89 % | 91.04 % | 94.15 % | P2 | 76.00 % |
| | 4 | 94.75 % | 96.26 % | 89.83 % | 93.96 % | P2 | 74.50 % |
| | 5 | 96.09 % | 97.63 % | 95.49 % | 96.89 % | P2 | 73.00 % |
| | 6 | 97.28 % | 97.77 % | 96.24 % | 96.78 % | P2 | 71.50 % |
| | 7 | 96.96 % | 97.93 % | 96.67 % | 97.75 % | P2 | 70.00 % |
| FFT 1.0 | 1 | 57.72 % | 49.68 % | 77.75 % | 53.96 % | P3 | 68.50 % |
| | 2 | 65.46 % | 62.73 % | 81.31 % | 59.67 % | P3 | 67.00 % |
| | 3 | 65.67 % | 64.57 % | 84.15 % | 60.74 % | P3 | 65.50 % |
| | 4 | 72.83 % | 72.18 % | 84.42 % | 70.04 % | P3 | 64.00 % |
| | 5 | 70.46 % | 71.28 % | 84.70 % | 66.70 % | P3 | 62.50 % |
| | 6 | 76.92 % | 78.14 % | 85.99 % | 75.90 % | P3 | 61.00 % |
| | 7 | 73.59 % | 75.42 % | 85.04 % | 71.66 % | P3 | 59.50 % |
| FFT 1.5 | 1 | 89.01 % | 92.17 % | 77.55 % | 86.70 % | P2 | 58.00 % |
| | 2 | 95.84 % | 97.66 % | 92.18 % | 96.63 % | P2 | 56.50 % |
| | 3 | 92.74 % | 96.55 % | 85.32 % | 93.54 % | P2 | 55.00 % |
| | 4 | 96.47 % | 98.29 % | 95.63 % | 98.04 % | P2 | 53.50 % |
| | 5 | 94.54 % | 97.89 % | 89.49 % | 96.34 % | P2 | 52.00 % |
| | 6 | 97.02 % | 98.80 % | 96.53 % | 98.69 % | P2 | 50.50 % |
| | 7 | 95.67 % | 98.52 % | 92.36 % | 97.64 % | P2 | 49.00 % |

The results of the second and the third rounds proved the superiority of the feature FFT 1.5 over the VEL RMS in terms of classification accuracy, in addition to its superiority in computational efficiency. Therefore, the feature FFT 1.5 was chosen for the classification tasks of the fourth round. The differences in the classification accuracies between using one of the two features, ACC ABS or ACC PWR, were marginal.

Therefore, the features ACC PWR and ACC ABS were both paired with the feature FFT 1.5 for the fourth round.

*Table 9. Main results of the fourth round: classification accuracies using the SVM RBF algorithm*

| Cycles | Feature Comb. with FFT 1.5 | Point P1 | Point P2 | Point P3 | Point P4 | Best Combination | Colour bar |
|---|---|---|---|---|---|---|---|
| 1 | **ACC PWR** | 96.34 % | 93.74 % | 95.56 % | 89.23 % | P1 | 100.0 % |
| | **ACC ABS** | 96.50 % | 93.85 % | 95.40 % | 88.78 % | ACC ABS | 99.08 % |
| 2 | **ACC PWR** | 99.27 % | 98.41 % | 98.39 % | 98.43 % | P1 | 98.15 % |
| | **ACC ABS** | 99.12 % | 98.45 % | 98.51 % | 98.22 % | ACC PWR | 97.23 % |
| 3 | **ACC PWR** | 98.72 % | 97.84 % | 98.25 % | 95.97 % | P1 | 96.31 % |
| | **ACC ABS** | 98.81 % | 97.94 % | 98.35 % | 95.69 % | ACC ABS | 95.38 % |
| 4 | **ACC PWR** | 99.76 % | 99.24 % | 99.39 % | 99.45 % | P1 | 94.46 % |
| | **ACC ABS** | 99.63 % | 99.26 % | 99.54 % | 99.33 % | ACC PWR | 93.54 % |
| 5 | **ACC PWR** | 99.37 % | 98.92 % | 98.97 % | 98.30 % | P1 | 92.62 % |
| | **ACC ABS** | 99.38 % | 98.96 % | 99.08 % | 98.17 % | ACC ABS | 91.69 % |
| 6 | **ACC PWR** | 99.86 % | 99.53 % | 99.62 % | 99.71 % | P1 | 90.77 % |
| | **ACC ABS** | 99.77 % | 99.54 % | 99.76 % | 99.65 % | ACC PWR | 89.85 % |
| 7 | **ACC PWR** | 99.68 % | 99.40 % | 99.35 % | 99.27 % | P1 | 88.92 % |
| | **ACC ABS** | 99.63 % | 99.42 % | 99.45 % | 99.18 % | ACC ABS | 88.00 % |

The best result is achieved using the combination of the features FFT 1.5 and ACC PWR extracted using a sequence length of six engine cycles from the signals measured at point P1. The classification accuracies, training times and prediction rates (thousands of samples per second) for the five different algorithms trained and tested using the features FFT 1.5 and ACC PWR extracted using all sequence lengths from the signals measured at point P1 are presented in 0, in Table 11, and in Table 12 respectively.

*Table 10. The results of the fourth round: Classification accuracies by the five different algorithms using the features FFT 1.5 and ACC PWR extracted using all sequence lengths from the signals measured at point P1 combined*

| Point | Classifier | Cycles 1 | 2 | 3 | 4 | 5 | 6 | 7 | Colour bar |
|---|---|---|---|---|---|---|---|---|---|
| P1 | LR | 95.14 % | 98.71 % | 97.81 % | 99.46 % | 98.77 % | 99.68 % | 99.22 % | 100.0 % |
| | SVM | 96.34 % | 99.27 % | 98.72 % | 99.76 % | 99.37 % | 99.86 % | 99.68 % | 99.00 % |
| | DT | 95.49 % | 98.60 % | 98.21 % | 99.25 % | 98.97 % | 99.40 % | 99.13 % | 98.00 % |
| | KNN | 95.14 % | 99.01 % | 98.26 % | 99.62 % | 99.21 % | 99.80 % | 99.59 % | 95.00 % |
| | GNB | 92.84 % | 97.27 % | 96.10 % | 97.94 % | 97.29 % | 98.27 % | 97.87 % | 92.00 % |

*Table 11. The results of the fourth round: Training times by the five different algorithms using the features FFT 1.5 and ACC PWR extracted using all sequence lengths from the signals measured at point P1 combined*

| Point | Classifier | Cycles 1 | 2 | 3 | 4 | 5 | 6 | 7 | Colour bar |
|---|---|---|---|---|---|---|---|---|---|
| P1 | LR | 733.8 | 670.6 | 810.2 | 566.1 | 640.8 | 529.8 | 585.6 | 3000 |
| | SVM | 3031.4 | 678.0 | 1191.8 | 308.9 | 634.2 | 207.0 | 386.2 | 2250 |
| | DT | 19.6 | 15.0 | 15.5 | 13.6 | 13.7 | 13.5 | 14.8 | 1500 |
| | KNN | 5.8 | 5.7 | 6.7 | 6.0 | 6.4 | 6.8 | 6.2 | 750 |
| | GNB | 0.5 | 0.5 | 0.6 | 0.6 | 0.6 | 0.6 | 0.6 | 0 |

*Table 12. The results of the fourth round: Prediction rates in thousands of samples per second by the five different algorithms using the features FFT 1.5 and ACC PWR extracted using all sequence lengths from the signals measured at point P1 combined*

| Point | Classifier | Cycles 1 | 2 | 3 | 4 | 5 | 6 | 7 | Colour bar |
|---|---|---|---|---|---|---|---|---|---|
| P1 | LR | 1972.2 | 1703.7 | 2304.8 | 2108.1 | 2603.6 | 2914.1 | 1972.8 | 3000 |
| | SVM | 0.0 | 0.1 | 0.1 | 0.3 | 0.1 | 0.5 | 0.2 | 2000 |
| | DT | 1812.6 | 1658.2 | 1726.4 | 2026.3 | 2046.0 | 2564.0 | 2022.1 | 1000 |
| | KNN | 0.6 | 0.6 | 0.6 | 0.7 | 0.7 | 0.6 | 0.7 | 500 |
| | GNB | 366.4 | 365.6 | 322.3 | 350.2 | 314.3 | 260.7 | 311.3 | 0 |

The accuracy of the most accurate classifier model was further improved by tuning the parameters C and γ of the SVM classifier. The value of the parameter C, used previously in all classification tasks of this study, was 10. The default value in scikit-learn for the parameter γ is relational to the size of the dataset and to the variance of the data, if not given as input parameter. Considering the dataset which gave the best classification result, the value of the parameter gamma was 0.1667.

A search grid was formed around the previously used values of the parameters C and γ by using powers -1 to 10 of 10 as the values for C and powers -2 to 2 of 10 for γ. As all previous classification tasks, the classification tasks of the grid search were performed using fivefold stratified cross-validation. The results of the grid search are presented in Table 13.

*Table 13. Grid search results*

| C | γ 0.01 | 0.1 | 1 | 10 | 100 | Colour bar |
|---|---|---|---|---|---|---|
| $10^{-1}$ | 99.237 % | 99.691 % | 99.863 % | 99.924 % | 99.668 % | 100.00 % |
| $10^{0}$ | 99.638 % | 99.792 % | 99.886 % | 99.938 % | 99.927 % | 99.927 % |
| $10^{1}$ | 99.705 % | 99.849 % | 99.911 % | 99.948 % | 99.929 % | 99.855 % |
| $10^{2}$ | 99.760 % | 99.875 % | 99.924 % | 99.945 % | 99.924 % | 99.782 % |
| $10^{3}$ | 99.842 % | 99.894 % | 99.934 % | 99.927 % | 99.921 % | 99.709 % |
| $10^{4}$ | 99.873 % | 99.912 % | 99.939 % | 99.911 % | 99.921 % | 99.636 % |
| $10^{5}$ | 99.889 % | 99.924 % | 99.939 % | 99.894 % | 99.921 % | 99.564 % |
| $10^{6}$ | 99.895 % | 99.930 % | 99.935 % | 99.889 % | 99.921 % | 99.491 % |
| $10^{7}$ | 99.894 % | 99.930 % | 99.924 % | 99.889 % | 99.921 % | 99.418 % |
| $10^{8}$ | 99.892 % | 99.930 % | 99.925 % | 99.889 % | 99.921 % | 99.345 % |
| $10^{9}$ | 99.893 % | 99.930 % | 99.922 % | 99.889 % | 99.921 % | 99.273 % |
| $10^{10}$ | 99.894 % | 99.930 % | 99.924 % | 99.889 % | 99.921 % | 99.200 % |

Parameter value combinations C = 10, γ = 10 and C = $10^{10}$, γ = 0.1 were used in the final round of classification training and testing. The first combination was chosen because it gave the best accuracy, and the second was chosen because it is the fastest for predicting. The combination of the FFT 1.5 and ACC PWR features, extracted using all sequence lengths from the signals measured at point P1, were used in the final round.

During the feature extraction part of this study, datasets of normal operation data were created containing 300 000 feature values for each class. Only one-third of the samples had been used so far during the rounds of classifier training and testing. Therefore, contrary to the preceding rounds, cross-validation was not used, and all the previously used 100 000 data samples per class were used in the classifier trainings of the final round. The testing was done using the unused data samples in the datasets of 300 000 samples per class. The results of the final round, including the accuracies, testing times in minutes and prediction rates in samples per second, are presented in 0.

*Table 14. Results of the final round*

| | Accuracy | | Training time [min] | | Prediction rate [sample/s] | |
|---|---|---|---|---|---|---|
| **Cycles** | **C=10, γ = 10** | **C=$10^{10}$, γ = 0.1** | **C=10, γ = 10** | **C=$10^{10}$, γ = 0.1** | **C=10, γ = 10** | **C=$10^{10}$, γ = 0.1** |
| **1** | 96.422 % | 96.578 % | 105 | 15799 | 156 | 271 |
| **2** | 99.444 % | 99.416 % | 15 | 1430 | 758 | 1442 |
| **3** | 99.041 % | 99.013 % | 20 | 2164 | 475 | 649 |
| **4** | 99.876 % | 99.855 % | 9 | 369 | 1688 | 4151 |
| **5** | 99.652 % | 99.614 % | 11 | 844 | 947 | 1779 |
| **6** | 99.950 % | 99.933 % | 5 | 76 | 4240 | 10549 |
| **7** | 99.872 % | 99.837 % | 8 | 359 | 1806 | 3777 |

The worst accuracy of the final round was achieved by using the sequence length of one cycle, and the best accuracy by using the sequence length of six cycles. The confusion matrices corresponding to the worst, and to the best, results using the combination C = 10, γ = 10 are presented in Figure 22 and in Figure 23 respectively.

| | Class | | | | | |
|---|---|---|---|---|---|---|
| **Class** | **100 %** | **95 %** | **90 %** | **75 %** | **50 %** | **0 %** |
| **100 %** | 177252 | 22455 | 293 | 0 | 0 | 0 |
| **95 %** | 18783 | 180896 | 321 | 0 | 0 | 0 |
| **90 %** | 254 | 268 | 199173 | 305 | 0 | 0 |
| **75 %** | 5 | 0 | 258 | 199737 | 0 | 0 |
| **50 %** | 0 | 0 | 0 | 0 | 200000 | 0 |
| **0 %** | 0 | 0 | 0 | 0 | 0 | 200000 |

*Figure 22. Results of the final round: Confusion matrix using sequence length of one engine cycles*

| | Class | | | | | |
|---|---|---|---|---|---|---|
| **Class** | **100 %** | **95 %** | **90 %** | **75 %** | **50 %** | **0 %** |
| **100 %** | 199743 | 257 | 0 | 0 | 0 | 0 |
| **95 %** | 345 | 199655 | 0 | 0 | 0 | 0 |
| **90 %** | 0 | 0 | 200000 | 0 | 0 | 0 |
| **75 %** | 0 | 0 | 0 | 200000 | 0 | 0 |
| **50 %** | 0 | 0 | 0 | 0 | 200000 | 0 |
| **0 %** | 0 | 0 | 0 | 0 | 0 | 200000 |

*Figure 23. Results of the final round: Confusion matrix using sequence length of six engine cycles*

## 4.4 Novelty detection

Two parameter sweeps were performed to find suitable values for the parameters ν and k of the two novelty detector algorithms One-class SVM and LOF. The best-performing features in the previous classification step, that is, the features FFT 1.5 and ACC PWR extracted using a sequence length of six engine cycles from the signals measured at point P1, were selected for the training of the novelty detectors used in the parameter sweeps. The features used were combined.

The data used previously for training the classifiers of normal operation was used for the training of the novelty detectors of each of the six different groups of power output level. Therefore, each dataset used for training a novelty detector consisted of 100 000 samples. The testing of the novelty detectors used in the parameter sweeps was done using the remaining 200 000 samples of data per class that was sampled in the datasets of normal operation data.

The goodness of the novelty detectors trained using the One-class SVM algorithm was evaluated based on two different properties: their ability to classify an equal or smaller proportion of new data from their own class as novel, as was indicated by the parameter ν, and their ability to classify data from another class as novel.

The second property was used as well when evaluating the goodness of the novelty detectors trained using the LOF algorithm. A smaller number of new data from the same class as the training data classified as novel was considered better when evaluating the novelty detectors trained using the LOF algorithm.

The results of the parameter sweep describing the first-mentioned property for novelty detectors trained using the One-class SVM algorithm are presented in Table 15. The values presented in Table 15 are the ratios of the values of parameter ν to the proportions of new data classified as novel by the trained novelty detector. Hence, values close to zero indicate a very large proportion of the new data classified as novel compared to the value of parameter ν and are, therefore, considered bad. Values close to one indicate that the proportion of as novel classified new data coincides with the value of parameter ν, which was desired. Values greater than one should be considered equally as good as one, because the parameter ν sets a limit for maximum amount of abnormal data in the training data.

*Table 15. Parameter sweep results for One-class SVM: Novelty detection against data from the same class as trained*

| | Value of Parameter v | | | | | | | Colour |
|---|---|---|---|---|---|---|---|---|
| Group | 0.00001 | 0.0001 | 0.001 | 0.005 | 0.01 | 0.02 | 0.05 | bar |
| 100 % | 0.007 | 0.074 | 0.592 | 0.903 | 0.951 | 0.969 | 0.988 | 1.000 |
| 95 % | 0.004 | 0.042 | 0.413 | 0.855 | 0.927 | 0.994 | 1.013 | 0.950 |
| 90 % | 0.012 | 0.122 | 0.791 | 0.993 | 1.006 | 0.986 | 1.006 | 0.900 |
| 75 % | 0.006 | 0.060 | 0.525 | 0.932 | 0.962 | 0.951 | 1.000 | 0.750 |
| 50 % | 0.007 | 0.068 | 0.585 | 0.883 | 0.918 | 0.927 | 0.978 | 0.500 |
| 0 % | 0.007 | 0.067 | 0.621 | 0.986 | 1.029 | 1.031 | 0.995 | 0.000 |

The number of samples in the test data, which belongs to the same class as the training data classified as novel by the novelty detectors trained by the LOF algorithm using different values of parameter k, are presented in Table 16. Smaller values of new data from the same class as the training data classified as novel were considered better in the case of the novelty detectors trained by the LOF algorithm.

*Table 16. Parameter sweep results for LOF: Novelty detection against data from the same class as trained*

| | Value of Parameter k | | | | | | | Colour |
|---|---|---|---|---|---|---|---|---|
| Group | 8 | 16 | 32 | 64 | 128 | 256 | 512 | bar |
| 100 % | 776 | 653 | 691 | 848 | 1062 | 1267 | 1486 | 2000 |
| 95 % | 447 | 381 | 442 | 599 | 896 | 1326 | 1926 | 1600 |
| 90 % | 842 | 447 | 330 | 397 | 562 | 884 | 1170 | 1200 |
| 75 % | 576 | 403 | 381 | 447 | 624 | 792 | 1131 | 800 |
| 50 % | 730 | 539 | 564 | 689 | 857 | 1057 | 1287 | 400 |
| 0 % | 415 | 339 | 372 | 535 | 756 | 1098 | 1622 | 0 |

The results of the parameter sweep describing the second-mentioned property for the novelty detectors trained by the One-class SVM algorithm, and for the novelty detectors trained by the LOF algorithm, are presented in Table 17 and in Table 18 respectively. The values presented in Table 17 and in Table 18 are the ratio of the number of new data samples classified as novel by the trained novelty detector to the total number of new data samples. Hence, zero indicates that no new data was classified as novel, and one indicates that all new data was classified as novel.

*Table 17. Parameter sweep result for One-class SVM: Novelty detection against data from the other classes*

| | Value of Parameter v | | | | | | | Colour |
|---|---|---|---|---|---|---|---|---|
| Group | 0.00001 | 0.0001 | 0.001 | 0.005 | 0.01 | 0.02 | 0.05 | bar |
| 100 % | 0.846 | 0.846 | 0.847 | 0.878 | 0.893 | 0.911 | 0.943 | 1.000 |
| 95 % | 0.967 | 0.967 | 0.967 | 0.972 | 0.975 | 0.980 | 0.988 | 0.968 |
| 90 % | 1.000 | 1.000 | 1.000 | 1.000 | 1.000 | 1.000 | 1.000 | 0.936 |
| 75 % | 1.000 | 1.000 | 1.000 | 1.000 | 1.000 | 1.000 | 1.000 | 0.904 |
| 50 % | 1.000 | 1.000 | 1.000 | 1.000 | 1.000 | 1.000 | 1.000 | 0.872 |
| 0 % | 1.000 | 1.000 | 1.000 | 1.000 | 1.000 | 1.000 | 1.000 | 0.840 |

*Table 18. Parameter sweep result for LOF: Novelty detection against data from the other classes*

| | Value of Parameter k | | | | | | | Colour |
|---|---|---|---|---|---|---|---|---|
| **Group** | **8** | **16** | **32** | **64** | **128** | **256** | **512** | **bar** |
| **100 %** | 0.960 | 0.957 | 0.954 | 0.948 | 0.937 | 0.922 | 0.902 | 1.000 |
| **95 %** | 0.966 | 0.968 | 0.969 | 0.971 | 0.974 | 0.976 | 0.978 | 0.980 |
| **90 %** | 1.000 | 1.000 | 1.000 | 0.996 | 0.999 | 1.000 | 1.000 | 0.960 |
| **75 %** | 1.000 | 1.000 | 1.000 | 1.000 | 1.000 | 1.000 | 1.000 | 0.940 |
| **50 %** | 1.000 | 1.000 | 1.000 | 1.000 | 1.000 | 1.000 | 1.000 | 0.920 |
| **0 %** | 1.000 | 1.000 | 1.000 | 1.000 | 1.000 | 1.000 | 1.000 | 0.900 |

The results presented in Table 17 and in Table 18 show that the novelty detectors trained using data from groups 0 % to 90 % classify new data almost ideally. The novelty detectors trained using data from groups 95 % and 100 % are not able to classify all new data from other groups as novel. It is mostly data from the 95 % group that is not classified correctly by the novelty detector trained using data from the 100 % group and vice versa. This can be seen if the ratios of the number of new data samples classified as novel by the trained novelty detector to the total number of new data samples are studied groupwise. The ratios are presented groupwise in Table 19.

*Table 19. Parameter sweep result for One-class SVM: Novelty detection against data from the other classes presented groupwise*

| **New Data** | **Novelty Detector Group** | | | | | | **Colour** |
|---|---|---|---|---|---|---|---|
| **Group** | **100 %** | **95 %** | **90 %** | **75 %** | **50 %** | **0 %** | **bar** |
| **100 %** | x | 0.877 | 1.000 | 1.000 | 1.000 | 1.000 | 1.000 |
| **95 %** | 0.467 | x | 1.000 | 1.000 | 1.000 | 1.000 | 0.890 |
| **90 %** | 1.000 | 1.000 | x | 1.000 | 1.000 | 1.000 | 0.780 |
| **75 %** | 1.000 | 1.000 | 1.000 | x | 1.000 | 1.000 | 0.670 |
| **50 %** | 1.000 | 1.000 | 1.000 | 1.000 | x | 1.000 | 0.560 |
| **0 %** | 1.000 | 1.000 | 1.000 | 1.000 | 1.000 | x | 0.450 |

A series of ones and zeros can be formed from the results of the novelty detection by denoting the novelties as ones and the inliers as zeros. Six such series, formed from the parameter sweep results for the novelty detectors trained by the One-class SVM and LOF algorithms using data from the 100 % group, are presented in Figure 24 and in Figure 25 respectively. The series presented in Figure 24 and Figure 25 were smoothed by calculating the moving average of the series of zeros and ones with a subset size of one engine cycle, that is 328 samples.


*Figure 24. Parameter sweep results for One-class SVM novelty detector fitted to 100 % group data, ν=0.01*

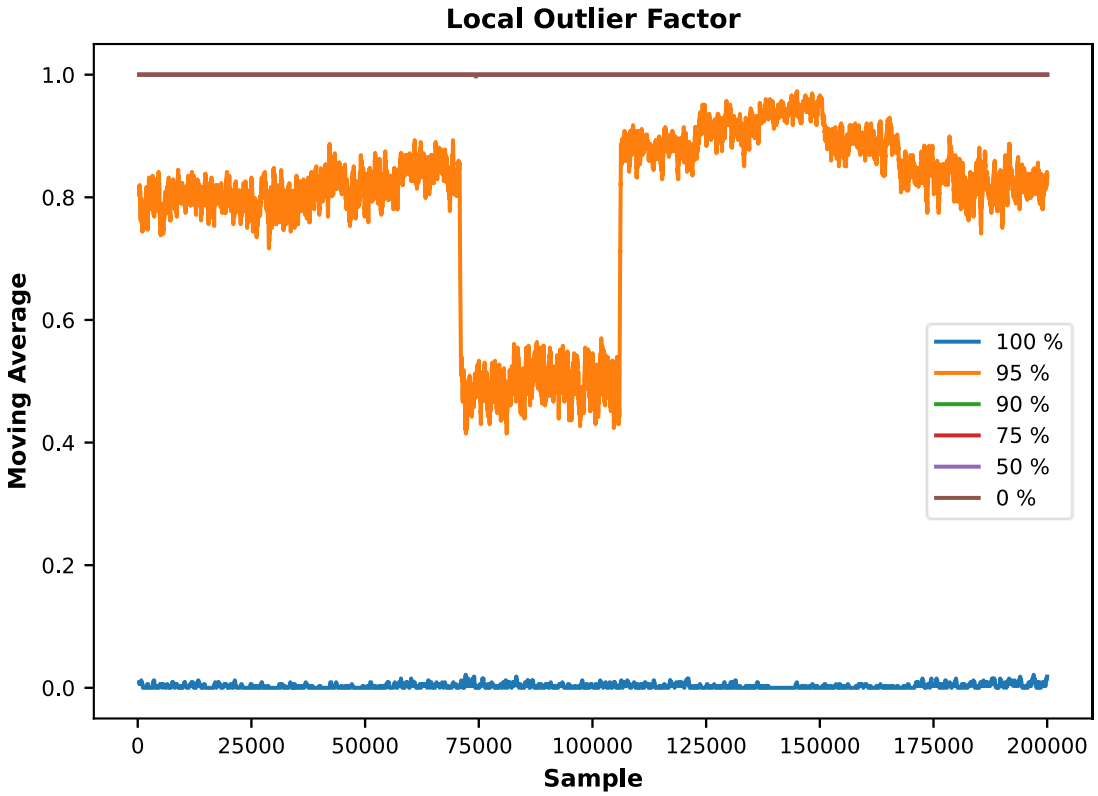


*Figure 25. Parameter sweep results for LOF novelty detector fitted to 100 % group data, k=16*

Based on the results of the parameter sweeps, values 0.01 and 16 were chosen for parameters ν and k of the One-class SVM and LOF algorithms, respectively. Novelty detectors were trained using the chosen parameter values for all groups except for the 0 % group, because no corresponding abnormal operation data was sampled. The training and testing of the novelty detectors were done using the features FFT 1.5 and ACC PWR, extracted using the 7 different sequence lengths from the signals measured at point P1. The two features were first used as combined, and then separately, for training the novelty detectors. The trained novelty detectors were run against the data sampled in the subsets of abnormal operation of their corresponding group. The number of the subsets of abnormal operation data per group was presented in Table 3 and anew below in Table 20.

*Table 20. The number of subsets of abnormal operation data by genset power output group.*

| Group | | | | |
|---|---|---|---|---|
| **100 %** | **95 %** | **90 %** | **75 %** | **50 %** |
| 8 | 6 | 6 | 12 | 8 |

The results of all novelty detection runs, using the features combined, using only the feature ACC PWR, and using only the feature FFT 1.5, are presented in Table 21, Table 22, and Table 23, respectively. The values presented in Table 21, Table 22 and Table 23 are the percentage of novel, or in this particular case, abnormal data, found in a subset by the trained novelty detector. The cells in Table 21, Table 22 and Table 23 are coloured green if the percentage of abnormal data is below the threshold.

Considering the results of the novelty detectors trained using the One-class SVM algorithm, a value below 1 % indicates that no abnormal data was found from the subset, because the value of parameter ν was 0.01. That is, the threshold value for the novelty detectors trained using the One-class SVM algorithm is 1 %. According to the parameter sweep results, proportions smaller than 0.35 % of the samples of new data from the same group as the training data were classified as novel by the novelty detectors trained using the LOF algorithm, and the value of the parameter k was 16. Therefore, values lower than 0.35 % indicate that no abnormal data was found by the novelty detectors trained using the LOF algorithm. That is, the threshold value for the novelty detectors trained using the LOF algorithm is 1 %. Independent of the algorithm used for training, a value of 100 % indicates that all data in the subset was abnormal or from another group of power output level.

*Table 21. Results for novelty detection runs using the features FFT 1.5 and ACC PWR combined, percentage of abnormal data found in the subsets of abnormal data by the trained novelty detectors*

| | | Cycles | | | | | | | | | | | | | |
|---|---|---|---|---|---|---|---|---|---|---|---|---|---|---|---|
| | | 1 | | 2 | | 3 | | 4 | | 5 | | 6 | | 7 | |
| Group | Subset | SVM | LOF | SVM | LOF | SVM | LOF | SVM | LOF | SVM | LOF | SVM | LOF | SVM | LOF |
| 100 % | 1 | 67 % | 60 % | 75 % | 70 % | 76 % | 66 % | 80 % | 73 % | 81 % | 70 % | 83 % | 82 % | 85 % | 75 % |
| | 2 | 15 % | 13 % | 18 % | 16 % | 16 % | 15 % | 17 % | 16 % | 17 % | 17 % | 19 % | 20 % | 18 % | 17 % |
| | 3 | 9 % | 7 % | 11 % | 10 % | 9 % | 9 % | 9 % | 10 % | 10 % | 10 % | 10 % | 13 % | 11 % | 12 % |
| | 4 | 25 % | 22 % | 31 % | 28 % | 31 % | 27 % | 36 % | 31 % | 36 % | 31 % | 41 % | 41 % | 39 % | 34 % |
| | 5 | 19 % | 16 % | 22 % | 21 % | 22 % | 20 % | 23 % | 23 % | 23 % | 21 % | 25 % | 26 % | 24 % | 24 % |
| | 6 | 45 % | 35 % | 53 % | 45 % | 54 % | 43 % | 59 % | 54 % | 58 % | 47 % | 63 % | 69 % | 63 % | 54 % |
| | 7 | 53 % | 51 % | 54 % | 54 % | 54 % | 52 % | 56 % | 57 % | 56 % | 54 % | 57 % | 65 % | 57 % | 56 % |
| | 8 | 32 % | 27 % | 43 % | 38 % | 43 % | 36 % | 45 % | 45 % | 47 % | 42 % | 49 % | 54 % | 48 % | 47 % |
| 95 % | 1 | 58 % | 57 % | 59 % | 58 % | 58 % | 57 % | 59 % | 59 % | 59 % | 59 % | 59 % | 60 % | 59 % | 59 % |
| | 2 | 58 % | 56 % | 60 % | 59 % | 61 % | 60 % | 62 % | 61 % | 62 % | 61 % | 63 % | 62 % | 63 % | 62 % |
| | 3 | 70 % | 63 % | 82 % | 75 % | 86 % | 79 % | 91 % | 86 % | 92 % | 87 % | 94 % | 91 % | 95 % | 91 % |
| | 4 | 61 % | 59 % | 63 % | 61 % | 63 % | 61 % | 63 % | 63 % | 64 % | 63 % | 64 % | 64 % | 64 % | 63 % |
| | 5 | 64 % | 61 % | 67 % | 65 % | 67 % | 65 % | 68 % | 66 % | 69 % | 66 % | 70 % | 69 % | 71 % | 68 % |
| | 6 | 61 % | 59 % | 63 % | 62 % | 62 % | 61 % | 63 % | 62 % | 63 % | 62 % | 63 % | 63 % | 64 % | 63 % |
| 90 % | 1 | 56 % | 49 % | 65 % | 63 % | 61 % | 55 % | 66 % | 75 % | 64 % | 63 % | 69 % | 86 % | 66 % | 70 % |
| | 2 | 58 % | 56 % | 62 % | 63 % | 61 % | 59 % | 61 % | 70 % | 62 % | 64 % | 62 % | 79 % | 62 % | 69 % |
| | 3 | 24 % | 22 % | 30 % | 32 % | 28 % | 29 % | 32 % | 39 % | 32 % | 37 % | 38 % | 49 % | 37 % | 46 % |
| | 4 | 21 % | 18 % | 26 % | 30 % | 24 % | 26 % | 27 % | 38 % | 27 % | 34 % | 28 % | 45 % | 28 % | 39 % |
| | 5 | 26 % | 23 % | 34 % | 33 % | 32 % | 31 % | 34 % | 41 % | 34 % | 37 % | 38 % | 53 % | 37 % | 45 % |
| | 6 | 21 % | 17 % | 34 % | 35 % | 27 % | 24 % | 35 % | 39 % | 31 % | 30 % | 40 % | 54 % | 33 % | 35 % |
| 75 % | 1 | 36 % | 31 % | 45 % | 45 % | 45 % | 44 % | 45 % | 45 % | 46 % | 47 % | 46 % | 47 % | 47 % | 47 % |
| | 2 | 38 % | 32 % | 45 % | 44 % | 44 % | 42 % | 43 % | 41 % | 45 % | 45 % | 45 % | 45 % | 47 % | 45 % |
| | 3 | 32 % | 25 % | 41 % | 39 % | 39 % | 38 % | 39 % | 36 % | 41 % | 40 % | 41 % | 40 % | 42 % | 40 % |
| | 4 | 66 % | 59 % | 80 % | 79 % | 81 % | 79 % | 81 % | 78 % | 85 % | 86 % | 86 % | 87 % | 87 % | 87 % |
| | 5 | 39 % | 34 % | 46 % | 44 % | 47 % | 46 % | 47 % | 47 % | 49 % | 50 % | 49 % | 51 % | 49 % | 52 % |
| | 6 | 37 % | 34 % | 41 % | 38 % | 40 % | 38 % | 39 % | 39 % | 40 % | 39 % | 41 % | 41 % | 41 % | 41 % |
| | 7 | 32 % | 29 % | 39 % | 36 % | 39 % | 36 % | 38 % | 37 % | 40 % | 40 % | 41 % | 42 % | 41 % | 44 % |
| | 8 | 36 % | 32 % | 46 % | 43 % | 46 % | 46 % | 46 % | 46 % | 48 % | 49 % | 48 % | 52 % | 48 % | 53 % |
| | 9 | 36 % | 32 % | 44 % | 43 % | 44 % | 45 % | 43 % | 45 % | 45 % | 48 % | 44 % | 51 % | 44 % | 51 % |
| | 10 | 28 % | 26 % | 35 % | 36 % | 36 % | 38 % | 36 % | 39 % | 38 % | 42 % | 39 % | 43 % | 39 % | 44 % |
| | 11 | 39 % | 35 % | 49 % | 48 % | 50 % | 50 % | 50 % | 51 % | 51 % | 54 % | 52 % | 55 % | 52 % | 54 % |
| | 12 | 40 % | 35 % | 47 % | 44 % | 46 % | 44 % | 45 % | 44 % | 47 % | 46 % | 48 % | 47 % | 48 % | 47 % |
| 50 % | 1 | 31 % | 30 % | 34 % | 32 % | 34 % | 33 % | 34 % | 35 % | 34 % | 37 % | 35 % | 40 % | 35 % | 42 % |
| | 2 | 7 % | 5 % | 13 % | 10 % | 14 % | 14 % | 15 % | 19 % | 17 % | 22 % | 20 % | 24 % | 24 % | 31 % |
| | 3 | 23 % | 16 % | 48 % | 33 % | 59 % | 41 % | 62 % | 50 % | 71 % | 55 % | 77 % | 60 % | 82 % | 68 % |
| | 4 | 15 % | 11 % | 19 % | 16 % | 17 % | 14 % | 14 % | 14 % | 18 % | 17 % | 17 % | 19 % | 16 % | 20 % |
| | 5 | 20 % | 17 % | 25 % | 24 % | 26 % | 26 % | 28 % | 26 % | 32 % | 34 % | 33 % | 33 % | 34 % | 34 % |
| | 6 | 14 % | 12 % | 16 % | 15 % | 18 % | 17 % | 18 % | 17 % | 21 % | 24 % | 23 % | 24 % | 24 % | 24 % |
| | 7 | 10 % | 9 % | 12 % | 10 % | 13 % | 12 % | 13 % | 12 % | 14 % | 12 % | 14 % | 14 % | 16 % | 19 % |
| | 8 | 10 % | 10 % | 12 % | 13 % | 12 % | 13 % | 12 % | 14 % | 14 % | 16 % | 15 % | 17 % | 15 % | 18 % |

*Table 22. Results for novelty detection runs using only the feature ACC PWR, percentage of abnormal data found in the subsets of abnormal data by the trained novelty detectors*

| | | Cycles & Algorithm | | | | | | | | | | | | | |
|---|---|---|---|---|---|---|---|---|---|---|---|---|---|---|---|
| | | 1 | | 2 | | 3 | | 4 | | 5 | | 6 | | 7 | |
| Group | Subset | SVM | LOF | SVM | LOF | SVM | LOF | SVM | LOF | SVM | LOF | SVM | LOF | SVM | LOF |
| 100 % | 1 | 63 % | 54 % | 76 % | 65 % | 75 % | 63 % | 79 % | 66 % | 80 % | 67 % | 84 % | 73 % | 84 % | 71 % |
| | 2 | 14 % | 10 % | 15 % | 13 % | 15 % | 13 % | 16 % | 15 % | 17 % | 15 % | 17 % | 16 % | 18 % | 16 % |
| | 3 | 7 % | 4 % | 9 % | 6 % | 9 % | 7 % | 8 % | 8 % | 8 % | 8 % | 9 % | 15 % | 9 % | 10 % |
| | 4 | 23 % | 18 % | 27 % | 22 % | 29 % | 23 % | 31 % | 26 % | 32 % | 27 % | 35 % | 30 % | 34 % | 30 % |
| | 5 | 18 % | 12 % | 23 % | 17 % | 24 % | 17 % | 24 % | 20 % | 25 % | 21 % | 27 % | 27 % | 27 % | 25 % |
| | 6 | 33 % | 26 % | 37 % | 31 % | 38 % | 32 % | 41 % | 33 % | 42 % | 35 % | 42 % | 37 % | 44 % | 39 % |
| | 7 | 50 % | 47 % | 52 % | 50 % | 53 % | 49 % | 55 % | 51 % | 56 % | 52 % | 57 % | 54 % | 57 % | 54 % |
| | 8 | 33 % | 23 % | 40 % | 34 % | 43 % | 35 % | 44 % | 39 % | 45 % | 38 % | 45 % | 39 % | 46 % | 40 % |
| 95 % | 1 | 54 % | 52 % | 56 % | 54 % | 56 % | 54 % | 57 % | 56 % | 57 % | 56 % | 57 % | 56 % | 57 % | 57 % |
| | 2 | 48 % | 45 % | 53 % | 50 % | 55 % | 52 % | 57 % | 54 % | 57 % | 56 % | 57 % | 57 % | 57 % | 56 % |
| | 3 | 60 % | 53 % | 73 % | 62 % | 79 % | 68 % | 82 % | 73 % | 86 % | 77 % | 89 % | 83 % | 91 % | 88 % |
| | 4 | 58 % | 53 % | 61 % | 59 % | 62 % | 60 % | 63 % | 62 % | 64 % | 63 % | 64 % | 63 % | 64 % | 63 % |
| | 5 | 58 % | 54 % | 62 % | 59 % | 62 % | 58 % | 65 % | 60 % | 66 % | 61 % | 67 % | 63 % | 68 % | 63 % |
| | 6 | 56 % | 50 % | 60 % | 55 % | 60 % | 56 % | 60 % | 59 % | 61 % | 58 % | 63 % | 60 % | 63 % | 61 % |
| 90 % | 1 | 53 % | 43 % | 62 % | 52 % | 62 % | 50 % | 67 % | 57 % | 70 % | 58 % | 74 % | 63 % | 75 % | 63 % |
| | 2 | 45 % | 40 % | 49 % | 45 % | 50 % | 47 % | 50 % | 48 % | 51 % | 48 % | 52 % | 51 % | 53 % | 53 % |
| | 3 | 23 % | 17 % | 26 % | 20 % | 27 % | 22 % | 29 % | 25 % | 30 % | 26 % | 33 % | 31 % | 33 % | 32 % |
| | 4 | 18 % | 14 % | 23 % | 18 % | 24 % | 20 % | 25 % | 24 % | 26 % | 24 % | 26 % | 26 % | 27 % | 26 % |
| | 5 | 24 % | 18 % | 30 % | 23 % | 31 % | 26 % | 33 % | 28 % | 33 % | 28 % | 36 % | 32 % | 36 % | 32 % |
| | 6 | 15 % | 10 % | 18 % | 13 % | 18 % | 13 % | 19 % | 16 % | 19 % | 16 % | 21 % | 19 % | 21 % | 19 % |
| 75 % | 1 | 31 % | 25 % | 39 % | 30 % | 42 % | 36 % | 44 % | 38 % | 45 % | 40 % | 47 % | 43 % | 47 % | 45 % |
| | 2 | 32 % | 24 % | 37 % | 30 % | 39 % | 33 % | 39 % | 35 % | 40 % | 37 % | 40 % | 38 % | 42 % | 40 % |
| | 3 | 24 % | 17 % | 27 % | 23 % | 30 % | 25 % | 31 % | 25 % | 34 % | 28 % | 35 % | 30 % | 36 % | 32 % |
| | 4 | 42 % | 32 % | 50 % | 40 % | 52 % | 44 % | 52 % | 48 % | 54 % | 51 % | 56 % | 52 % | 57 % | 55 % |
| | 5 | 33 % | 24 % | 36 % | 29 % | 38 % | 32 % | 39 % | 33 % | 42 % | 36 % | 44 % | 39 % | 45 % | 39 % |
| | 6 | 32 % | 25 % | 37 % | 32 % | 38 % | 36 % | 40 % | 38 % | 41 % | 39 % | 41 % | 40 % | 40 % | 41 % |
| | 7 | 26 % | 20 % | 31 % | 26 % | 33 % | 31 % | 33 % | 32 % | 33 % | 33 % | 34 % | 35 % | 35 % | 36 % |
| | 8 | 29 % | 22 % | 33 % | 27 % | 36 % | 31 % | 37 % | 35 % | 38 % | 37 % | 39 % | 39 % | 40 % | 41 % |
| | 9 | 29 % | 23 % | 33 % | 28 % | 34 % | 30 % | 36 % | 33 % | 37 % | 34 % | 38 % | 36 % | 38 % | 36 % |
| | 10 | 21 % | 17 % | 26 % | 21 % | 28 % | 25 % | 29 % | 27 % | 30 % | 29 % | 31 % | 29 % | 32 % | 30 % |
| | 11 | 34 % | 29 % | 37 % | 33 % | 38 % | 35 % | 38 % | 38 % | 39 % | 39 % | 39 % | 42 % | 39 % | 42 % |
| | 12 | 33 % | 28 % | 34 % | 31 % | 34 % | 32 % | 35 % | 34 % | 35 % | 36 % | 36 % | 38 % | 36 % | 38 % |
| 50 % | 1 | 21 % | 17 % | 25 % | 21 % | 28 % | 24 % | 29 % | 27 % | 30 % | 29 % | 31 % | 31 % | 31 % | 32 % |
| | 2 | 10 % | 4 % | 17 % | 10 % | 19 % | 13 % | 20 % | 17 % | 22 % | 22 % | 26 % | 25 % | 28 % | 29 % |
| | 3 | 27 % | 15 % | 50 % | 42 % | 57 % | 51 % | 61 % | 58 % | 68 % | 67 % | 73 % | 70 % | 76 % | 74 % |
| | 4 | 5 % | 2 % | 8 % | 6 % | 9 % | 7 % | 10 % | 9 % | 10 % | 9 % | 10 % | 9 % | 10 % | 9 % |
| | 5 | 15 % | 11 % | 17 % | 14 % | 18 % | 17 % | 20 % | 20 % | 21 % | 24 % | 23 % | 26 % | 23 % | 28 % |
| | 6 | 9 % | 6 % | 10 % | 8 % | 10 % | 8 % | 11 % | 10 % | 10 % | 10 % | 11 % | 11 % | 11 % | 12 % |
| | 7 | 10 % | 7 % | 13 % | 9 % | 17 % | 11 % | 21 % | 15 % | 21 % | 16 % | 25 % | 19 % | 29 % | 25 % |
| | 8 | 10 % | 9 % | 11 % | 10 % | 13 % | 12 % | 14 % | 13 % | 15 % | 15 % | 16 % | 15 % | 16 % | 16 % |

*Table 23. Results for novelty detection runs using only the feature FFT 1.5, percentage of abnormal data found in the subsets of abnormal data by the trained novelty detectors*

| | | Cycles & Algorithm | | | | | | | | | | | | | |
|---|---|---|---|---|---|---|---|---|---|---|---|---|---|---|---|
| | | 1 | | 2 | | 3 | | 4 | | 5 | | 6 | | 7 | |
| Group | Subset | SVM | LOF | SVM | LOF | SVM | LOF | SVM | LOF | SVM | LOF | SVM | LOF | SVM | LOF |
| 100 % | 1 | 31 % | 27 % | 44 % | 38 % | 33 % | 30 % | 44 % | 47 % | 35 % | 32 % | 53 % | 56 % | 39 % | 38 % |
| | 2 | 5 % | 3 % | 7 % | 5 % | 3 % | 2 % | 2 % | 1 % | 2 % | 1 % | 2 % | 2 % | 1 % | 0 % |
| | 3 | 5 % | 3 % | 7 % | 5 % | 3 % | 2 % | 3 % | 2 % | 2 % | 1 % | 2 % | 1 % | 1 % | 1 % |
| | 4 | 10 % | 6 % | 16 % | 11 % | 6 % | 3 % | 5 % | 2 % | 3 % | 1 % | 6 % | 4 % | 3 % | 1 % |
| | 5 | 10 % | 7 % | 13 % | 11 % | 7 % | 4 % | 5 % | 3 % | 5 % | 2 % | 7 % | 5 % | 4 % | 1 % |
| | 6 | 28 % | 17 % | 46 % | 34 % | 37 % | 24 % | 53 % | 40 % | 42 % | 30 % | 66 % | 62 % | 52 % | 38 % |
| | 7 | 32 % | 25 % | 43 % | 39 % | 37 % | 31 % | 40 % | 37 % | 39 % | 35 % | 41 % | 41 % | 38 % | 35 % |
| | 8 | 10 % | 7 % | 18 % | 15 % | 10 % | 6 % | 13 % | 10 % | 12 % | 9 % | 19 % | 18 % | 13 % | 10 % |
| 95 % | 1 | 48 % | 43 % | 55 % | 53 % | 51 % | 49 % | 51 % | 50 % | 50 % | 49 % | 53 % | 51 % | 50 % | 49 % |
| | 2 | 51 % | 46 % | 57 % | 54 % | 55 % | 52 % | 57 % | 54 % | 56 % | 54 % | 58 % | 55 % | 56 % | 53 % |
| | 3 | 37 % | 30 % | 49 % | 38 % | 39 % | 33 % | 48 % | 41 % | 42 % | 36 % | 54 % | 45 % | 47 % | 41 % |
| | 4 | 39 % | 30 % | 55 % | 46 % | 51 % | 42 % | 53 % | 47 % | 53 % | 48 % | 56 % | 51 % | 53 % | 50 % |
| | 5 | 32 % | 28 % | 45 % | 38 % | 36 % | 32 % | 46 % | 40 % | 41 % | 35 % | 52 % | 45 % | 45 % | 38 % |
| | 6 | 43 % | 36 % | 54 % | 49 % | 50 % | 44 % | 54 % | 49 % | 53 % | 48 % | 56 % | 52 % | 54 % | 50 % |
| 90 % | 1 | 26 % | 24 % | 49 % | 47 % | 41 % | 42 % | 49 % | 59 % | 46 % | 53 % | 51 % | 62 % | 47 % | 59 % |
| | 2 | 45 % | 43 % | 58 % | 58 % | 55 % | 57 % | 55 % | 64 % | 55 % | 62 % | 58 % | 74 % | 54 % | 69 % |
| | 3 | 15 % | 13 % | 25 % | 23 % | 18 % | 17 % | 20 % | 19 % | 19 % | 19 % | 22 % | 25 % | 20 % | 20 % |
| | 4 | 15 % | 13 % | 28 % | 23 % | 18 % | 17 % | 26 % | 23 % | 20 % | 21 % | 30 % | 28 % | 22 % | 26 % |
| | 5 | 14 % | 12 % | 26 % | 24 % | 19 % | 18 % | 21 % | 23 % | 21 % | 22 % | 23 % | 27 % | 20 % | 22 % |
| | 6 | 15 % | 13 % | 36 % | 28 % | 21 % | 19 % | 46 % | 33 % | 29 % | 27 % | 56 % | 50 % | 34 % | 29 % |
| 75 % | 1 | 21 % | 15 % | 38 % | 34 % | 37 % | 31 % | 35 % | 27 % | 38 % | 37 % | 37 % | 36 % | 37 % | 34 % |
| | 2 | 25 % | 17 % | 44 % | 39 % | 42 % | 38 % | 40 % | 34 % | 42 % | 42 % | 41 % | 41 % | 41 % | 39 % |
| | 3 | 22 % | 13 % | 40 % | 33 % | 37 % | 33 % | 36 % | 27 % | 40 % | 38 % | 39 % | 37 % | 39 % | 36 % |
| | 4 | 53 % | 39 % | 78 % | 71 % | 78 % | 74 % | 77 % | 72 % | 81 % | 85 % | 82 % | 84 % | 81 % | 84 % |
| | 5 | 21 % | 15 % | 33 % | 24 % | 34 % | 29 % | 32 % | 29 % | 35 % | 33 % | 35 % | 33 % | 34 % | 33 % |
| | 6 | 20 % | 15 % | 29 % | 21 % | 30 % | 24 % | 29 % | 25 % | 32 % | 28 % | 33 % | 29 % | 33 % | 29 % |
| | 7 | 19 % | 14 % | 33 % | 25 % | 34 % | 29 % | 32 % | 29 % | 36 % | 32 % | 36 % | 33 % | 35 % | 33 % |
| | 8 | 25 % | 18 % | 40 % | 30 % | 44 % | 38 % | 44 % | 41 % | 48 % | 45 % | 49 % | 47 % | 49 % | 48 % |
| | 9 | 19 % | 13 % | 34 % | 24 % | 36 % | 31 % | 34 % | 32 % | 36 % | 35 % | 35 % | 34 % | 34 % | 34 % |
| | 10 | 18 % | 13 % | 30 % | 22 % | 31 % | 28 % | 32 % | 30 % | 35 % | 34 % | 36 % | 33 % | 36 % | 33 % |
| | 11 | 20 % | 16 % | 36 % | 27 % | 38 % | 33 % | 38 % | 36 % | 40 % | 40 % | 40 % | 40 % | 41 % | 40 % |
| | 12 | 25 % | 18 % | 40 % | 33 % | 39 % | 36 % | 40 % | 38 % | 42 % | 40 % | 42 % | 40 % | 42 % | 42 % |
| 50 % | 1 | 24 % | 21 % | 27 % | 24 % | 28 % | 26 % | 28 % | 26 % | 28 % | 26 % | 29 % | 27 % | 29 % | 28 % |
| | 2 | 2 % | 1 % | 2 % | 1 % | 1 % | 1 % | 2 % | 1 % | 1 % | 1 % | 1 % | 2 % | 1 % | 2 % |
| | 3 | 4 % | 2 % | 9 % | 4 % | 7 % | 4 % | 4 % | 2 % | 11 % | 6 % | 9 % | 6 % | 9 % | 6 % |
| | 4 | 15 % | 8 % | 18 % | 11 % | 12 % | 6 % | 6 % | 3 % | 13 % | 6 % | 12 % | 5 % | 7 % | 3 % |
| | 5 | 7 % | 5 % | 9 % | 5 % | 12 % | 8 % | 13 % | 9 % | 15 % | 10 % | 16 % | 13 % | 17 % | 15 % |
| | 6 | 8 % | 6 % | 9 % | 6 % | 12 % | 8 % | 13 % | 9 % | 12 % | 9 % | 15 % | 11 % | 17 % | 14 % |
| | 7 | 2 % | 1 % | 3 % | 1 % | 2 % | 1 % | 1 % | 1 % | 1 % | 1 % | 1 % | 1 % | 1 % | 0 % |
| | 8 | 4 % | 2 % | 5 % | 3 % | 5 % | 3 % | 4 % | 2 % | 5 % | 3 % | 6 % | 4 % | 7 % | 5 % |

The minimum and the maximum values in Table 21, considering the novelty detectors trained by One-class SVM algorithm, are 6.9 % and 94.6 %, and considering the novelty detectors trained by the LOF algorithm are 5.1 % and 91.4 %. Corresponding maximum and minimum values in Table 22 are 5.4 % and 91.1 %, considering the novelty detectors trained by One-class SVM algorithm, and 2.2 % and 87.8 %, considering the novelty detectors trained by LOF algorithm, and correspondingly in Table 23 they are 0.9 % and 81.8 %, considering the novelty detectors trained by One-class SVM algorithm and 0.4 % and 84.6 %, considering the novelty detectors trained by LOF algorithm.

The average ratio of the abnormal predictions made using novelty detectors trained by the two algorithms with only the feature ACC PWR to abnormal predictions made using novelty detectors trained by the two algorithms with the features combined were 88.6 % for One-class SVM and 79.6 % for LOF. The corresponding average ratios, considering feature FFT 1.5 instead of feature ACC PWR, were 64.8 % (One-class SVM) and 56.4 % (LOF).

The chronological order of the samples in the subsets of abnormal operation data was conserved. Therefore, the results of a novelty detection run can be plotted against time forming a series of ones and zeros as was done previously for the results of the parameter sweep. As an example, the moving averages of the results of novelty detection runs with different levels of detected abnormal data are presented in the following three figures. All three figures include the moving average of the serialised results for novelty detectors trained by the two algorithms and with the features ACC PWR and FFT 1.5, extracted using a sequence length of six engine cycles combined.

First, the results for the novelty detections run against data from subset 3 of group 100 %, which have a relatively small proportion of abnormal data detected, that is 10 % by One-class SVM and 13 % by LOF, are presented in Figure 26. Then, the results for the novelty detections run against data from subset 5 of group 95 %, which have a relatively large proportion of abnormal data detected, that is 70 % by One-class SVM and 69 % by LOF, are presented in Figure 27. Finally, the results for the novelty detections run against data from subset 8 of group 75 %, which have balanced proportions of normal and abnormal data, that is 48 % by One-class SVM and 52 % by LOF, are presented in Figure 28.

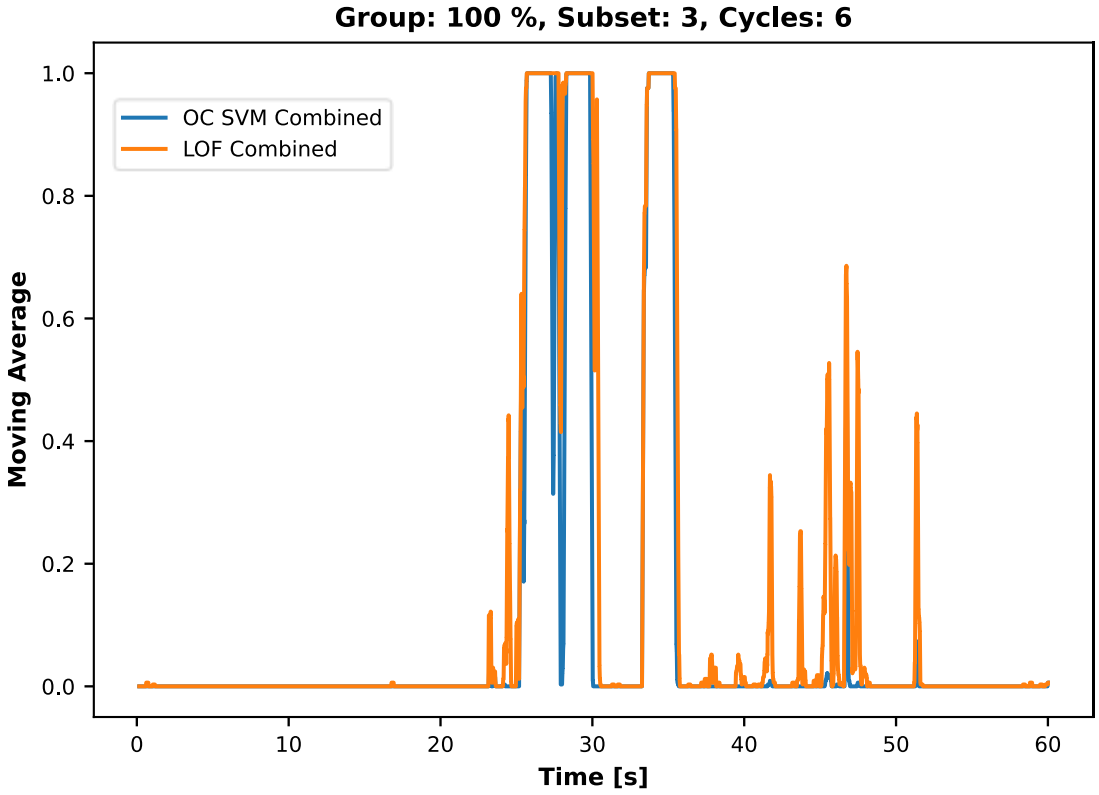


*Figure 26. Results for novelty detections run against data from subset 3 of group 100 %: Low proportion of test data classified as abnormal*

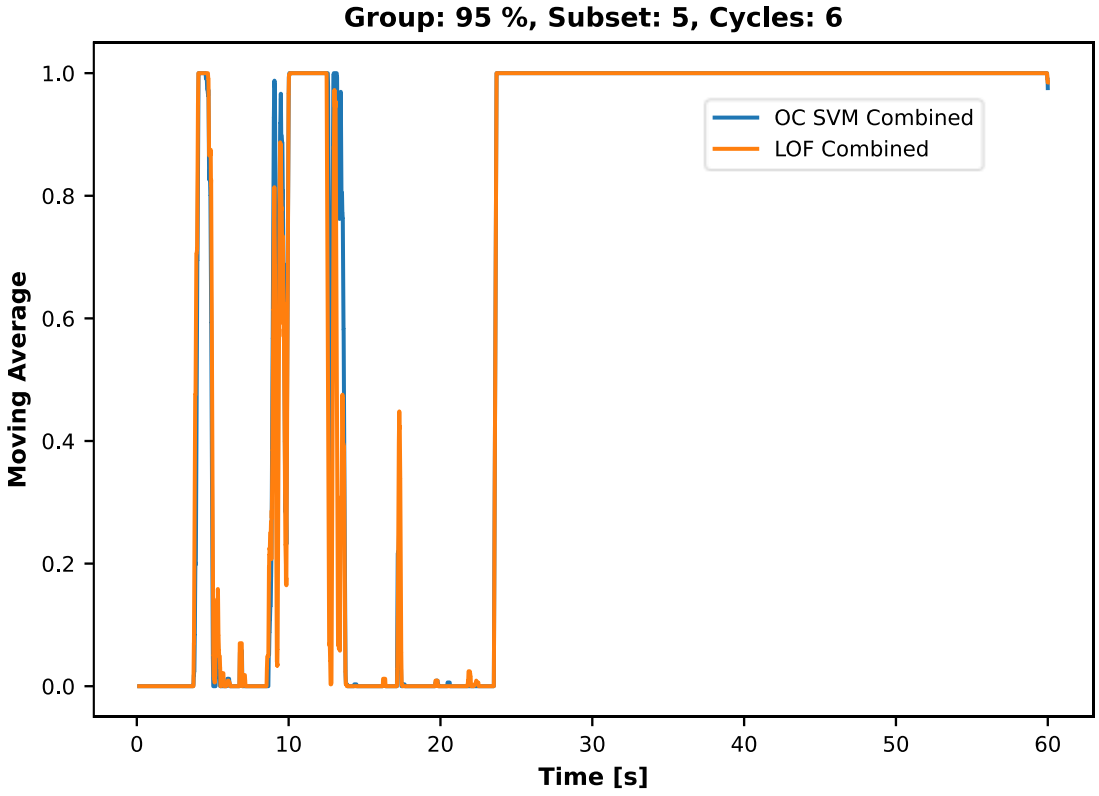


*Figure 27. Results for novelty detections run against data from subset 5 of group 95 %: High proportion of test data classified as abnormal*

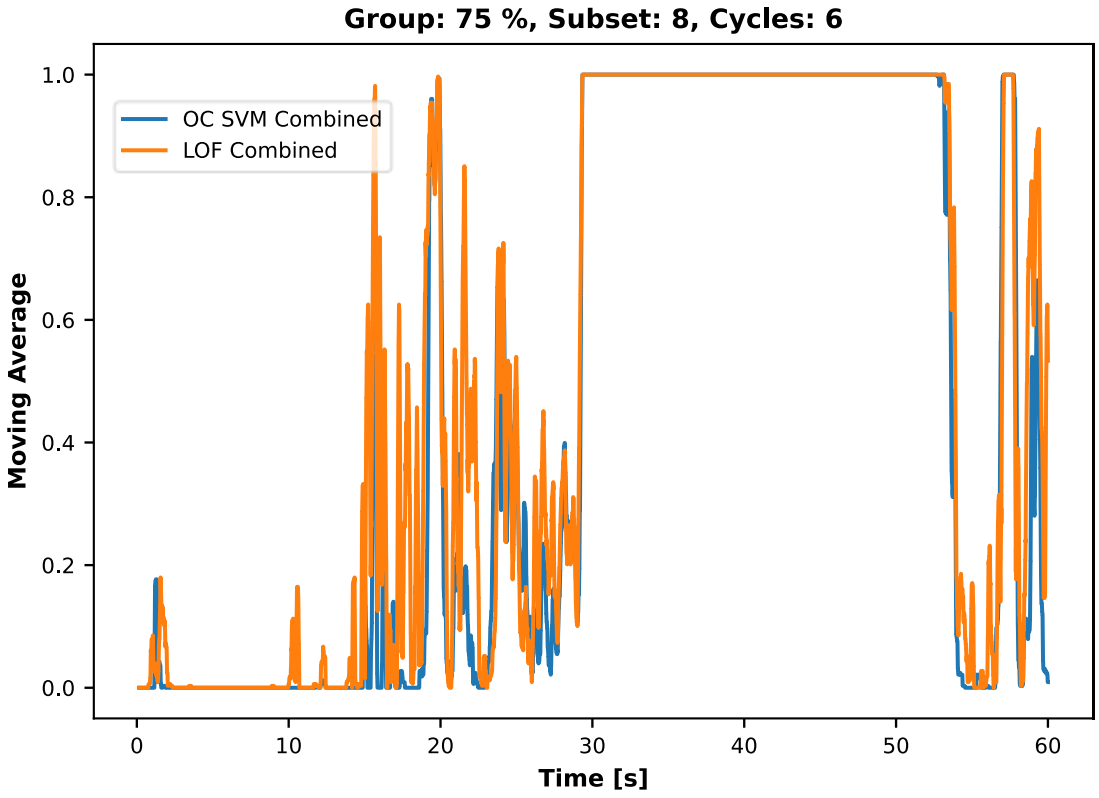


*Figure 28. Results for novelty detections run against data from subset 5 of group 95 %: balanced proportions of data classified as normal or abnormal*

As mentioned before, there are substantial differences in the average ratios of abnormal predictions made using novelty detectors trained with only one feature to abnormal predictions made using novelty detectors trained with the two features combined, especially considering the novelty detectors trained by the LOF algorithm and with only the feature FFT 1.5. The results for novelty detections, run using the novelty detectors trained by the LOF algorithm with the two features combined, and separately against data from subset 5 of group 50 %, are presented in Figure 29. The ratios of abnormal predictions to the total amount of data samples by the three novelty detectors were 33 % for the novelty detector trained with the features combined, 26 % for the novelty detector trained with only the ACC PWR feature, and 13 % for the novelty detector trained with only the FFT 1.5 feature.

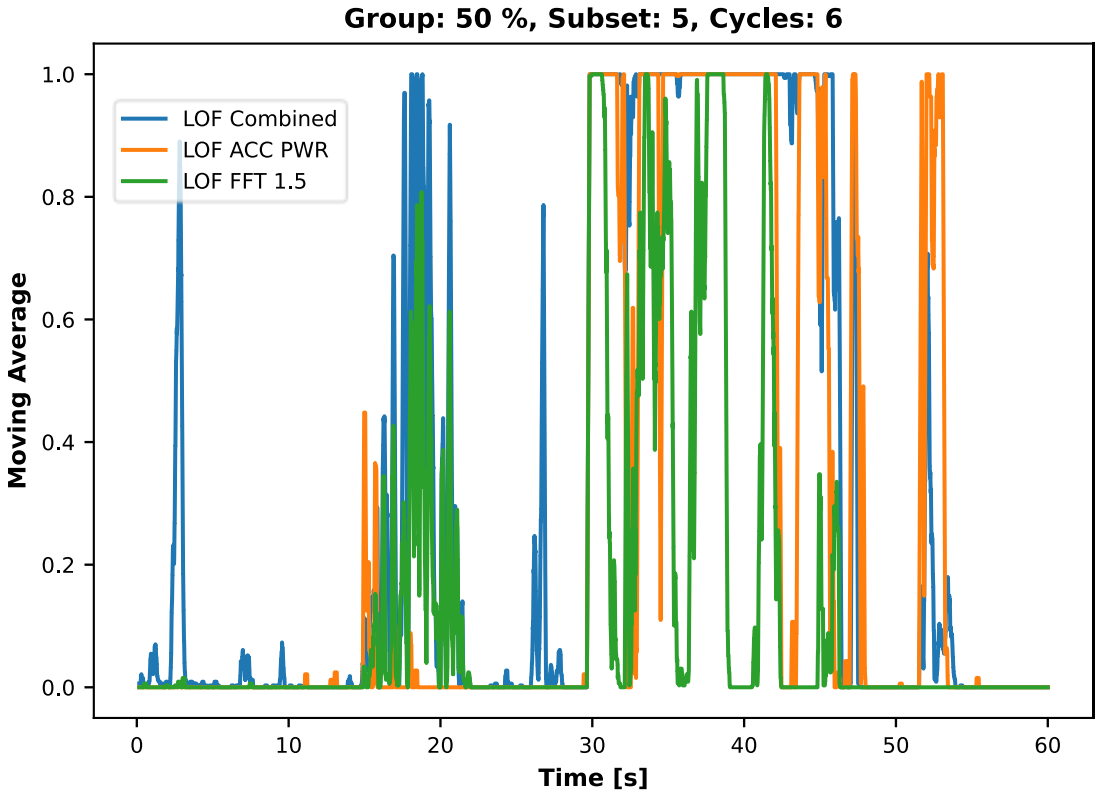


*Figure 29. Unbalanced ratios of data classified as abnormal to total amount of data in subset between the novelty detectors trained with features combined and separately*

The effect of the length of the sequence used in feature extraction can be seen in the novelty detection results presented in Table 21, Table 22 and Table 23. The novelty detectors trained with features extracted from shorter sequences of signal tend to find fewer abnormal samples from the training data than the novelty detectors trained with features extracted from longer sequences of signal. The results for three different novelty detection runs, using novelty detectors trained by the LOF algorithm with the features ACC PWR and FFT 1.5, combined against data from subset 2 of group 100 %, are presented in Figure 30. The difference between the three novelty detectors for which the results are shown in Figure 30 is that the features used in the training of the three novelty detectors were extracted using different lengths of signal sequences. The different lengths of signal sequences were one, two and six engine cycles.

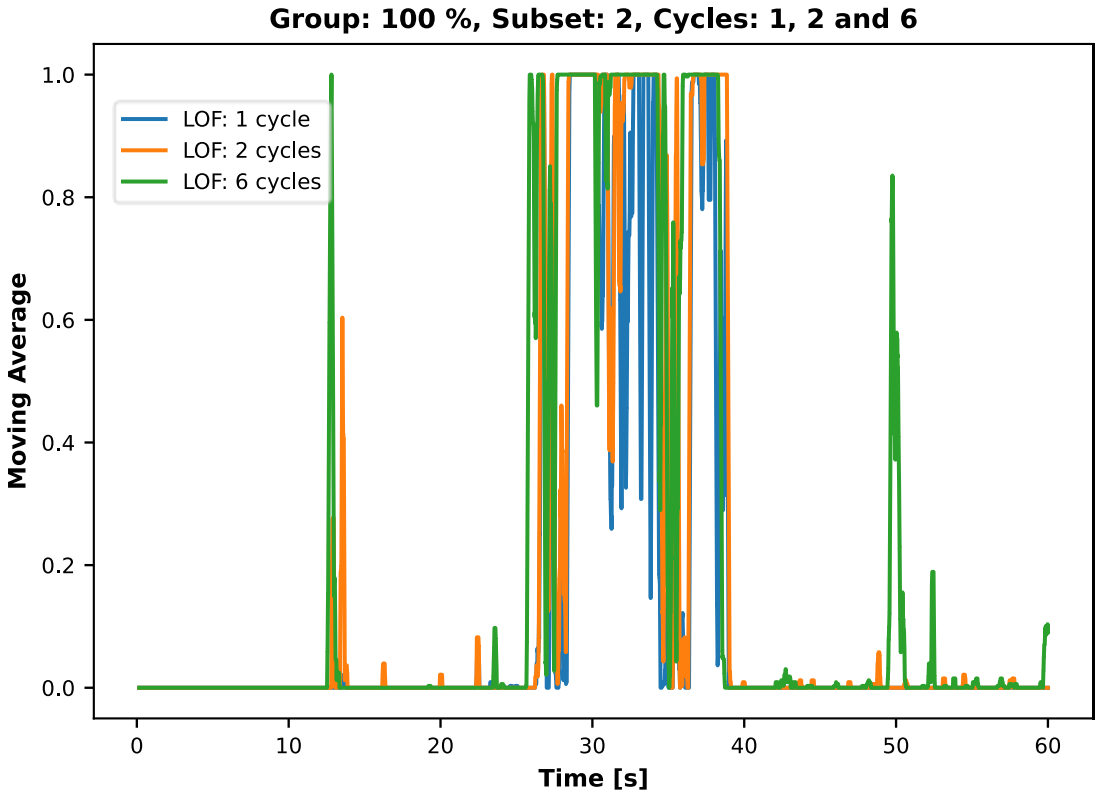


*Figure 30. Effect of training novelty detectors with features extracted using different lengths of signal sequences*

The training of a novelty detector by the One-class SVM algorithm took, on average, 15.2 s with the features combined, 22.6 s with only the feature ACC PWR and 23.5 s with only the feature FFT 1.5. The corresponding average training times of a novelty detector trained using the LOF algorithm were 7.7 s, 1.3 s and 1.3 using one CPU and 4.4 s, 0.9 s and 1.0 using four CPUs.

The testing of all 40 subsets of abnormal operation data, using a novelty detector trained by the One-class SVM algorithm, took, on average, 546.5 s with the features combined, 514.8 s with only the feature ACC PWR and 508.8 s with only the feature FFT 1.5. The aforementioned testing times correspond to prediction rates of 8 994, 9 548 and 9 661 samples classified per second respectively. The corresponding average testing times, using a novelty detector trained by the LOF algorithm, were 400.6 s, 48.2 s and 66.2 s using 1 CPU and 223.0 s, 37.5 s and 48.2 s using 4 CPUs. The testing times of the novelty detectors trained by the LOF algorithm correspond to prediction rates of 12 268, 101 948 and 74 239 samples classified per second using one CPU, and 21 392, 130 901 and 101 954 samples classified per second using 4 CPUs, respectively.

# 5 DISCUSSION AND CONCLUSIONS

This study was formed of three clear predefined steps, which lead to achieving the proposed objective. The number of results produced during the three steps and presented in the previous chapter is substantial. The most notable findings of each step are summed up and discussed in detail in this chapter. Some of the results already presented in the previous chapter are repeated partly or entirely in this chapter for ease of reading and better understanding. Finally, the conclusions made based on the summarised results are presented.

## 5.1 Discussion

The objective of this study was to provide a data-based model for operational state recognition and detection of abnormal operation of a gas engine genset in near real-time. Three different tasks to be fulfilled were defined in the beginning of the study to achieve this objective. The first task was to identify and sample data that represents different operational states of the genset into labelled datasets from the provided data.

A comprehensive dataset, or a collection of subsets of measured mechanical vibration data representing both normal and abnormal states of operation of the studied genset, was sampled from the provided data. Altogether, 442 minutes of the twelve different signals were sampled in subsets of normal operation data at six different levels of power output of the genset. The six different power output levels were 100 %, 95 %, 90 %, 75 %, 50 % and 0 %. The different power output levels were used for labelling the data into six different groups. Forty subsets of abnormal operation data were sampled from the provided data. The subsets of abnormal operation data contained one-minute-long sequences of the twelve signals.

The statistical analyses performed on the sampled data showed that the average signal power generally becomes higher as the power input increases. However, some exceptions to the rule were revealed when the average signal powers of the measurement points and directions were studied individually. For example, the average signal power measured at points P2 in X- and Y-directions, and P4 in X-direction are higher at 95 % than at 100 % of power output. The statistical analyses revealed also substantial variation in the average signal power between the subsets of normal operation data belonging to the same group

of power output level. Also, the differences between the signal powers of the signals sampled into the subsets of normal operation data compared to the signal powers of the signals sampled into the subsets of abnormal operation data are moderate. Hence, the statistical analysis proved that it is not possible to directly estimate the power output level of the genset, nor can the normal operation be distinguished from abnormal operation based on the average signal power. Therefore, the utilisation of ML algorithms to achieve the objective of this study is justified.

The second task was to extract computationally light features that are sensitive to the changes in the operational state of the genset from the sampled data. Five different computationally light functions were defined for extracting five different features. The functions were applied on short sequences of the sampled signals. The lengths of the sequences were integer multiples from one to seven of the duration of an engine cycle. Basing the sequence lengths on the duration of the engine cycle represents the cyclic nature of the operation of an ICE at constant rotation speed. Using longer sequences was assumed to smoothen the effect of the fluctuations between engine cycles that are typical, especially for SI engines.

The number of different extracted features was therefore 420, that is five different functions for feature extraction, times seven different sequence lengths, times twelve different measured signals. So, 300 000 feature values were extracted from the subsets of normal operation data per class for each of the 420 different features. These 300 000 feature values per class cover only approximately 3.3 % of the maximum number of feature values possible to extract from the 442 minutes of data sampled to the subsets of normal operation data. Although the coverage is relatively small, all the sampled data was included in the feature values due to the length of the sequence, due to dividing the number of samples extracted from the subsets relative to the size of the subsets and due to using random selection of the starting points of the sequences without duplicates. The minimum sequence length used in feature extraction was 328 samples.

The sensitivity of the features to the changes in the operational state of the genset, that is changes in the power output level of the genset, was studied by performing four rounds of classifier training and testing, meaning classification tasks. Six different classification algorithms were chosen for performing the classification tasks to find the most suitable classification algorithm for the purposes of this study. In addition, the effect of the size

of the dataset used in the classification tasks on the classification accuracy was studied during the first of the four rounds of classification tasks. The results of the first round considering the LR, SVM RBF and SVM LIN algorithms are presented in Table 24.

*Table 24. Results of the first round: LR, SVM RBF, and SVM LIN algorithms*

| | | Samples per Class | | | | | | |
|---|---|---|---|---|---|---|---|---|
| **Classifier** | **Cycles** | **100** | **500** | **1000** | **5000** | **10000** | **50000** | **100000** |
| **LR** | **1** | 94.67 % | 96.10 % | 96.27 % | 96.80 % | 96.88 % | 96.89 % | 96.95 % |
| | **2** | 97.50 % | 98.40 % | 98.28 % | 98.61 % | 98.63 % | 98.65 % | 98.69 % |
| | **3** | 97.83 % | 98.63 % | 98.87 % | 99.02 % | 99.12 % | 99.19 % | 99.18 % |
| | **4** | 98.50 % | 98.90 % | 99.13 % | 99.38 % | 99.41 % | 99.44 % | 99.45 % |
| | **5** | 99.17 % | 99.03 % | 99.22 % | 99.43 % | 99.56 % | 99.58 % | 99.58 % |
| | **6** | 99.17 % | 99.20 % | 99.28 % | 99.60 % | 99.63 % | 99.68 % | 99.69 % |
| | **7** | 99.17 % | 99.20 % | 99.42 % | 99.67 % | 99.71 % | 99.74 % | 99.75 % |
| **SVM RBF** | **1** | 96.50 % | 96.53 % | 96.93 % | 97.20 % | 97.34 % | 97.37 % | 97.45 % |
| | **2** | 98.50 % | 98.73 % | 98.83 % | 98.88 % | 98.99 % | 99.03 % | 99.08 % |
| | **3** | 98.83 % | 99.20 % | 99.28 % | 99.36 % | 99.40 % | 99.51 % | 99.52 % |
| | **4** | 99.33 % | 99.40 % | 99.53 % | 99.62 % | 99.67 % | 99.72 % | 99.74 % |
| | **5** | 99.33 % | 99.47 % | 99.65 % | 99.71 % | 99.76 % | 99.81 % | 99.83 % |
| | **6** | 99.67 % | 99.63 % | 99.65 % | 99.80 % | 99.83 % | 99.87 % | 99.89 % |
| | **7** | 100.0 % | 99.80 % | 99.70 % | 99.85 % | 99.87 % | 99.91 % | 99.92 % |
| **SVM LIN** | **1** | 90.83 % | 92.70 % | 92.53 % | 93.06 % | 92.90 % | 92.99 % | 92.99 % |
| | **2** | 96.17 % | 96.57 % | 97.00 % | 96.93 % | 97.11 % | 97.12 % | 97.15 % |
| | **3** | 97.50 % | 96.97 % | 97.60 % | 97.84 % | 97.94 % | 97.99 % | 97.98 % |
| | **4** | 98.00 % | 97.97 % | 98.37 % | 98.52 % | 98.64 % | 98.73 % | 98.74 % |
| | **5** | 98.17 % | 98.37 % | 98.33 % | 98.74 % | 98.90 % | 98.93 % | 98.94 % |
| | **6** | 98.50 % | 98.60 % | 98.60 % | 99.03 % | 99.15 % | 99.20 % | 99.23 % |
| | **7** | 98.83 % | 98.73 % | 98.85 % | 99.10 % | 99.21 % | 99.29 % | 99.31 % |

The main result of the first round was that the dataset size of 100 000 samples per class proved to be sufficient for the purposes of this study. Also, one of the classification algorithms, the SVM with linear kernel function, was left out from the following rounds based on the results of the first round. The effect of the different lengths of sequences used in the feature extraction could be seen from the results of the first round. It was clear that using longer sequences for extracting the feature ACC PWR increased the sensitivity to the changes in power output levels. The best result of the first round in terms of accuracy was achieved using a very small dataset size of 100 samples per class. However, it does not mean that 100 samples per class would be an appropriate size for the dataset to be used in the classification tasks; that it is too small to cover all the feature space.

The results of the second round revealed the principal differences between and similarities of the different features. Using the features ACC PWR or ACC ABS for the classification tasks gave similar classification results, as could be expected due to their similar definition. Overall, the classification results using the ACC ABS feature were better than using the ACC PWR feature. Increasing the sequence length used in the feature extraction steadily increases the resulting classification accuracy considering the ACC ABS, ACC PWR and FFT 1.0 features. The results of the second round considering the SVM RBF and KNN algorithms are presented in Table 25.

*Table 25. Results of the second round: SVM RBF and KNN algorithms*

| | | Feature | | | | | Best |
|---|---|---|---|---|---|---|---|
| **Classifier** | **Cycles** | **ACC PWR** | **ACC ABS** | **VEL RMS** | **FFT 1.0** | **FFT 1.5** | **Feature** |
| **SVM RBF** | **1** | 97.45 % | 97.46 % | 97.59 % | 89.18 % | 96.53 % | VEL RMS |
| | **2** | 99.08 % | 99.15 % | 99.62 % | 93.74 % | 99.72 % | FFT 1.5 |
| | **3** | 99.52 % | 99.54 % | 98.38 % | 94.93 % | 99.29 % | ACC ABS |
| | **4** | 99.74 % | 99.77 % | 98.61 % | 96.50 % | 99.94 % | FFT 1.5 |
| | **5** | 99.83 % | 99.85 % | 99.44 % | 96.46 % | 99.74 % | ACC ABS |
| | **6** | 99.89 % | 99.91 % | 99.53 % | 97.62 % | 99.98 % | FFT 1.5 |
| | **7** | 99.92 % | 99.94 % | 99.62 % | 97.31 % | 99.90 % | ACC ABS |
| **KNN** | **1** | 96.14 % | 95.84 % | 96.62 % | 82.22 % | 94.82 % | VEL RMS |
| | **2** | 98.27 % | 98.00 % | 99.44 % | 90.04 % | 99.46 % | FFT 1.5 |
| | **3** | 98.90 % | 98.70 % | 97.48 % | 90.52 % | 98.76 % | ACC PWR |
| | **4** | 99.36 % | 99.19 % | 97.53 % | 94.25 % | 99.87 % | FFT 1.5 |
| | **5** | 99.54 % | 99.41 % | 99.14 % | 93.08 % | 99.54 % | ACC PWR |
| | **6** | 99.69 % | 99.59 % | 99.31 % | 95.93 % | 99.95 % | FFT 1.5 |
| | **7** | 99.75 % | 99.68 % | 99.41 % | 94.99 % | 99.79 % | FFT 1.5 |

The relation between the classification accuracy and the sequence length used in the extraction of the features VEL RMS and FFT 1.5 is more complex. Considering the feature FFT 1.5, the classification accuracy was higher if the sequence length used in extracting the features is divisible by two. Considering both features, the classification accuracy is considerably high when using sequence length of two engine cycles for extracting them. In fact, using sequence length of two engine cycles for extracting the feature VEL RMS gives the best classification accuracy depending on the classification algorithm. The reason behind these phenomena needs further study.

The highest classification accuracies of the second round are over 99.9 %. Classification accuracies higher than 99.9 % were achieved using the features ACC PWR, ACC ABS and FFT 1.5 and the algorithms SVM RBF and KNN. Overall, the best classification results of the second round were achieved using the feature FFT 1.5.

In the classification tasks of the second round, the features extracted from the twelve signals measured at all four measurement points were included in the same classification task. Whereas, in the classification tasks of the third round, they were divided according to the measurement points into four different tasks, that is the effect of measurement point location was studied.

Considering the features ACC PWR, ACC ABS and FFT 1.0, the best classification results are achieved if they are extracted from the signals measured at point P3. Whereas, considering the features VEL RMS and FFT 1.5, the best classification results are achieved if they are extracted from the signals measured at point P2 or P4. In fact, the classification results are the worst considering the features ACC PWR, ACC ABS and FFT 1.0 if they are extracted from the signals measured at points P2 or P4. The above-described relations between the different signal sources and functions used in the feature extraction imply that the function to be applied in the feature extraction process should be considered in the selection of the measurement point location or vice versa.

Looking at the results of the second and the third rounds, the assumption that was made about the feature FFT 1.0 having low sensitivity to the changes in the power output level of the genset was clearly accurate. The assumption was based on the possibility of strong dependency on the inertial torque of the vibration acceleration amplitude at order 1.0. The inertial torques are only dependent on the rotation speed of the engine, which remains constant at levels of power output. The classification accuracies using the feature FFT 1.0 are notably lower than the rest. On the other hand, the assumption made about the feature FFT 1.5 being a good replacement, in terms of sensitivity, due to its independency of the inertial torque, for the computationally heavier feature VEL RMS, was also proven correct. Using the feature FFT 1.5 in the classification tasks gives better results overall than using the feature VEL RMS. The results of the third round considering the SVM RBF algorithm are presented in Figure 28.

*Table 26. Results of the second round: SVM RBF algorithm*

| Feature | Cycles | Point P1 | P2 | P3 | P4 | Best Point | Colour bar |
|---|---|---|---|---|---|---|---|
| ACC PWR | 1 | 91.49 % | 79.19 % | 93.64 % | 70.12 % | P3 | 100.0 % |
| | 2 | 93.54 % | 83.97 % | 96.21 % | 78.22 % | P3 | 98.50 % |
| | 3 | 94.12 % | 85.83 % | 96.94 % | 81.51 % | P3 | 97.00 % |
| | 4 | 94.62 % | 87.02 % | 97.59 % | 83.49 % | P3 | 95.50 % |
| | 5 | 94.85 % | 87.74 % | 97.86 % | 84.63 % | P3 | 94.00 % |
| | 6 | 95.08 % | 88.34 % | 98.12 % | 85.45 % | P3 | 92.50 % |
| | 7 | 95.18 % | 88.80 % | 98.25 % | 86.02 % | P3 | 91.00 % |
| ACC ABS | 1 | 91.97 % | 78.82 % | 93.35 % | 67.42 % | P3 | 89.50 % |
| | 2 | 93.96 % | 84.17 % | 96.61 % | 76.25 % | P3 | 88.00 % |
| | 3 | 94.57 % | 86.26 % | 97.33 % | 79.96 % | P3 | 86.50 % |
| | 4 | 95.00 % | 87.56 % | 98.03 % | 82.11 % | P3 | 85.00 % |
| | 5 | 95.24 % | 88.30 % | 98.24 % | 83.43 % | P3 | 83.50 % |
| | 6 | 95.44 % | 89.02 % | 98.57 % | 84.35 % | P3 | 82.00 % |
| | 7 | 95.53 % | 89.51 % | 98.68 % | 85.08 % | P3 | 80.50 % |
| VEL RMS | 1 | 91.17 % | 93.66 % | 93.52 % | 92.40 % | P2 | 79.00 % |
| | 2 | 96.43 % | 97.44 % | 97.15 % | 97.95 % | P4 | 77.50 % |
| | 3 | 93.74 % | 95.89 % | 91.04 % | 94.15 % | P2 | 76.00 % |
| | 4 | 94.75 % | 96.26 % | 89.83 % | 93.96 % | P2 | 74.50 % |
| | 5 | 96.09 % | 97.63 % | 95.49 % | 96.89 % | P2 | 73.00 % |
| | 6 | 97.28 % | 97.77 % | 96.24 % | 96.78 % | P2 | 71.50 % |
| | 7 | 96.96 % | 97.93 % | 96.67 % | 97.75 % | P2 | 70.00 % |
| FFT 1.0 | 1 | 57.72 % | 49.68 % | 77.75 % | 53.96 % | P3 | 68.50 % |
| | 2 | 65.46 % | 62.73 % | 81.31 % | 59.67 % | P3 | 67.00 % |
| | 3 | 65.67 % | 64.57 % | 84.15 % | 60.74 % | P3 | 65.50 % |
| | 4 | 72.83 % | 72.18 % | 84.42 % | 70.04 % | P3 | 64.00 % |
| | 5 | 70.46 % | 71.28 % | 84.70 % | 66.70 % | P3 | 62.50 % |
| | 6 | 76.92 % | 78.14 % | 85.99 % | 75.90 % | P3 | 61.00 % |
| | 7 | 73.59 % | 75.42 % | 85.04 % | 71.66 % | P3 | 59.50 % |
| FFT 1.5 | 1 | 89.01 % | 92.17 % | 77.55 % | 86.70 % | P2 | 58.00 % |
| | 2 | 95.84 % | 97.66 % | 92.18 % | 96.63 % | P2 | 56.50 % |
| | 3 | 92.74 % | 96.55 % | 85.32 % | 93.54 % | P2 | 55.00 % |
| | 4 | 96.47 % | 98.29 % | 95.63 % | 98.04 % | P2 | 53.50 % |
| | 5 | 94.54 % | 97.89 % | 89.49 % | 96.34 % | P2 | 52.00 % |
| | 6 | 97.02 % | 98.80 % | 96.53 % | 98.69 % | P2 | 50.50 % |
| | 7 | 95.67 % | 98.52 % | 92.36 % | 97.64 % | P2 | 49.00 % |

In the fourth round, the best combination of two different features extracted from the signals of a single measurement point was searched. Two combinations of two features were studied: the feature FFT 1.5 combined with the feature ACC PWR, and the feature FFT 1.5 combined with the feature ACC ABS. The combinations were chosen based on the results of the preceding rounds. Remarkably more accurate classification models were

achieved by using two features combined than when using a single feature. The accuracy of the classification models trained using the features combined are comparable with the accuracies of the classification models trained using a single feature extracted from all four measurement points, that is the classification models of the second round.

The differences in the accuracies between the classification models trained using the two different combinations of features were small. The best result was achieved using the combination of the features FFT 1.5 and ACC PWR extracted using a sequence length of six engine cycles from the signals measured at point P1. The classification accuracies and prediction rates (thousands of samples per second) for the five different algorithms trained and tested using the features FFT 1.5 and ACC PWR extracted using all sequence lengths from the signals measured at point P1 are presented in Table 27 and in Table 28 respectively.

*Table 27. The results of the fourth round: Classification accuracies by the five different algorithms using the features FFT 1.5 and ACC PWR extracted using all sequence lengths from the signals measured at point P1 combined*

| | | Cycles | | | | | | | Colour |
|---|---|---|---|---|---|---|---|---|---|
| Point | Classifier | 1 | 2 | 3 | 4 | 5 | 6 | 7 | bar |
| P1 | LR | 95.14 % | 98.71 % | 97.81 % | 99.46 % | 98.77 % | 99.68 % | 99.22 % | 100.0 % |
| | SVM | 96.34 % | 99.27 % | 98.72 % | 99.76 % | 99.37 % | 99.86 % | 99.68 % | 99.00 % |
| | DT | 95.49 % | 98.60 % | 98.21 % | 99.25 % | 98.97 % | 99.40 % | 99.13 % | 98.00 % |
| | KNN | 95.14 % | 99.01 % | 98.26 % | 99.62 % | 99.21 % | 99.80 % | 99.59 % | 95.00 % |
| | GNB | 92.84 % | 97.27 % | 96.10 % | 97.94 % | 97.29 % | 98.27 % | 97.87 % | 92.00 % |

The training time of the classification models is not as important as the prediction rate considering the objective of this study. A classification model for the recognition of the operational state of a genset does not need to be trained but once, and only possibly updated occasionally, if changes that affect the structural dynamics of the genset are made. The prediction rate, however, is of crucial importance considering the requirement of continuous state recognition in near real-time. Ideally, a prediction of the power output level should be given at the sampling frequency of the measured signal. To achieve this, the measured data should be processed and given as input to the classifier model, and the classification should be made before the next sample is ready. However, the necessity of making predictions at the sampling rate can be questioned since subsequent feature values are extracted from almost the same data.

*Table 28. The results of the fourth round: Prediction rates (thousands of samples per second) by the five different algorithms using the features FFT 1.5 and ACC PWR, extracted using all sequence lengths from the signals measured at point P1 combined*

| Point | Classifier | Cycles 1 | 2 | 3 | 4 | 5 | 6 | 7 | Colour bar |
|---|---|---|---|---|---|---|---|---|---|
| P1 | LR | 1972.2 | 1703.7 | 2304.8 | 2108.1 | 2603.6 | 2914.1 | 1972.8 | 3000 |
| | SVM | 0.0 | 0.1 | 0.1 | 0.3 | 0.1 | 0.5 | 0.2 | 2000 |
| | DT | 1812.6 | 1658.2 | 1726.4 | 2026.3 | 2046.0 | 2564.0 | 2022.1 | 1000 |
| | KNN | 0.6 | 0.6 | 0.6 | 0.7 | 0.7 | 0.6 | 0.7 | 500 |
| | GNB | 366.4 | 365.6 | 322.3 | 350.2 | 314.3 | 260.7 | 311.3 | 0 |

The data used in this study was measured at a sampling rate of 2048 Hz. The classification models trained by the LR, DT and GNB algorithms have prediction rates which are hundredths of times higher than the sampling rate used in the measurements. The prediction rate of the classifier models trained by the KNN algorithm is independent of the accuracy of the model and is notably below the sampling rate used in the measurements. The prediction rate of the classifier model trained by the SVM RBF algorithm is even worse. However, it is clearly dependent on the accuracy of the model: that is, the more accurate the model, the higher the prediction rate.

Although the classification accuracy achieved using the classification models trained by the SVM RBF algorithm was already very high, it could be further improved by tuning the parameters of the SVM algorithm. The highest prediction rates achieved were 4 240 and 10 549 samples per second, which are higher than the sampling rate used in the measurements. The corresponding classification accuracies were 99.948 % and 99.930 %.

It is notable that significantly more misclassification exists between the groups 100 % and 95 % than between the groups 95 % and 90 %, although the percentual difference in the power output level is equal between the two pairs of groups. The most accurate classification models trained in this study can classify all other groups of power output levels perfectly, except for the highest two. This can be observed from the confusion matrix of the classifier trained using the tuned parameter values and with the features FFT 1.5 and ACC PWR, extracted using a sequence length of six engine cycles from the signals measured at point P1 presented in Figure 31.

| | Class | | | | | |
|---|---|---|---|---|---|---|
| **Class** | **100 %** | **95 %** | **90 %** | **75 %** | **50 %** | **0 %** |
| **100 %** | 199743 | 257 | 0 | 0 | 0 | 0 |
| **95 %** | 345 | 199655 | 0 | 0 | 0 | 0 |
| **90 %** | 0 | 0 | 200000 | 0 | 0 | 0 |
| **75 %** | 0 | 0 | 0 | 200000 | 0 | 0 |
| **50 %** | 0 | 0 | 0 | 0 | 200000 | 0 |
| **0 %** | 0 | 0 | 0 | 0 | 0 | 200000 |

*Figure 31. Results of the classification model trained using the tuned parameter values*

Tuning the parameters of the algorithm can cause overfitting, which in general should be avoided. However, when considering a genset it can be ignored if the data used for training the model covers the states of normal operation of the genset comprehensively, since it can be assumed that a classification model is trained for each genset individually, using the data measured from the genset itself. Gathering the necessary amount of data for building a model is not very time consuming. The amount of data sampled and used in this study could be measured in one day. Therefore, it could be done, for example, as part of the commissioning of the genset of which the measurement of mechanical vibration levels is an obligatory part.

Considering the results of the classification and feature selection part of this study in general, it can be said that a combination of sensitive features for the recognition of different states of normal operation was found. The effect of increasing the length of the sequence used in the feature extraction to the sensitivity of the extracted feature is the most significant when moving from one to two cycles. The classification accuracy is notably higher when the classification models are trained with features extracted from sequences equal or longer than two engine cycles. The highest accuracy was achieved with features extracted using the length of six or seven engine cycles, depending on the feature.

The choice of measurement point location was proven to be an important factor in the sensitivity of the features extracted from the measured signal. It is remarkable that an accurate classification model can be built using measured data from only one measurement point, that is using only one triaxial accelerometer. It significantly simplifies and reduces the cost of a real-world state recognition application of a genset, or any related type of machinery.

In addition, the applicability of different algorithms for building a near real-time classification model in terms of accuracy and prediction rate was studied. The prediction of the classification models trained by LR, DT and GNB algorithms are more than adequate, whereas the classification models trained by the SVM RBF algorithm must be very accurate for them to be fast enough to predict at speeds comparable to the sampling rate used in the measurement of mechanical vibration. A classification model trained by the KNN algorithm has a considerably lower prediction rate compared to the others. In terms of accuracy, the classification models trained by the SVM RBF algorithm were the best; but compared to classification models trained by the LR or DT algorithms, the difference in classification accuracy was relatively small. Also, the effect of parameter tuning was not experimented with the classification models trained by the LR or DT algorithms. Therefore, the accuracy of the classification models trained by the LR and DT algorithms could probably still be increased.

The first and the second tasks for reaching the objective of this study were clearly completed by the end of the classification and feature selection part of this study. Representative data was sampled and features sensitive to the changes in the power output level were found. In fact, the third task was also half-done, since a fast-performing classifier model for the recognition of the normal operational state of the genset was successfully built. The remaining half of the third and the last task was to develop an accurate and fast-performing model for detecting the abnormal operation of the genset.

The applicability of two algorithms, One-class SVM and LOF, to the detection of abnormal operation of the studied genset was analysed. The novelty detectors were first validated using only normal operation data. The novelty detectors trained by both algorithms classified the new unseen test samples correctly into normal and abnormal, with two exceptions. The novelty detectors trained with data from the 100 % group classifies a significant proportion of test data from the 95 % group as inliers and vice versa. The novelty detector trained by the LOF algorithm made less false positive predictions compared to the novelty detector trained by the One-class SVM algorithm, as can be seen when comparing the parameter sweep results presented in Figure 32 and in Figure 33.


*Figure 32. Parameter sweep results for One-class SVM novelty detector fitted to 100 % group data, ν=0.01*

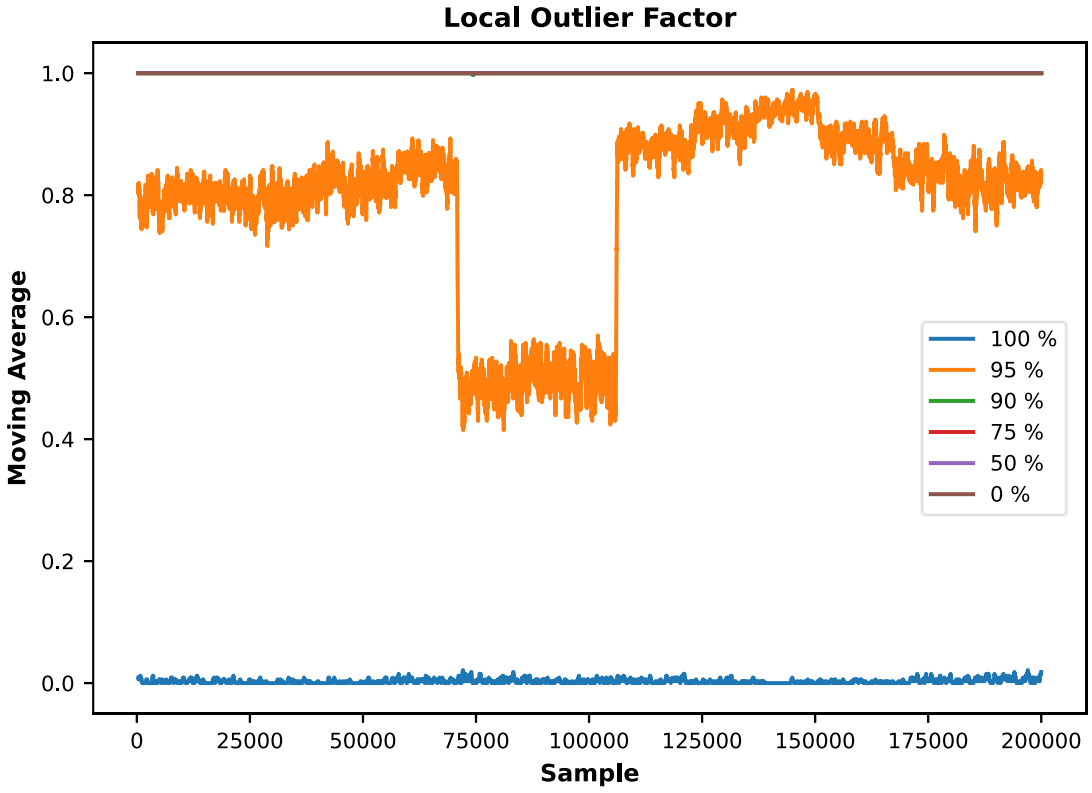


*Figure 33. Parameter sweep results for LOF novelty detector fitted to 100 % group data, k=16*

After the evaluation of the novelty detectors, using normal operation data, the novelty detectors were run against the data sampled in the subsets of abnormal operation of their corresponding group. The training and testing of the novelty detectors were done using the features FFT 1.5 and ACC PWR, extracted using the seven different sequence lengths from the signals measured at point P1. The two features were first used as combined and then separately for training the novelty detectors. The novelty detectors trained with the features combined, or with only the feature ACC PWR, found proportions of abnormal operation greater than the threshold value from all subsets of abnormal operation. In two of the 280 runs against the subsets of abnormal data, the novelty detectors trained using One-class SVM, with only the feature FFT 1.5, did not find a proportion of abnormal operation greater than the threshold value.

In general, the proportions of abnormal operation found from the subsets of abnormal operation data by the novelty detectors varied greatly, from 0.4 % to 94.6. This is most likely due to different types of fault situations run during the performance tests of the genset. The novelty detectors trained by the One-class SVM algorithm found more abnormal data in the subsets of abnormal data than the novelty detectors trained by the LOF algorithm, but the difference was small. Also, the novelty detectors trained with the two features combined found the largest proportions of abnormal data in the subsets of abnormal data, and the novelty detectors that were trained with only the feature FFT 1.5 found the smallest proportions.

The prediction rates of the trained novelty detectors were high compared to the sampling rate used in the measurements. The novelty detectors trained by the LOF algorithm were notably faster than the novelty detectors trained by the One-class SVM algorithm. Also, training the novelty detectors by the LOF algorithm with only one feature, instead of the two combined, increased the prediction rate almost tenfold at best. The highest prediction rates using novelty detectors trained by the LOF algorithm were 130 901 samples per second using four CPUs, and 101 948 samples per second using one CPU.

Plotting some novelty detection results against time revealed that the predictions made by the differently trained novelty detectors were very similar in general. It could be seen that sampling only one minute of normal operation data into the subsets of abnormal operation data was not enough in some of the cases. The subset 5 of the 95 % group,

which had a relatively large proportions of abnormal data detected, that is 70 % by One-class SVM and 69 % by LOF, presented in Figure 34, is a good example.

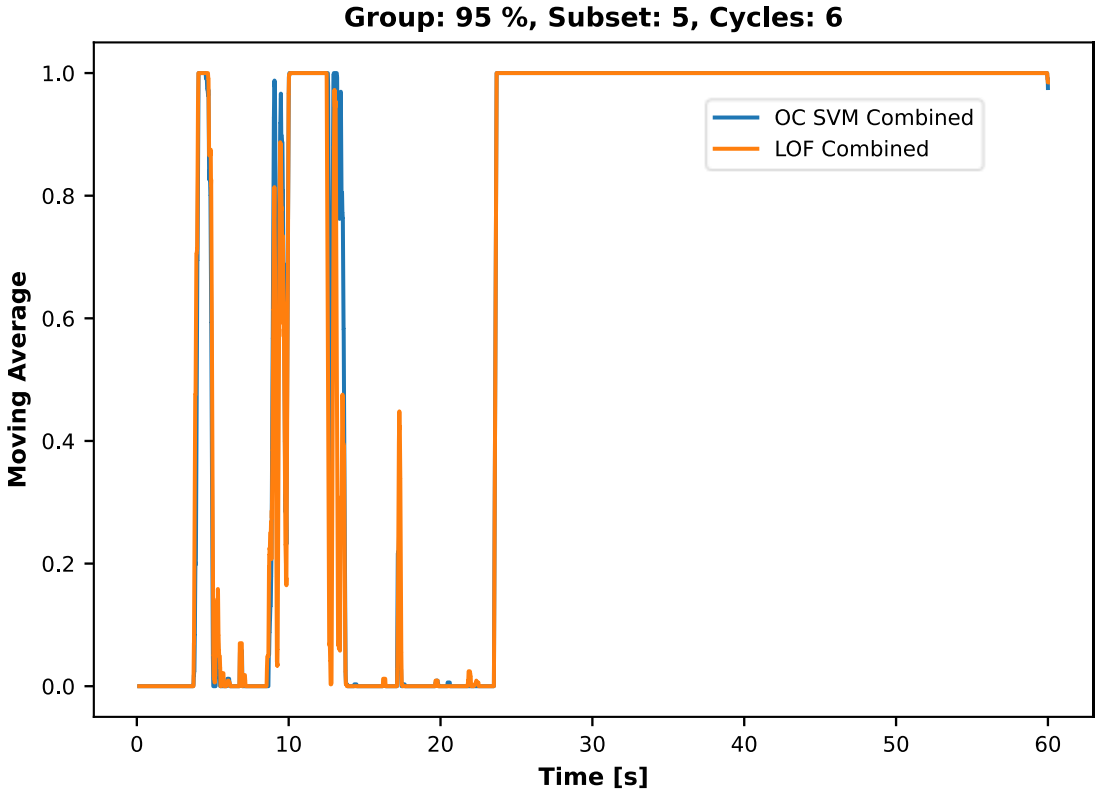


*Figure 34. Results for novelty detections run against data from subset 5 of group 95 %: High proportion of test data classified as abnormal*

If abnormal operation data was included in the subsets of abnormal operation data, as was intended, it can then be said that the novelty detectors trained by both algorithms are applicable to the detection of abnormal operation of the studied genset in near real-time. Therefore, also the third and last step for reaching the objective of the study was completed. Based on the results of the novelty detection part, the LOF algorithm is more suitable for the purposes of this study than the One-class SVM algorithm. The novelty detectors trained by the LOF algorithm had higher prediction rates and gave less false positive predictions when evaluated using normal operation data, compared to the novelty detectors trained by the One-class SVM algorithm. The predictions made by the novelty detectors trained by both algorithms against data sampled in the subsets of abnormal operation were similar. Training the novelty detectors with features extracted using a sequence length of only one cycle should be further studied, since no evident reason for not using them was found based on the results of the novelty detection part. Also, the

option of using only the feature ACC PWR should be considered when using novelty detectors trained by the LOF algorithm, since it results in notably higher prediction rates.

The novelty detectors trained individually for each group of power output level could be combined with the previously defined classification model of the power output levels so that first the classification model identifies the current power output level and then activates the corresponding novelty detector. By doing so, it would not be necessary to run all the novelty detectors trained for the different groups simultaneously.

## 5.2 Conclusions

Tools and methods for near real-time operational state recognition of a genset based on measured mechanical vibration data for DT applications were developed and analysed in this study. It was proven that accurate classification of the normal operation of a genset into different classes of power output level and detection of abnormal operation of the genset is possible using measured mechanical vibration data using only one triaxial accelerometer. The delay of the state recognition of a genset can be less than one second using the methods developed in this study.

The state recognition models developed in this study were built using common ML classification, data analysis and signal processing methods. The extraction methods for the features used in the machine learning tasks of this study were based on the cyclic nature of the operation of an ICE at constant rotation speed. A combination of two features sensitive to the changes in the power output levels of the genset was identified.

Two different types of models were trained using the feature combination for the state recognition of the genset. The first, a classification model, can identify the current power output level of the genset using the measured mechanical vibration data. The second, a novelty detection model, can detect abnormal operation of the genset in fault situations at a specific power output level. A two-step state recognition model can be built by combining the classification and novelty detection models.

## 5.3 Future work

A logical addition to the two-step state recognition model developed in this study would be a model that can recognise the type of the fault situation when the novelty detector model detects abnormal operation. Currently there is not enough data, let alone labelled data, measured during different fault situations; therefore, it should be first gathered and labelled before attempting to build such a model. The two-step state recognition model can be used as a trigger for saving the data measured during the fault situations, but, for example, the method for labelling the data according to the different fault situations should be found.

# REFERENCES


Bevilacqua, M. et. al., 2020. Digital Twin Reference Model Development to Prevent Operators' Risk in Process Plants. In: *Sustainability Vol.* 12*, no. 3* : 1088. https://doi.org/10.3390/su12031088

Breeze, P., 2017. *Piston Engine-Based Power Plants*, Elsevier Science & Technology, San Diego, ISBN 978-0-12-812905-0.

Breunig, M., et. al., 2000, LOF: Identifying Density-Based Local Outliers. In: *Association for Computing Machinery 29, no. 2*. DOI: https://doi.org/10.1145/335191.335388

Caesarendra, Wahyu; Tjahjowidodo, Tegoeh. 2017. A Review of Feature Extraction Methods in Vibration-Based Condition Monitoring and Its Application for Degradation Trend Estimation of Low-Speed Slew Bearing. In: *Machines* 5, *no. 4* : 21. DOI: https://doi.org/10.3390/machines5040021

Den Hartog, J.P., 1985. *Mechanical Vibrations*, Dover Publications, New York, United States, ISBN 9780486647852.

Eriksson, L. and Andersson, I. 2002. *An Analytic Model for Cylinder Pressure in a Four Stroke SI Engine*, Society of Automotive Engineers, Inc., 10.4271/2001-10-0371.

Grieves, M. 2014. *Digital Twin: Manufacturing Excellence through Virtual Factory Replication*. White paper. Available from: https://www.researchgate.net/publication/275211047_Digital_Twin_Manufacturing_Excellence_through_Virtual_Factory_Replication

ISO, 1995. *Reciprocating internal combustion engine driven alternating current generating sets – Part 9: Measurement and evaluation of mechanical vibrations*, International Organization for Standardization, Geneve, Switzerland, ISO 8528-9:1995(E).

Jablonski, A., 2021. *Condition Monitoring Algorithms in MATLAB®*, Springer Tracts in Mechanical Engineering, Springer Nature Switzerland AG, Cham Switzerland, ISBN 978-3-030-62749-2. DOI: https://doi.org/10.1007/978-3-030-62749-2.

Johansen, S.S., and Nejad, A.R., 2019. On Digital Twin Condition Monitoring Approach for Drivetrains in Marine Applications. In: *Proceedings of the ASME 2019 38th International Conference on Ocean, Offshore and Arctic Engineering. Volume 10: Ocean Renewable Energy*. Glasgow, Scotland, UK. V010T09A013. ASME. DOI: https://doi.org/10.1115/OMAE2019-95152

Lackie, J., 2007. *Chambers Dictionary of Science and Technology*, Chambers Harrap Publishers Ltd, Edinburgh, ISBN-13: 978 0550 100719

Lämsä, V., Nieminen, V., 2019. Benefits, Advantages, Added Values & Enabled Business Opportunities through Digital Twins, Digital Twin Platforms and Digital Threads. In: *Proceedings of the 3rd Annual SMACC Research Seminar 2018*, Tampere, pp. 10-13. ISBN 978-952-03-0975-6

Lyons, R.G., 2010. *Understanding Digital Signal Processing*, 3rd edition, Pearson Education, Inc. ISBN 978-0-13-702741-5

Markou, M. and Singh, S., 2003. Novelty detection: a review—part 1: statistical approaches. In: *Signal Processing*, vol. 83, no. 12, pp. 2481-2497. Available from: https://www.sciencedirect.com/science/article/pii/S0165168403002020 , ISSN 0165-1684. DOI: https://doi.org/10.1016/j.sigpro.2003.07.018.

Müller, A.C. and Guido, S., 2016. *Introduction to Machine Learning with Python*, O'Reilly Media, Inc., Sebastopol, CA. ISBN 978-1-449-36941-5

Nairac, A. & Al., 1997, Choosing an Appropriate Model for Novelty Detection. In: *Proceedings of the 5th IEEE International Conference on Artificial Neural Networks*, Cambridge, pp. 227-232.

National Instruments, Inc., 2020. *Using Fast Fourier Transforms and Power Spectra in LabVIEW*, National Instruments, Inc.. Available from: https://www.ni.com/fi-fi/innovations/white-papers/06/using-fast-fourier-transforms-and-power-spectra-in-labview.html

Oppenheim, A.V., Willsky, A.S., 1997. Signals & Systems, 2nd edition, Prentice Hall Signal Processing Series, Prentice-Hall, Inc., New Jersey. ISBN 0-13-814757-4

Palestini, C., Gallici, I., 2019. *Multi-body Dynamic Simulation for Identification of Operating Scenarios on a Powerplant Genset Using Machine Learning*, European GT Conference 2019, Frankfurt. Available from: https://www.gtisoft.com/wp-content/uploads/2019/11/Multi-body-dynamic-simulation-for-identification-of-operating-scenarios-on-a-powerplant-genset-using-machine-learning-W%C3%A4rtsil%C3%A4-Cesare-Palestini.pdf

Porter, F.P., 1943, Harmonic Coefficients of Engine Torque Curves. In: *ASME, Journal of Applied Mecchanics*, 10(1): A33-A48. DOI: https://doi.org/10.1115/1.4009248

Randall, R.B., 2011, *Vibration-Based Condition Monitoring, Industrial, Aerospace and Automotive Applications*. John Wiley & Sons Ltd, ISBN 9780470977651.

Rasheed, A. et. al., 2020, Digital Twin: Values, Challenges and Enablers from a Modeling Perspective. In: *IEEE Access*, vol. 8, pp. 21980-22012, DOI: 10.1109/ACCESS.2020.2970143.

Shafto, M. et. al., 2010, *DRAFT Modeling, Simulation, Inofrmation Technology & Processing Roadmap, Technology area 11*. National Aeronautics and Space Administration. Available from: https://www.nasa.gov/pdf/501321main_TA11-MSITP-DRAFT-Nov2010-A1.pdf

Tiainen, T. et. al., 2019, Digital Twin and Virtual Sensor for a Rotor System. In: *Proceedings of the 30th International DAAAM Symposium "Intelligent Manufacturing & Automation"*, DAAAM International. ISBN 978-3-902734-22-8 Available from: 10.2507/30th.daaam.proceedings.156

Tao, F., et. Al., 2019, Digital Twin in Industry: State-of-the-Art : *IEEE Transactions on Industrial Informatics*. vol. 15, no. 4, pp. 2405-2415, doi: 10.1109/TII.2018.2873186.

Van Basshuysen, R. and Schäfer, F., 2016, *Internal Combustion Engine Handbook - Basics, Components, System, and Perspectives*, 2nd Edition, SAE International, ISBN 9780-768080247.

*Wärtsilä*, 2021. Available from: https://www.wartsila.com/marine/build/engines-and-generating-sets/pure-gas-engines/wartsila-31sg Accessed on May 14th 2021.

# APPENDIX A

The complete results of the third and the fourth rounds of classification tasks are presented in the following tables.

*Table 29. Results of the third round for point P1*

| Feature | Classifier | Cycles 1 | 2 | 3 | 4 | 5 | 6 | 7 | Colour bar |
|---|---|---|---|---|---|---|---|---|---|
| ACC ABS | LR | 91.87 % | 93.82 % | 94.40 % | 94.82 % | 95.01 % | 95.21 % | 95.32 % | 100.0 % |
| | SVM | 91.94 % | 93.97 % | 94.54 % | 95.03 % | 95.23 % | 95.44 % | 95.52 % | 99.0 % |
| | DT | 91.82 % | 93.89 % | 94.49 % | 95.03 % | 95.20 % | 95.42 % | 95.49 % | 98.0 % |
| | KNN | 91.90 % | 93.99 % | 94.57 % | 95.08 % | 95.25 % | 95.51 % | 95.59 % | 97.0 % |
| | GNB | 90.51 % | 93.05 % | 93.64 % | 94.27 % | 94.51 % | 94.81 % | 94.91 % | 96.0 % |
| ACC PWR | LR | 91.39 % | 93.43 % | 93.99 % | 94.49 % | 94.70 % | 94.94 % | 95.07 % | 95.0 % |
| | SVM | 91.49 % | 93.54 % | 94.12 % | 94.62 % | 94.85 % | 95.08 % | 95.18 % | 94.0 % |
| | DT | 91.37 % | 93.48 % | 94.06 % | 94.64 % | 94.84 % | 95.14 % | 95.22 % | 93.0 % |
| | KNN | 91.44 % | 93.55 % | 94.11 % | 94.69 % | 94.90 % | 95.20 % | 95.28 % | 92.0 % |
| | GNB | 90.07 % | 92.77 % | 93.42 % | 94.08 % | 94.30 % | 94.59 % | 94.69 % | 91.0 % |
| VEL RMS | LR | 90.19 % | 96.13 % | 93.23 % | 93.93 % | 95.70 % | 96.92 % | 96.56 % | 90.0 % |
| | SVM | 91.17 % | 96.43 % | 93.74 % | 94.75 % | 96.09 % | 97.28 % | 96.96 % | 88.0 % |
| | DT | 91.06 % | 96.46 % | 93.84 % | 94.97 % | 96.17 % | 97.40 % | 97.00 % | 86.0 % |
| | KNN | 91.25 % | 96.61 % | 93.98 % | 95.05 % | 96.34 % | 97.62 % | 97.24 % | 84.0 % |
| | GNB | 89.54 % | 95.54 % | 92.87 % | 92.68 % | 95.09 % | 95.76 % | 95.66 % | 82.0 % |
| FFT 1.0 | LR | 44.81 % | 63.79 % | 61.28 % | 70.05 % | 67.43 % | 73.38 % | 70.65 % | 80.0 % |
| | SVM | 57.72 % | 65.46 % | 65.67 % | 72.83 % | 70.46 % | 76.92 % | 73.59 % | 77.5 % |
| | DT | 56.94 % | 64.87 % | 65.28 % | 72.36 % | 69.96 % | 76.46 % | 73.10 % | 75.0 % |
| | KNN | 57.72 % | 65.42 % | 65.82 % | 72.82 % | 70.55 % | 77.00 % | 73.66 % | 70.0 % |
| | GNB | 55.28 % | 63.38 % | 63.25 % | 69.26 % | 67.28 % | 72.30 % | 70.08 % | 65.0 % |
| FFT 1.5 | LR | 88.10 % | 94.94 % | 91.31 % | 95.74 % | 93.32 % | 96.04 % | 94.55 % | 60.0 % |
| | SVM | 89.03 % | 95.87 % | 92.78 % | 96.52 % | 94.59 % | 97.06 % | 95.73 % | 55.0 % |
| | DT | 88.97 % | 95.89 % | 92.99 % | 96.86 % | 94.70 % | 97.54 % | 95.90 % | 50.0 % |
| | KNN | 88.96 % | 96.02 % | 93.03 % | 96.99 % | 94.89 % | 97.61 % | 96.07 % | 45.0 % |
| | GNB | 87.11 % | 94.49 % | 91.40 % | 95.17 % | 93.38 % | 95.45 % | 94.48 % | 40.0 % |

*Table 30. Results of the third round for point P2*

| Feature | Classifier | Cycles 1 | 2 | 3 | 4 | 5 | 6 | 7 | Colour bar |
|---|---|---|---|---|---|---|---|---|---|
| ACC ABS | LR | 78.53 % | 83.71 % | 85.68 % | 87.03 % | 87.71 % | 88.37 % | 88.81 % | 100.0 % |
| | SVM | 78.83 % | 84.13 % | 86.16 % | 87.51 % | 88.28 % | 89.00 % | 89.51 % | 99.0 % |
| | DT | 78.55 % | 83.84 % | 86.01 % | 87.31 % | 88.13 % | 88.89 % | 89.39 % | 98.0 % |
| | KNN | 78.84 % | 84.11 % | 86.21 % | 87.55 % | 88.37 % | 89.15 % | 89.67 % | 97.0 % |
| | GNB | 76.73 % | 81.85 % | 83.99 % | 85.22 % | 85.87 % | 86.39 % | 86.76 % | 96.0 % |
| ACC PWR | LR | 78.82 % | 83.54 % | 85.38 % | 86.47 % | 87.13 % | 87.68 % | 88.08 % | 95.0 % |
| | SVM | 79.19 % | 83.97 % | 85.83 % | 87.02 % | 87.74 % | 88.34 % | 88.80 % | 94.0 % |
| | DT | 78.84 % | 83.69 % | 85.63 % | 86.84 % | 87.61 % | 88.23 % | 88.67 % | 93.0 % |
| | KNN | 79.19 % | 84.01 % | 85.86 % | 87.07 % | 87.85 % | 88.48 % | 89.03 % | 92.0 % |
| | GNB | 76.53 % | 81.50 % | 83.52 % | 84.67 % | 85.41 % | 85.90 % | 86.21 % | 91.0 % |
| VEL RMS | LR | 93.13 % | 97.03 % | 95.33 % | 95.47 % | 97.09 % | 97.50 % | 97.56 % | 90.0 % |
| | SVM | 93.66 % | 97.44 % | 95.89 % | 96.26 % | 97.63 % | 97.77 % | 97.93 % | 88.0 % |
| | DT | 93.69 % | 97.56 % | 96.41 % | 96.87 % | 97.87 % | 98.12 % | 98.16 % | 86.0 % |
| | KNN | 93.68 % | 97.60 % | 96.45 % | 96.88 % | 97.89 % | 98.11 % | 98.20 % | 84.0 % |
| | GNB | 92.21 % | 96.77 % | 94.77 % | 94.73 % | 96.80 % | 97.09 % | 97.26 % | 82.0 % |
| FFT 1.0 | LR | 39.17 % | 61.22 % | 61.81 % | 71.00 % | 69.53 % | 76.65 % | 73.92 % | 80.0 % |
| | SVM | 49.68 % | 62.73 % | 64.57 % | 72.18 % | 71.28 % | 78.14 % | 75.42 % | 77.5 % |
| | DT | 49.13 % | 62.14 % | 63.99 % | 71.68 % | 70.75 % | 77.69 % | 74.99 % | 75.0 % |
| | KNN | 49.73 % | 62.67 % | 64.60 % | 72.18 % | 71.31 % | 78.21 % | 75.47 % | 70.0 % |
| | GNB | 47.49 % | 61.30 % | 62.84 % | 70.87 % | 69.73 % | 76.73 % | 74.09 % | 65.0 % |
| FFT 1.5 | LR | 91.10 % | 96.18 % | 94.48 % | 97.16 % | 95.75 % | 97.83 % | 96.39 % | 60.0 % |
| | SVM | 92.19 % | 97.66 % | 96.61 % | 98.32 % | 97.92 % | 98.80 % | 98.54 % | 55.0 % |
| | DT | 92.19 % | 97.55 % | 96.57 % | 98.27 % | 97.86 % | 98.65 % | 98.46 % | 50.0 % |
| | KNN | 92.09 % | 97.64 % | 96.57 % | 98.36 % | 97.92 % | 98.83 % | 98.53 % | 45.0 % |
| | GNB | 91.04 % | 96.80 % | 95.25 % | 97.37 % | 96.59 % | 97.69 % | 97.26 % | 40.0 % |

*Table 31. Results of the third round for point P3*

| Feature | Classifier | Cycles 1 | 2 | 3 | 4 | 5 | 6 | 7 | Colour bar |
|---|---|---|---|---|---|---|---|---|---|
| ACC ABS | LR | 93.22 % | 96.50 % | 97.29 % | 97.96 % | 98.21 % | 98.50 % | 98.64 % | 100.0 % |
| | SVM | 93.34 % | 96.59 % | 97.35 % | 98.04 % | 98.27 % | 98.56 % | 98.70 % | 99.0 % |
| | DT | 93.17 % | 96.46 % | 97.26 % | 97.92 % | 98.13 % | 98.47 % | 98.59 % | 98.0 % |
| | KNN | 93.30 % | 96.58 % | 97.33 % | 98.03 % | 98.26 % | 98.55 % | 98.67 % | 97.0 % |
| | GNB | 92.70 % | 95.66 % | 96.51 % | 97.10 % | 97.42 % | 97.67 % | 97.86 % | 96.0 % |
| ACC PWR | LR | 93.53 % | 96.06 % | 96.84 % | 97.42 % | 97.70 % | 97.96 % | 98.10 % | 95.0 % |
| | SVM | 93.64 % | 96.21 % | 96.94 % | 97.59 % | 97.86 % | 98.12 % | 98.25 % | 94.0 % |
| | DT | 93.49 % | 96.09 % | 96.80 % | 97.51 % | 97.75 % | 98.10 % | 98.21 % | 93.0 % |
| | KNN | 93.61 % | 96.23 % | 96.94 % | 97.63 % | 97.89 % | 98.22 % | 98.32 % | 92.0 % |
| | GNB | 92.85 % | 95.17 % | 96.01 % | 96.56 % | 96.85 % | 97.12 % | 97.32 % | 91.0 % |
| VEL RMS | LR | 91.77 % | 95.55 % | 89.89 % | 87.10 % | 94.56 % | 95.55 % | 95.67 % | 90.0 % |
| | SVM | 93.52 % | 97.15 % | 91.04 % | 89.83 % | 95.49 % | 96.24 % | 96.67 % | 88.0 % |
| | DT | 93.20 % | 96.91 % | 91.24 % | 89.60 % | 95.68 % | 96.22 % | 96.75 % | 86.0 % |
| | KNN | 93.53 % | 97.18 % | 91.50 % | 89.96 % | 95.93 % | 96.61 % | 97.02 % | 84.0 % |
| | GNB | 92.42 % | 95.79 % | 88.32 % | 84.10 % | 94.13 % | 94.34 % | 95.51 % | 82.0 % |
| FFT 1.0 | LR | 64.17 % | 75.06 % | 75.70 % | 77.13 % | 77.65 % | 78.33 % | 78.14 % | 80.0 % |
| | SVM | 77.75 % | 81.31 % | 84.15 % | 84.42 % | 84.70 % | 85.99 % | 85.04 % | 77.5 % |
| | DT | 77.12 % | 81.15 % | 83.69 % | 84.29 % | 84.51 % | 85.89 % | 85.00 % | 75.0 % |
| | KNN | 78.13 % | 81.53 % | 84.41 % | 84.72 % | 85.04 % | 86.33 % | 85.37 % | 70.0 % |
| | GNB | 74.11 % | 76.87 % | 80.07 % | 78.03 % | 80.21 % | 78.72 % | 79.76 % | 65.0 % |
| FFT 1.5 | LR | 75.89 % | 88.48 % | 82.16 % | 91.43 % | 86.25 % | 92.47 % | 88.92 % | 60.0 % |
| | SVM | 77.56 % | 92.12 % | 85.36 % | 95.55 % | 89.46 % | 96.51 % | 92.34 % | 55.0 % |
| | DT | 78.35 % | 91.81 % | 86.34 % | 95.33 % | 89.71 % | 96.34 % | 92.20 % | 50.0 % |
| | KNN | 79.00 % | 92.13 % | 86.65 % | 95.63 % | 90.10 % | 96.60 % | 92.54 % | 45.0 % |
| | GNB | 75.56 % | 87.56 % | 80.17 % | 90.95 % | 83.83 % | 92.32 % | 86.71 % | 40.0 % |

*Table 32. Results of the third round for point P4*

| Feature | Classifier | Cycles 1 | 2 | 3 | 4 | 5 | 6 | 7 | Colour bar |
|---|---|---|---|---|---|---|---|---|---|
| ACC ABS | LR | 65.86 % | 74.07 % | 77.68 % | 79.60 % | 80.88 % | 81.82 % | 82.43 % | 100.0 % |
| | SVM | 67.32 % | 76.19 % | 79.95 % | 82.13 % | 83.46 % | 84.39 % | 85.08 % | 99.0 % |
| | DT | 67.00 % | 75.82 % | 79.53 % | 81.83 % | 83.09 % | 84.13 % | 84.84 % | 98.0 % |
| | KNN | 67.37 % | 76.27 % | 80.03 % | 82.28 % | 83.58 % | 84.62 % | 85.32 % | 97.0 % |
| | GNB | 63.95 % | 72.13 % | 75.69 % | 77.78 % | 79.17 % | 80.25 % | 80.95 % | 96.0 % |
| ACC PWR | LR | 68.70 % | 76.27 % | 79.35 % | 81.18 % | 82.21 % | 82.89 % | 83.45 % | 95.0 % |
| | SVM | 70.12 % | 78.22 % | 81.51 % | 83.49 % | 84.63 % | 85.45 % | 86.02 % | 94.0 % |
| | DT | 69.70 % | 77.85 % | 81.13 % | 83.09 % | 84.22 % | 85.19 % | 85.80 % | 93.0 % |
| | KNN | 70.10 % | 78.26 % | 81.60 % | 83.60 % | 84.79 % | 85.62 % | 86.30 % | 92.0 % |
| | GNB | 66.00 % | 73.77 % | 77.10 % | 79.03 % | 80.24 % | 81.09 % | 81.75 % | 91.0 % |
| VEL RMS | LR | 91.48 % | 97.56 % | 92.81 % | 90.94 % | 95.93 % | 94.84 % | 97.09 % | 90.0 % |
| | SVM | 92.40 % | 97.95 % | 94.15 % | 93.96 % | 96.89 % | 96.78 % | 97.75 % | 88.0 % |
| | DT | 92.32 % | 97.96 % | 94.45 % | 94.84 % | 97.20 % | 97.50 % | 98.00 % | 86.0 % |
| | KNN | 92.62 % | 98.11 % | 94.65 % | 94.83 % | 97.38 % | 97.60 % | 98.18 % | 84.0 % |
| | GNB | 91.33 % | 97.33 % | 92.58 % | 90.23 % | 96.04 % | 94.32 % | 96.83 % | 82.0 % |
| FFT 1.0 | LR | 40.45 % | 56.87 % | 53.83 % | 64.97 % | 60.81 % | 69.48 % | 65.18 % | 80.0 % |
| | SVM | 53.96 % | 59.67 % | 60.74 % | 70.04 % | 66.70 % | 75.90 % | 71.66 % | 77.5 % |
| | DT | 53.65 % | 59.29 % | 60.35 % | 69.63 % | 66.29 % | 75.42 % | 71.34 % | 75.0 % |
| | KNN | 54.07 % | 59.79 % | 60.91 % | 70.10 % | 66.78 % | 75.95 % | 71.78 % | 70.0 % |
| | GNB | 52.56 % | 57.58 % | 58.48 % | 66.55 % | 63.83 % | 71.54 % | 68.19 % | 65.0 % |
| FFT 1.5 | LR | 85.29 % | 96.06 % | 91.71 % | 97.14 % | 94.82 % | 97.51 % | 96.33 % | 60.0 % |
| | SVM | 86.74 % | 96.66 % | 93.58 % | 98.04 % | 96.38 % | 98.72 % | 97.71 % | 55.0 % |
| | DT | 87.20 % | 96.85 % | 93.97 % | 98.44 % | 96.68 % | 98.93 % | 97.94 % | 50.0 % |
| | KNN | 87.68 % | 97.03 % | 94.08 % | 98.57 % | 96.86 % | 99.09 % | 98.16 % | 45.0 % |
| | GNB | 85.29 % | 95.97 % | 92.68 % | 96.86 % | 95.23 % | 97.25 % | 96.32 % | 40.0 % |

*Table 33. Results of the fourth round for combination FFT 1.5 and ACC ABS*

| Point | Classifier | Cycles 1 | 2 | 3 | 4 | 5 | 6 | 7 | Colour bar |
|---|---|---|---|---|---|---|---|---|---|
| P1 | LR | 95.14 % | 98.71 % | 97.81 % | 99.46 % | 98.77 % | 99.68 % | 99.22 % | 100.0 % |
| | SVM | 96.34 % | 99.27 % | 98.72 % | 99.76 % | 99.37 % | 99.86 % | 99.68 % | 99.90 % |
| | DT | 95.49 % | 98.60 % | 98.21 % | 99.25 % | 98.97 % | 99.40 % | 99.13 % | 99.80 % |
| | KNN | 95.14 % | 99.01 % | 98.26 % | 99.62 % | 99.21 % | 99.80 % | 99.59 % | 99.70 % |
| | GNB | 92.84 % | 97.27 % | 96.10 % | 97.94 % | 97.29 % | 98.27 % | 97.87 % | 99.55 % |
| P2 | LR | 92.19 % | 96.66 % | 95.47 % | 97.91 % | 96.60 % | 98.54 % | 97.26 % | 99.40 % |
| | SVM | 93.74 % | 98.41 % | 97.84 % | 99.24 % | 98.92 % | 99.53 % | 99.40 % | 99.20 % |
| | DT | 93.33 % | 98.08 % | 97.32 % | 98.90 % | 98.39 % | 99.14 % | 98.94 % | 99.00 % |
| | KNN | 90.56 % | 97.21 % | 95.94 % | 98.46 % | 97.65 % | 98.96 % | 98.45 % | 98.75 % |
| | GNB | 92.43 % | 97.35 % | 96.50 % | 97.90 % | 97.65 % | 98.22 % | 98.16 % | 98.50 % |
| P3 | LR | 95.05 % | 97.73 % | 97.69 % | 98.85 % | 98.51 % | 99.20 % | 98.92 % | 98.25 % |
| | SVM | 95.56 % | 98.39 % | 98.25 % | 99.39 % | 98.97 % | 99.62 % | 99.35 % | 98.00 % |
| | DT | 95.00 % | 97.88 % | 97.78 % | 98.91 % | 98.47 % | 99.22 % | 98.85 % | 97.50 % |
| | KNN | 95.31 % | 98.33 % | 98.14 % | 99.39 % | 98.95 % | 99.64 % | 99.33 % | 97.00 % |
| | GNB | 94.52 % | 97.34 % | 97.24 % | 98.50 % | 98.09 % | 98.86 % | 98.53 % | 96.00 % |
| P4 | LR | 87.79 % | 97.35 % | 93.64 % | 98.64 % | 96.31 % | 99.07 % | 97.70 % | 95.00 % |
| | SVM | 89.23 % | 98.43 % | 95.97 % | 99.45 % | 98.30 % | 99.71 % | 99.27 % | 93.50 % |
| | DT | 88.58 % | 97.87 % | 95.34 % | 99.16 % | 97.69 % | 99.48 % | 98.87 % | 92.00 % |
| | KNN | 88.66 % | 97.94 % | 94.88 % | 99.17 % | 97.65 % | 99.54 % | 98.92 % | 90.00 % |
| | GNB | 87.50 % | 97.26 % | 94.51 % | 98.33 % | 97.08 % | 98.83 % | 98.15 % | 87.00 % |

*Table 34. Results of the fourth round for combination FFT 1.5 and ACC ABS*

| Point | Classifier | Cycles 1 | 2 | 3 | 4 | 5 | 6 | 7 | Colour bar |
|---|---|---|---|---|---|---|---|---|---|
| P1 | LR | 95.48 % | 98.58 % | 98.08 % | 99.31 % | 98.88 % | 99.55 % | 99.23 % | 100.0 % |
| | SVM | 96.50 % | 99.12 % | 98.81 % | 99.63 % | 99.38 % | 99.77 % | 99.63 % | 99.90 % |
| | DT | 95.68 % | 98.59 % | 98.33 % | 99.18 % | 98.84 % | 99.37 % | 99.17 % | 99.80 % |
| | KNN | 95.49 % | 98.86 % | 98.43 % | 99.48 % | 99.21 % | 99.67 % | 99.52 % | 99.70 % |
| | GNB | 93.33 % | 97.29 % | 96.34 % | 97.88 % | 97.38 % | 98.16 % | 97.83 % | 99.55 % |
| P2 | LR | 92.28 % | 96.71 % | 95.57 % | 97.97 % | 96.67 % | 98.57 % | 97.32 % | 99.40 % |
| | SVM | 93.85 % | 98.45 % | 97.94 % | 99.26 % | 98.96 % | 99.54 % | 99.42 % | 99.20 % |
| | DT | 93.39 % | 98.10 % | 97.43 % | 98.88 % | 98.45 % | 99.17 % | 98.97 % | 99.00 % |
| | KNN | 90.76 % | 97.35 % | 96.20 % | 98.58 % | 97.83 % | 99.06 % | 98.59 % | 98.75 % |
| | GNB | 92.59 % | 97.44 % | 96.68 % | 98.04 % | 97.80 % | 98.37 % | 98.30 % | 98.50 % |
| P3 | LR | 94.84 % | 98.03 % | 97.94 % | 99.21 % | 98.78 % | 99.51 % | 99.20 % | 98.25 % |
| | SVM | 95.40 % | 98.51 % | 98.35 % | 99.54 % | 99.08 % | 99.76 % | 99.45 % | 98.00 % |
| | DT | 94.76 % | 98.03 % | 97.95 % | 99.17 % | 98.70 % | 99.42 % | 99.09 % | 97.50 % |
| | KNN | 95.05 % | 98.42 % | 98.17 % | 99.48 % | 98.99 % | 99.75 % | 99.38 % | 97.00 % |
| | GNB | 94.27 % | 97.58 % | 97.50 % | 98.80 % | 98.37 % | 99.14 % | 98.80 % | 96.00 % |
| P4 | LR | 87.30 % | 97.09 % | 93.39 % | 98.43 % | 96.08 % | 98.91 % | 97.47 % | 95.00 % |
| | SVM | 88.78 % | 98.22 % | 95.69 % | 99.33 % | 98.17 % | 99.65 % | 99.18 % | 93.50 % |
| | DT | 88.22 % | 97.68 % | 95.06 % | 99.07 % | 97.53 % | 99.43 % | 98.75 % | 92.00 % |
| | KNN | 87.94 % | 97.57 % | 94.51 % | 99.00 % | 97.41 % | 99.42 % | 98.76 % | 90.00 % |
| | GNB | 87.00 % | 96.94 % | 94.19 % | 98.02 % | 96.79 % | 98.58 % | 97.89 % | 87.00 % |